Price Dynamics & Trading Strategies in the Commodities Market

Kevin Louis Guo

Submitted in partial fulfillment of the
requirements for the degree
of Doctor of Philosophy
in the Graduate School of Arts and Sciences

Columbia Univeristy

2018

ABSTRACT

Price Dynamics & Trading Strategies in the Commodities Market

Kevin Louis Guo

This thesis makes new observations of market phenomena for various commodities and trading strategies centered around these observations. In particular, our results imply that many aspects of the commodities markets, from delivery markets to producers and consumer derivative based ETFs can be modeled effectively using financial engineering techniques.

Chapter 2 examines what drives the returns of gold miner stocks and ETFs. Inspired by our real options model, we construct a method to dynamically replicate gold miner stocks using two factors: a spot gold ETF and a market equity portfolio. We find that our real options approach can explain a significant portion of the drivers of firm implied gold leverage.

Chapter 3 studies commodity exchange-traded funds (ETFs). From empirical data, we find that many commodity leveraged ETFs underperform significantly against our constructed dynamic benchmark, and we quantify such a discrepancy via the novel idea of *realized effective fee*. Finally, we consider a number of trading strategies and examine their performance by backtesting with historical price data.

Chapter 4 studies the phenomenon of non-convergence between futures and spot prices in the grains market. In our proposed approach, we incorporate stochastic spot price and storage cost, and solve an optimal double stopping problem to understand shipping certificate prices. Our new models for stochastic storage rates explain the spot-futures premium.

Contents

List of Figures

List of Tables

Acknowledgements

In terms of my greatest intellectual inspiration and personal motivator, I would like to acknowledge Ayn Rand's magnum opus Atlas Shrugged (see Rand (1957)). It taught me the importance of money, the virtue of self-interest, and the thrill of creating new knowledge:

> Money is the material shape of the principle that men who wish to deal with one another must deal by trade and give value for value. Money is not the tool of the moochers, who claim your product by tears, or of the looters, who take it from you by force. Money is made possible only by the men who produce ... Run for your life from any man who tells you that money is evil. That sentence is the leper's bell of an approaching looter. So long as men live together on earth and need means to deal with one another-their only substitute, if they abandon money, is the muzzle of a gun.

Most importantly, this defense couldn't have taken place without the hard work of my thesis committee: Garud Iyengar, Dylan Possamai, Miquel Alonso, David Yao, and my adviser Tim Leung. I especially wish to thank my adviser, who stuck with me all the way back when I was a junior in undergrad at Columbia. He always knows to which journal to submit, which research paths to pursue, and which parts of my writing to emphasize. Without his guidance, I'm certain I would have taken 3 additional years to graduate. Finally, I would like to acknowledge myself as well. I probably couldn't have written this thesis without me.

Chapter 1

Introduction

This thesis makes new observations of market phenomena for various commodities and trading strategies centered around these observations. Unlike equities, commodities cannot be easily modeled as claims to future cash flows. However, a pure supply-demand model for commodities as used in elementary economics courses also remains unsatisfactory because it cannot capture the rich set of incentives which drive the behavior of financial intermediaries, producers, and investors. Thus, we turn to the financial engineering literature to explain these market observations through micro-founded rational agent models. In particular, we study gold miners as agent optimized claims on future gold production; we show that non-convergence in grain markets can be explained by the CBOT delivery mechanisms which have hidden, embedded storage options; and finally, we demonstrate how commodity leveraged ETFs behave like a dynamic replicating portfolio of their underlying commodities. In all three chapters, we make heavy use of options pricing, optimal stopping, and optimal control techniques to understand the underlying dynamics of commodity markets.

Chapter 2 examines what drives the returns of gold miner stocks and ETFs by modeling them as real options on gold. We solve a double optimal control problem to determine the best production strategy and the value of the firm equity, demonstrating that gold miner equities behave like "real options on gold." Inspired by our real options model, we construct

a method to dynamically replicate gold miner stocks using two factors: a spot gold ETF and a market equity portfolio. Furthermore, through each firm's factor loadings on replicating portfolio, we can infer the implicit firm leverage parameters of our model using the Kalman Filter. We find that our real options approach can explain a significant portion of the drivers of firm implied gold leverage. We posit that gold miner companies hold additional real options which help mitigate firm volatility, but these real options cause lower returns relative to the replicating portfolio.

Chapter 3 studies commodity exchange-traded funds (ETFs), which can be modeled as a dynamic replicating portfolio of an underlying index. In this chapter, we analyze the tracking performance of commodity leveraged ETFs and discuss the associated trading strategies. It is known that leveraged ETF returns typically deviate from their tracking target over longer holding horizons due to the so-called volatility decay. This motivates us to construct a benchmark process that accounts for the volatility decay, and use it to examine the tracking performance of commodity leveraged ETFs. From empirical data, we find that many commodity leveraged ETFs underperform significantly against the benchmark, and we quantify such a discrepancy via the novel idea of *realized effective fee*. Finally, we consider a number of trading strategies and examine their performance by backtesting with historical price data.

Chapter 4 explains the market phenomenon of non-convergence between futures and spot prices in the grains market through an embedded storage option in the futures contract. We postulate that the positive basis observed at maturity stems from the futures holder's timing options to exercise the shipping certificate delivery item and subsequently liquidate the physical grain. In our proposed approach, we incorporate stochastic spot price and storage cost, and solve an optimal double stopping problem to give the optimal strategies to exercise and liquidate the grain. Our new models for stochastic storage rates lead to explicit no-arbitrage prices for the shipping certificate and associated futures contract. We calibrate our models to empirical futures data during the periods of observed non-convergence, and illustrate the premium generated by the shipping certificate.

Our results imply that many newly observed aspects of the commodities markets, from delivery markets to producers and consumer derivative based ETFs can be modeled effectively using financial engineering techniques based on rational optimizing agent models. All technical proofs are delegated to the appendices.

Chapter 2

How to Mine Gold Without Digging through Dynamic Replication

This chapter examines what drives the returns of gold miner stocks and ETFs between 2006-2017. We solve a double optimal control problem to determine the best production strategy and the value of the firm equity, demonstrating that gold miner equities behave like "real options on gold." Inspired by our real options model, we construct a method to dynamically replicate gold miner stocks using two factors: a spot gold ETF and a market equity portfolio. Furthermore, through each firm's factor loadings on replicating portfolio, we can infer the implicit firm leverage parameters of our model using the Kalman Filter. We find that our real options approach can explain a significant portion of the drivers of firm implied gold leverage. We posit that gold miner companies hold additional real options which help mitigate firm volatility, but these real options cause lower returns relative to the replicating portfolio.

2.1 Introduction

As is well established in literature (Ghosh et al., 2004; Baur and McDermott, 2010), gold is an asset class that can be viewed as a safe haven or a hedge against market turmoils, currency

depreciation, and other economic or political events. For instance, during the credit crisis, major market indices, including the Dow and the S&P 500, declined by about 20% while gold prices rose from $850 to $1,100 per troy ounce. To achieve these diversification goals, there are a number of products traded that are related to gold including gold exchange traded funds (ETFs), leveraged ETFs (LETFs), gold futures, and gold miner equities. For example, Leung and Ward (2015) find that gold ETFs are relatively cost-effective products for gaining exposure to physical gold.

However, the price of gold does not exist in a vacuum. Gold must be mined and the companies that perform this mining process are themselves traded companies. This gives another avenue for investors to achieve exposure to gold, while allowing them to determine investment decisions through standard equity research techniques. In addition to the spot gold, there are a number of single-name gold miner stocks and (L)ETFs available for trading. Even though general equity sector ETFs are by far the largest by market capitalization, gold miner (L)ETFs are some of the most popular vehicles for short-term trading available on the market. In fact, amongst the top 10 ETFs traded by volume (either dollar or share weighted) there are four directly related to gold miner stocks![1] On the other hand, not a single gold miner ETF appears in the top 20 when ranked by AUM, which suggests that the recent primary interest in gold and gold miner stocks is heavily driven by speculative traders seeking gold-like exposure. Therefore, understanding the underlying factor dynamics of gold miner ETF returns are practically useful for analyzing popular trading strategies, such as pairs trading (see e.g. Triantafyllopoulos and Montana (2009), Leung and Li (2015), and Naylor et al. (2011)).

Standard equity market research has established several rules of thumb to understand the differences of investing in gold miners vs. gold itself.[2] While in the long run there is a clear correlation between gold prices and miner equity prices, price divergence is not unusual.

[1] According to ETF Database `http://www.etfdb.com/compare/volume`.

[2] See `http://www.etf.com/etf-education-center/21023-commodity-etfs-gold-miners-vs-gold.html`.

For example, the short-term performance of gold miners is very sensitive to both the market discount rate and payments of future dividends, which are dictated by the general equity markets. Furthermore, at the individual firm level, management could have a significant impact on the equity returns through superior investment skills, mine openings and closures, cost cutting, or market timing. However, in the long run, the only way for gold miners to make money is to dig gold from the ground and sell it on the open market. Therefore, we propose a model to describe the connection between gold and miner stocks. We extend the structural model of Brennan and Schwartz (1985), directly relating gold prices to the value of gold miner equity via a combined optimal control and stopping problem. This real options model requires gold miners to set an internal production function, liquidating the company assets when gold prices decline past a certain level. In particular, our model suggests that a dynamic portfolio of physical gold would perform identically to an actual portfolio of gold miners.

The contributions of our chapter is twofold. First, we develop a tractable structural model which directly relates the price of physical gold to the performance of a gold miner's equity via the real options literature. Our model allows for explicit analytical expressions for the value of firm's assets, the value of the firm's equity, and precisely identifies the parameters which affect firm's leverage. In fact, we examine the predictions of our real options model, finding that a significant part of gold miner firm's leverage can be explained within the real options framework! Second, we use the insights from our structural model to develop a method to replicate gold miner stocks, using only physical gold and the market equity portfolio, that can explain about 70% of the variation in gold miner stock returns. Our main empirical insight suggests that gold-miner equities have a call-option-like payoff, which results in higher implied leverage and negative alpha relative to physical gold.

The rest of the chapter is organized as follows. Section 2.2 summarizes the relevant literature about the interconnection of gold miner stocks and physical gold. In Section 2.3 we present a valuation model for the gold miner's equity. Section 2.4 illustrates a model-

free dynamic replication strategy of gold miner equity returns using two factors. Section 2.5 studies the inference of the stochastic implied leverage with respect to spot gold using Kalman Filter. Section 2.6 analyzes the relationship between spot gold and gold miner's implied leverage. Section 2.7 concludes.

2.2 Related Studies

Our approach relates the value of a gold miner company's equity to that of an infinitely timed real option on the physical gold itself. To that end, we propose a structural model of optimal production to link the gold miner firm price to the gold it produces. In particular, the model must allow the producer to turn the mine on/off and permit him to vary the rate of production.

Benninga et al. (1985) consider an optimal production rule for a commodity export firm which faces both foreign exchange and commodity price risk. The earlier work by Florian and Klein (1971) solves a similar optimal production problem involving optimal discrete time multi-period commodity production with a concave cost and capacity constraints by deriving a dynamic programming algorithm in the stationary case. In their model, the miner optimizes consumption subject to production control, and the firm's production decision is proportional to the beta with respect to the unhedgeable consumption risk. In the current chapter, while we do not consider currency risk, we derive the total mining firm value in a similar fashion by solving an optimal production control problem for a risk-neutral firm owner. Our model yields a similar production decision rule to Benninga et al. (1985), which mandates a constant rate of production, and a firm consumption rate proportional to the price of physical gold.

We build our model based on the framework of Brennan and Schwartz (1985), where the mining company has a real option to open and close a mine, with a constant rate of production. The non-linearity of the firm payoff with respect to the resource, in other words

the option nature, comes from the option to close and re-open the mine. In contrast for our model, we derive the production rate endogenously by considering a firm with quadratic increasing fractional costs with respect to commodity price (when each marginal ounce of gold costs more to mine as a percentage of the gold price). Furthermore, while they only consider the total firm value, we decompose the firm into equity and debt in order to better understand the non-linear nature of gold miner equity returns. Our model also generates explicit comparative statics and expressions for the implied gold leverage with respect to the various model parameters, making it more useful for empirical validation.

Having derived the optimal production schedule and total firm value, we then split the firm value into two components: equity and debt. We view the equity as a call option on the firm's assets (Merton, 1974), and thus, determine the optimal investment timing for the associated real option (McDonald and Siegel, 1986; Dixit, 1994; Dahlgren and Leung, 2015). We extend the real options literature by not only showing that gold miner equities behave like options on gold, but also demonstrating how the resulting stochastic implied leverage evolves with respect to spot gold.

We develop a method to dynamically replicate gold miner's equity returns using a tradable, dynamic tracking portfolio. Some existing studies have focused on analyzing the price behaviors of the gold (L)ETFs rather than the gold miner stock and the firm's production model (Murphy and Wright, 2010; Guo and Leung, 2015). While common factors for equities in the asset pricing literature are the market portfolio, size, profitability, and value, (Fama and French, 1993), Johnson and Lamdin (2015) and Bloseand and Shieh (1995) have documented the poor performance of static multi-factor models in the gold miner equity space. In fact, gold miners are more similar to options on physical gold than to other equities. The non-linear payoff nature of gold miner stocks leads to implied loadings on physical gold which can vary significantly over respect to time, making consistent estimation extremely difficult. The problem of hedge fund replication has similar issues with replicating non-linear payoffs with linear securities. (Takahashi and Yamamoto, 2008) point out that early hedge fund

replication products tracked their indices very poorly over a long time. Jurek and Stafford (2013) mitigate this issue by introducing non-linear securities as a "factor," demonstrating that hedge funds were engaged in closeted put-selling behavior. In our chapter, we resolve these issues by allowing the factor loadings to vary over time. By using time-varying factor loadings to construct factor portfolios, we can perform our regression analysis utilizing longer holding intervals. Unlike existing factor models for gold miner equities, our model not only has high explanatory power, but a further analysis of the implied factor loadings confirms the intuitive economic relationship of the tracking portfolio with our real options model.

Another novel feature of our approach is the implied leverage of gold miner stocks with respect to gold. Specifically, we explicitly characterize how implied leverage evolves with respect to factors such as gold price, volatility, interest rates etc. The most comprehensive analyses of implied leverage of gold miners was performed by Tufano (1996, 1998), who use individual company level characteristics to explain implied leverage. Confirming economic intuition, they find that the implied leverage decreases with respect to gold price and the presence of firm hedging due to fewer fixed costs, but cash production costs, gold volatility and leverage have no effect on the implied leverage. Later Jorion (2006) presents similar findings on implied leverage for oil and gas companies. We add significantly to the literature by demonstrating exactly why marginal production costs, volatility, and the debt ratio all fail to explain much of the variation in firm implied gold leverage, while gold price remains the main driver of changes in beta over time. Furthermore, we show that our structural real options approach can explain much more of the variation in firm implied gold leverage while using zero firm level variables. Finally, we not only confirm previous results that gold miner stocks are less leveraged than their model would predict, but we also relate this result to extra real options the firm holds that discounted cash flow models do not consider. These real options allow firms to hedge during distressed periods of lower gold prices, resulting in lower implied gold leverage but at a cost of lower average returns.

2.3 Model

We consider a firm that chooses to mine an optimal quantity of gold in order to maximize the expectation of its total discounted future profit. The firm's cost of mining is affine and increasing in the mining rate. We derive both the value of the firm as a function of the current gold price and the optimal mining strategy. The value of the firm's assets serves as input to the valuation of the firm's equity. Finally, we derive an implicit leverage factor of the firm with respect to the gold price, and make predictions about the behavior of implied leverage with respect to the parameters of our model.

2.3.1 Asset Valuation

In the background, we fix a probability space $(\Omega, \mathbb{F}, \mathbb{Q})$. Under the theory of storage (Kaldor, 1939; Working, 1949; Brennan, 1958), the futures price should reflect the spot price plus storage cost less the convenience yield via a no-arbitrage relationship. This relationship was further empirically confirmed by Fama and French (1987) and Gorton et al. (2012) through examining inventories data and commodity prices. Finally, Schwartz (1997) connected the theory of storage to modern risk-neutral pricing with a stochastic convenience yield.

Therefore, given the literature on the theory of storage with stochastic convenience yields, under no-arbitrage principles, the deflated commodity price less convenience yield with the money market numeraire must be a martingale under the risk-neutral pricing measure. Therefore, we suppose that the spot price of gold follows a Geometric Brownian Motion (GBM) under the risk neutral measure $\mathbb{Q}$:

$$\frac{dS_t}{S_t} = (r - \delta)dt + \sigma dW_t, \tag{2.3.1}$$

where $r > 0$ is the risk-free interest rate, $\delta > 0$ is the net convenience yield, and $\sigma > 0$ is the volatility. We also require that $\delta > r$.

The gold mining company strategically controls the (positive) rate of production over time. Let the set of admissible controls as $\mathcal{A} := \{(u_t)_{t\geq 0} : u_t \geq 0,\ \forall t \geq 0\}$. Furthermore, let $K(u)$ be a cost function denoting the fractional costs of mining the gold. Therefore, the retained profit is $1 - K(u)$ fraction of the revenue from mining gold. When the firm mines at the rate u_t at time t, the gold mining company receives the infinitesimal cash flow,

$$u_t(1 - K(u_t))S_t dt.$$

In our model, the only source of randomness is through the gold price, so that the the market for gold derivatives is complete. Furthermore, since in a complete market, no-arbitrage requires investors to be indifferent between buying a portfolio of gold in the market and mining it at cost, so the firm must also be risk-neutral in our model. Therefore, the value of the mining company's assets is given by the discounted sum of all future cash flows from mining the gold under the risk-neutral measure $\mathbb{Q}$. The firm solves the following stochastic control problem:

$$V(S) = \sup_{u\in\mathcal{A}} \mathbb{E}\left[\int_t^\infty u_\xi(1 - K(u_\xi))S_\xi e^{-r(\xi-t)}d\xi \Big| S_t = S\right]. \tag{2.3.2}$$

The mining cost involves a positive fixed cost κ and is linear in the production rate u. That is,

$$K(u) = \kappa + \alpha u. \tag{2.3.3}$$

To better understand the cost function, a few remarks are in order. First, it is typical for resource extraction that costs, such as worker compensation and expenditures on mining equipment, all increase as with the gold price, since these resources can become scarce during a gold rush. Furthermore, a higher gold price also motivates miner to open or operate more difficult mines, again resulting in higher marginal costs. For example, a mining company may choose to open new mines in the arctic circle, or switch from surface cyanide mining to more

difficult extraction processes such as deep shafts. As a result, the total cost at time t, which is the product of the fraction $K(u_t)$ and revenue $u_t S_t$, is proportional to the production rate and price of gold.

In our model, we require $\alpha > 0$ so that the cost of extraction increases with the mining rate. Then, the instantaneous profit is non-negative as long as $0 \leq u_t \leq \frac{1-\kappa}{\alpha}$ and $0 \leq \kappa \leq 1$. If $\kappa > 1$ or $\alpha < 0$, then the firm would never produce and simply exit the market. If $\kappa = 1$ then the only strategy is $u_t \equiv 0$ so the firm is in the market but not producing. Finally, if $\alpha = 0$, then control is unbounded above, in other words $u_t \equiv \infty$, so the firm produces an infinite quantity of the commodity. Thus, the only possibility for non-trivial production is when $\kappa < 1$ and $\alpha > 0$, so we impose these conditions on the production costs for the rest of this section.

By standard dynamic programming arguments, the value function solves the following Hamilton-Jacobi-Bellman (HJB) equation:

$$0 = -rV + (r - \delta)S\frac{\partial V}{\partial S} + \frac{1}{2}\sigma^2 S^2 \frac{\partial^2 V}{\partial S^2} + \sup_{u \geq 0} \{u(1 - K(u))S\}.$$

To solve the inner optimization, we introduce the Lagrangian

$$\mathcal{L}(u, \lambda) = u(1 - K(u))S + \lambda u.$$

From this Lagrangian, we derive the Karush-Kuhn-Tucker (KKT) conditions for optimality:

1. $(1 - K(u))S - uK'(u)S + \lambda = 0$
2. $u \geq 0$
3. $\lambda \geq 0$
4. $\lambda u = 0$.

Multiplying the first condition by u, and using the fourth, we obtain

$$u(1 - K(u)) - u^2 K'(u) = 0. \tag{2.3.4}$$

Since $K(u)$ is affine in u (see (2.3.3)), equation (2.3.4) yields two candidate solutions:

1. $u_1^* = 0$, with $\lambda_1^* = -(1-\kappa)S$,
2. $u_2^* = \frac{1-\kappa}{2\alpha}$, with $\lambda_2^* = 0$.

The first achieves a trivial objective function value of 0, while the second achieves

$$\frac{(1-\kappa)^2}{4\alpha} S > 0.$$

The inequality holds given that $\kappa < 1$ and $\alpha > 0$. Thus, the optimal solution must be u_2^*. Since $\alpha, S > 0$, the second-order condition yields that

$$\frac{\partial^2}{\partial u^2}\mathcal{L}(u, \lambda) = -2K'(u)S = -2\alpha S < 0.$$

Notice that $u^* = \frac{1-\kappa}{2\alpha} \leq \frac{1-\kappa}{\alpha}$, so the optimal control is constant and below the maximum production rate. Applying the optimal control, we express the original value function (2.3.2) as

$$\begin{aligned} V(S) = \mathbb{E}\left[\int_t^\infty \frac{(1-\kappa)^2}{4\alpha} S_\xi e^{-r(\xi - t)} d\xi \middle| S_t = S\right] &= \frac{(1-\kappa)^2}{4\alpha} \int_t^\infty e^{-r(\xi-t)} \mathbb{E}\left[S_\xi \middle| S_t = s\right] d\xi \\ &= \frac{(1-\kappa)^2}{4\alpha\delta} S, \end{aligned}$$

where the step switching expectation and integration follows from Tonelli's Theorem. We arrive at the following theorem.

Theorem 2.3.1. *Under the spot model* (2.3.1) *and affine cost assumption* (2.3.3)*, the gold*

miner's asset value defined in (2.3.2) *is given by*

$$V(S_t) = \frac{(1-\kappa)^2}{4\alpha\delta} S_t.$$

Morevoer, the optimal production policy is

$$u^* = \frac{1-\kappa}{2\alpha}.$$

Finally, $V_t := V(S_t)$ *is a GBM under* $\mathbb{Q}$*:*

$$dV_t = \frac{(1-\kappa)^2}{4\alpha\delta} dS_t = \frac{(1-\kappa)^2}{4\alpha\delta}(r-\delta)dt + \frac{(1-\kappa)^2}{4\alpha\delta}\sigma dW_t.$$

As this result, the miner's asset value is a constant multiple of the spot price. The value function suggests that firm's asset value decreases if production cost increases (as measured by either κ or α). This is quite intuitive since higher production costs entail a less profitable enterprise. Furthermore, since the firm value is quadratically decreasing in the fixed cost, but only linearly in the marginal cost, we conclude that the fixed mining cost plays a bigger role in determining the firm value. We also observe that the value function is decreasing in the convenience yield δ. Since the firm sells the gold instantaneously with production, its profit is reduced by the value of the convenience yield which accrues to the physical holder of the commodity. Surprisingly, our simple production model suggests that the total firm value can be statically replicated with only a single asset, physical gold itself, with a multiplier analogous to the price-to-earnings ratio under the Gordon growth model. We will explore the implications of this fact in the next section.

2.3.2 Equity Valuation

Given the value of the firm's assets under the optimal production schedule, the firm's equity can be priced via the (Merton, 1974) firm model, wherein the equity value is equal to the

price of a call option on the firm's assets with a strike price equal to the total debt less accumulated coupons. We assume at time t the firm has perpetual debt with face value D and continuous coupon C. It pays back its debt at some stopping $\tau \in \mathcal{T}_t$, where $\mathcal{T}_t$ is the set of stopping times with respect to the filtration $\mathbb{F}$ generated by S such that $\tau \geq t$. Therefore, the value of the equity is essentially equal to the price of a perpetual American call option on the firm's asset value, V_t. The equity value is found from the optimal stopping problem:

$$J(V) = \sup_{\tau \in \mathcal{T}_t} \mathbb{E}\left[e^{-r(\tau - t)}(V_\tau - D)^+ - \int_t^\tau C e^{-r(u-t)} du \Big| V_t = V \right].$$

Note that $J(V) \geq 0$ for all V because stopping immediately (i.e. choosing $\tau = t$) yields the lower bound value of zero.

Since V_t can be expressed in terms of the spot gold price, we can rewrite the equity valuation problem in terms of S as

$$J(S) = \frac{(1-\kappa)^2}{4\alpha\delta} \sup_{\tau \in \mathcal{T}_t} \mathbb{E}\left[e^{-r(\tau - t)}(S_\tau - \bar{D})^+ - \int_t^\tau \bar{C} e^{-r(u-t)} du \Big| S_t = S \right], \tag{2.3.5}$$

where

$$\bar{D} = \frac{4\alpha\delta}{(1-\kappa)^2} D, \quad \text{and} \quad \bar{C} = \frac{4\alpha\delta}{(1-\kappa)^2}.$$

Hence, the optimal timing strategy can be derived from

$$\tilde{J}(S) = \sup_{\tau \in \mathcal{T}_t} \mathbb{E}\left[e^{-r(\tau - t)}(S_\tau - \bar{D})^+ - \int_t^\tau \bar{C} e^{-r(u-t)} du \Big| S_t = S \right],$$

and then multiplying through by the constant $\frac{(1-\kappa)^2}{4\alpha\delta}$ to derive $J(S)$. By standard calculations

(see e.g. McDonald and Siegel (1986)), we obtain

$$\tilde{J}(S) = \begin{cases} AS^{\gamma} - \frac{4\alpha\delta C}{r(1-\kappa)^2}, & \text{if } S \leq S^* \\ \\ S - \frac{4\alpha\delta D}{(1-\kappa)^2}, & \text{otherwise,} \end{cases}$$

where

$$\gamma = -\left(\frac{r-\delta}{\sigma^2} - \frac{1}{2}\right) + \sqrt{\left(\frac{r-\delta}{\sigma^2} - \frac{1}{2}\right)^2 + \frac{2r}{\sigma^2}}\,. \tag{2.3.6}$$

By inspection of (2.3.6), we know that the leverage parameter $\gamma > 0$, and for $\delta > r$ then $\gamma > 1$. Intuitively, the stock value is always increasing in the price of gold. From standard results, we can solve for the constants A and S^* by requiring $\bar{J}(S)$ satisfy the continuity and smooth pasting conditions:

$$\begin{aligned} \tilde{J}(S^*) &= S^* - \frac{4\alpha\delta D}{(1-\kappa)^2}, \\ \tilde{J}'(S^*) &= 1. \end{aligned}$$

In other words, at the debt buyback boundary S^*, the equity value should match both the level and rate of change as it was in the continuation region. This results in the solution

$$\begin{aligned} A &= \frac{1}{\gamma(S^*)^{\gamma-1}}, \\ S^* &= \frac{\gamma}{\gamma-1} \times \frac{4\alpha\delta}{(1-\kappa)^2} \times \left(D - \frac{C}{r}\right). \end{aligned}$$

Multiplying by the constant gives us the following result.

Theorem 2.3.2. *Under the spot model* (2.3.1) *and affine cost assumption* (2.3.3)*, the gold*

miner's equity value defined in (2.3.5) *is given by*

$$J(S_t) = \begin{cases} \frac{(1-\kappa)^2}{4\alpha\delta} A S_t^\gamma - \frac{C}{r}, & \text{if } S_t \leq S^* \\ \\ \frac{(1-\kappa)^2}{4\alpha\delta} S_t - D, & \text{otherwise,} \end{cases}$$

where

$$\begin{aligned} A &= \frac{1}{\gamma (S^*)^{\gamma-1}}, \\ S^* &= \frac{\gamma}{\gamma - 1} \times \frac{4\alpha\delta}{(1-\kappa)^2} \times \left(D - \frac{C}{r} \right), \\ \gamma &= -\left(\frac{r-\delta}{\sigma^2} - \frac{1}{2} \right) + \sqrt{\left(\frac{r-\delta}{\sigma^2} - \frac{1}{2} \right)^2 + \frac{2r}{\sigma^2}}. \end{aligned}$$

First, the price of the gold mining company is leveraged with respect to gold through the parameter γ. In addition, the equity value declines with respect to production costs κ and α. The fixed cost κ affects stock price quadratically and has a stronger effect while the marginal cost α affects it linearly. This is intuitive since fixed costs must always be paid and represent a lower bound on profit, while marginal costs are variable and only affect the upper bound.

The gold miner's equity is a function of the physical gold price. As a consequence, the equity J can be perfectly replicated using a portfolio of $\frac{\partial J}{\partial S}$ shares of physical gold and the rest composed of the money market account. Figure 1 illustrates the value of the gold miner equity compared to the immediate value of paying back the debt under different spot prices for gold. As we can see, the value function is convex and approaches the asset value less debt as the price of gold surpasses S^*. Under this model the gold miner's equity can always be spanned by some combination of physical gold and the money market account. Although

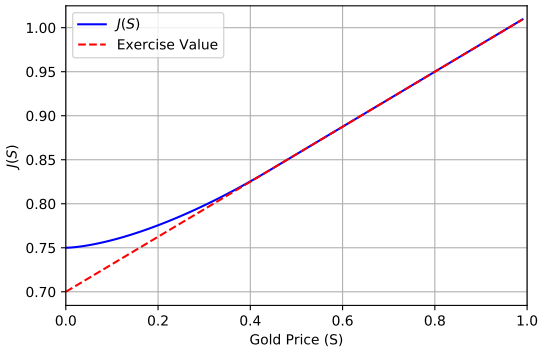

Figure 1: The value function $J(S)$ (blue) and the immediate exercise value $\frac{(1-\kappa)^2}{4\alpha\delta}S_t - D$ (red) vs the spot price of gold S. The parameters are $\alpha = 0.2$, $\kappa = 0.95$, $r = 0.02$, $\delta = 0.01$, $\sigma = 0.1$, $D = 0.33$, $C = 0.015$. The optimal exercise level is $S^* = 0.38$.

this result seems surprising, we will demonstrate in Section 2.4 that 70% of the gold miner equity returns can be explained by a tradable replicating portfolio consisting only of the equity market portfolio, risk free bonds, and physical gold. Thus, although replication is far from perfect, by buying the correct dynamic quantities of gold and risk-free bonds, we have thus managed to "mine gold without digging!"

2.3.3 Comparative Statics

We now set up the framework for our empirical asset pricing model by considering how the dynamic quantities of physical gold we need for replication vary with respect to time. In particular, since we care about comparing *returns* of the various assets in our sample, it is important to analyze how the *implied leverage* of the gold miner equity with respect to gold varies over time. The instantaneous return of the gold mining equity is related to the instantaneous returns of the physical gold and the money market account as follows:

$$\frac{dJ_t}{J_t} = \beta(S_t)\frac{dS_t}{S_t} + (1 - \beta(S_t))rdt.$$

In the non-trivial continuation region $S_t = S \leq S^*$, we have

$$\beta(S) = \frac{\partial J}{\partial S}\frac{S}{J} = \frac{A\gamma S^\gamma}{AS^\gamma - \frac{4\alpha\delta C}{r(1-\kappa)^2}} \tag{2.3.7}$$

We call $\beta(S)$ the **implied gold leverage** of the gold miner equity, choosing to suppress the time dependence for notational simplicity. When β is larger, the equity is more risky with higher risk premium and hence has lower price, and when β is smaller, the equity is less risky with lower risk premium and hence has higher price. We would like to understand how the gold miner implied leverage varies with the various explicit parameters of our company.

Proposition 1. *In the continuation region where $S \leq S^*$, the sensitivities of the implied gold leverage with respect to the gold price are given by*

$$\beta'(S) = \frac{-\frac{4\alpha\delta C}{(1-\kappa)^2 r}}{\left(AS^\gamma - \frac{4\alpha\delta C}{(1-\kappa)^2 r}\right)^2} < 0, \qquad \beta''(S) = -\frac{2\beta}{S} \times \beta'(S) > 0.$$

Furthermore, the stochastic evolution of the implied gold leverage $\beta(S_t)$ follows

$$\begin{aligned} d\beta(S_t) &= \beta'(S_t)dS_t + \frac{1}{2}\beta''(S_t)(dS_t)^2 \\ &= \beta'(S_t)\left(dS_t - \beta\sigma^2 S_t dt\right). \end{aligned} \tag{2.3.8}$$

Our model confirms a number of financial intuitions. As the spot gold price increases, the implied leverage of the gold company falls. Furthermore, the implied leverage is decreasing *convex* in the gold price S, so a higher price of physical gold decreases leverage by a smaller and smaller amount as $S \to \infty$. On the other hand, a fall in gold price would lead to implied leverage spiraling higher and higher by the same convexity property. By a replicating portfolio argument, we can imagine that a higher (relative) cost gold miner company borrows more in order to fund his positions in the physical gold, and as costs increase more and more

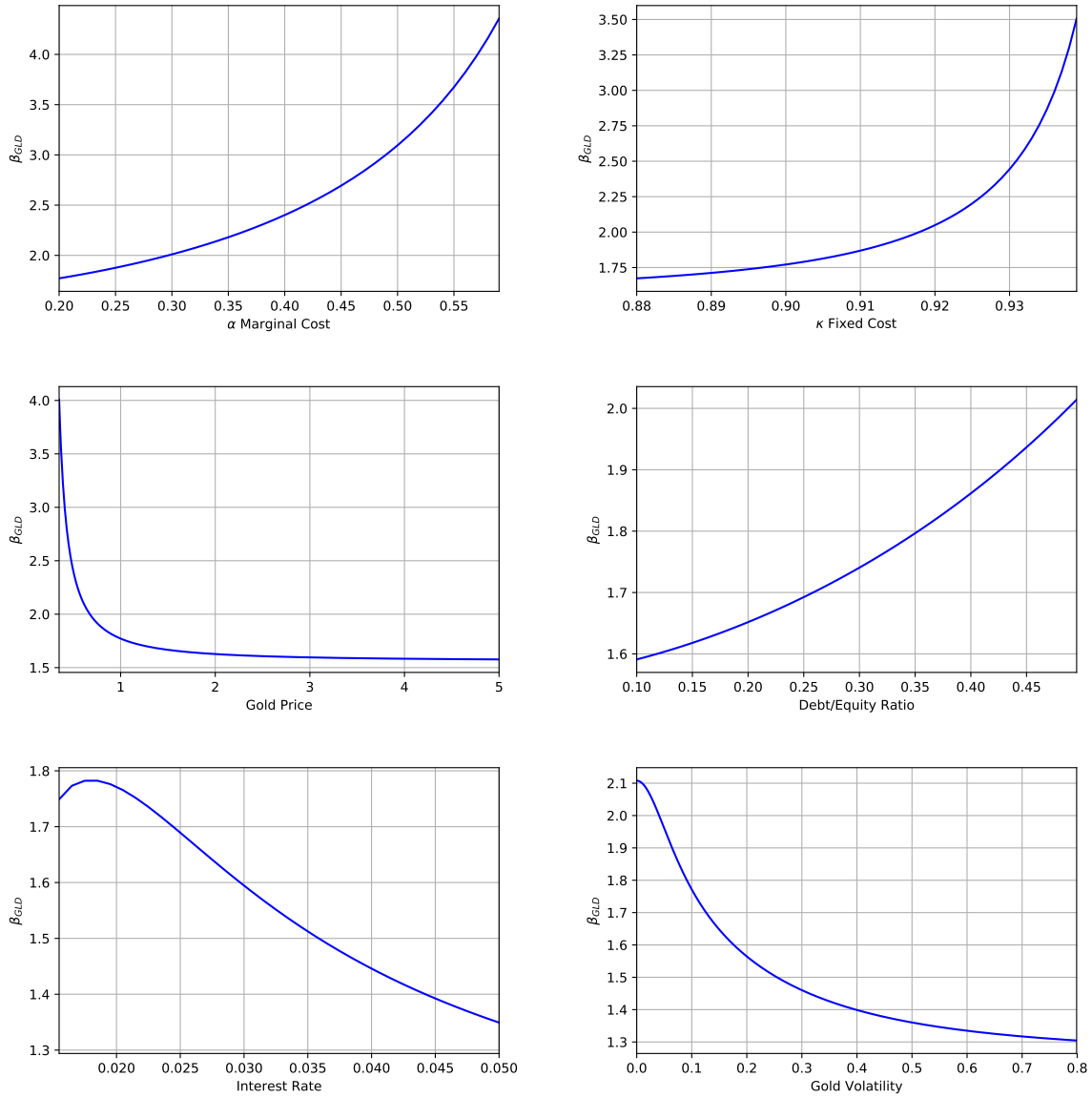

Figure 2: Implied leverage $\beta(S)$ vs our model parameters. From left to right top to bottom: α, κ, S_t, D, r, σ. The graphs vary one set of parameters while holding the others constant. The constant parameters are $\alpha = 0.2$, $\kappa = 0.9$, $r = 0.02$, $\delta = 0.01$, $\sigma = 0.1$, $D = 0.12$, $C = 0.003$, and $S_0 = 1.25$

as a percentage of the gold price, leverage will spiral out of control via the convexity property.

In fact, the decreasing convex evolution of β with respect to gold price results in an interesting dynamics of implied leverage. Suppose there is a positive shock to the physical gold dS_t. While the implied leverage initially falls linearly via the shock, it is mitigated by the convex component $\beta\sigma^2 S_t dt$. On the other hand, when there is a negative shock

to the physical gold price, then implied leverage increases even more through the convex component. Therefore, the convexity of beta acts as an anti-regulatory mechanism for high cost gold producers: even a small decrease in gold prices can cause a massive increase in implied leverage! Moreover, the implied leverage of a high-cost mining company should be extremely volatile and hence more difficult to estimate vs the implied leverage of a lower cost mining company.

On the other hand, as the cost parameters κ and α rise, the implied leverage of the gold company will increase as well, a mirror result to Proposition 1.

Proposition 2. *In the continuation region where $S \leq S^*$, the sensitivities of the implied leverage with respect to the gold miner's constant and linear production costs, κ and α, respectively, are*

$$\frac{\partial \beta}{\partial \kappa}(S) = \frac{\frac{8\alpha\delta C}{(1-\kappa)^3 r} \times A\gamma^2 S^\gamma}{\left(AS^\gamma - \frac{4\alpha\delta C}{(1-\kappa)^2 r}\right)^2} > 0, \qquad \frac{\partial \beta}{\partial \alpha}(S) = \frac{\frac{4\delta C}{(1-\kappa)^2 r} \times A\gamma^2 S^\gamma}{\left(AS^\gamma - \frac{4\alpha\delta C}{(1-\kappa)^2 r}\right)^2} > 0.$$

Intuitively, the higher the fixed costs of a gold miner company, the higher the leverage of equity. For example, if a company has revenue of \$100 with fixed cost of \$99 then a \$1 increase/decrease in revenue results in a 100% increase/decrease of earnings. On the other hand, if the fixed cost is only \$50 then a \$1 increase/decrease in revenue increases/decreases total earnings by only 2%. As a result, the higher the mining cost as a fraction of the revenue, in this case the spot gold price, the higher the implied leverage of our gold mining company. Thus, fixed mining costs and debt payments would result in similar implications for the profits of a the gold mining company. We remark that Tufano (1996) found several anomalies in how implied leverage was reflected in gold miner stocks (summarized in Table V & VI of their chapter). Although as predicted gold price and fixed mining costs all had the anticipated effect on firm's leverage, the debt/equity ratio had a much weaker effect on leverage. In particular, after taking fixed effects, he found that mining costs ceased to

be significant. In other words, while fixed mining costs were important, increased marginal costs had less effects on leverage. By appealing to our real options model of the gold mining firm, we can explain why they found such anomalies in the determinants of firm leverage.

Figure 2 illustrates the dependence of the gold miner equity's implied leverage on various model parameters. As predicted by Proposition 1, the leverage increases significantly as the gold price reaches a significant threshold, in this case around 0.5 times the original value S_0. Similarly, Proposition 2 predicts a similar "convexity" effect as both the fixed percentage cost κ and the marginal percentage cost α increases. For example, a small increase of 0.06 in the fixed cost results in leverage rising from 1.6 to 3.5. On the other hand, rises in the marginal cost α result in much less dramatic increases in the leverage. We need to almost triple α in order to generate the same rise in leverage. The intuition is that a larger fixed cost cannot be accommodated easily, while changes in marginal costs are usually offset by an increase in the gold price itself. After all, one would only choose to mine the high cost of production gold if the gold price itself was high! Finally, changes in the debt/equity structure leads to only moderate changes in implied leverage compared to changes in the mining costs. This is because typically most of the fixed costs of a gold miner are related to mining costs for the gold rather than payments of coupons for the bondholders, so the capital structure is less important than the mining cost structure. For example, Jorion (2006) reveals that the net profit margin for oil and gas drilling companies is typically 5%, suggesting that over 90% of the cost can be attributed to fixed costs and not coupon payments.

Furthermore, we can consider the variation of the gold miner implied leverage with respect to the implied growth parameters of our model.

Proposition 3. *In the continuation region where $S \leq S^*$, the sensitivities for the implied leverage with respect to the model parameters, namely, the interest rate r, net convenience yield δ, and volatility σ of the spot gold price, respectively, are given by*

$$\frac{\partial\beta}{\partial r}(S) = -\frac{AS^\gamma\left(\frac{\partial\gamma}{\partial r} - \frac{4\alpha\delta C}{(1-\kappa)^2 r}\left(\gamma\log S + \frac{S^*\log S^*}{\gamma-1}\right)\frac{\partial\gamma}{\partial r} - \gamma\frac{4\alpha\delta C}{(1-\kappa)^2 r^2}\right)}{\left(AS^\gamma - \frac{4\alpha\delta C}{(1-\kappa)^2 r}\right)^2} \times \frac{\partial\gamma}{\partial r},$$

$$\frac{\partial\beta}{\partial\delta}(S) = \frac{AS^\gamma\left(\frac{\partial\gamma}{\partial\delta} - \frac{4\alpha\delta C}{(1-\kappa)^2 r}\left(\gamma\log S + \frac{S^*\log S^*}{\gamma-1}\right)\frac{\partial\gamma}{\partial\delta} + \gamma\frac{4\alpha C}{(1-\kappa)^2 r}\right)}{\left(AS^\gamma - \frac{4\alpha\delta C}{(1-\kappa)^2 r}\right)^2} \times \frac{\partial\gamma}{\partial\delta},$$

$$\frac{\partial\beta}{\partial\sigma}(S) = \frac{AS^\gamma\left(1 - \frac{4\alpha\delta C}{(1-\kappa)^2 r}\left(\gamma\log S + \frac{S^*\log S^*}{\gamma-1}\right)\right)}{\left(AS^\gamma - \frac{4\alpha\delta C}{(1-\kappa)^2 r}\right)^2} \times \frac{\partial\gamma}{\partial\sigma},$$

where

$$\frac{\partial\gamma}{\partial r} = -\frac{\gamma-1}{\sigma^2\sqrt{\left(\frac{r-\delta}{\sigma^2} - \frac{1}{2}\right)^2 + \frac{2r}{\sigma^2}}}, \quad \frac{\partial\gamma}{\partial\delta} = \frac{\gamma}{\sigma^2\sqrt{\left(\frac{r-\delta}{\sigma^2} - \frac{1}{2}\right)^2 + \frac{2r}{\sigma^2}}}, \quad \frac{\partial\gamma}{\partial\sigma} = 2\frac{(r-\delta)\gamma - r}{\sigma^3\sqrt{\left(\frac{r-\delta}{\sigma^2} - \frac{1}{2}\right)^2 + \frac{2r}{\sigma^2}}}.$$

Under the further condition that

$$\gamma\log S + \frac{S^*\log S^*}{\gamma-1} < 0, \tag{2.3.9}$$

we have the signs for the following sensitivities:

$$\frac{\partial\beta}{\partial r}(S) < 0, \qquad \frac{\partial\beta}{\partial\delta}(S) > 0.$$

By imposing the condition (2.3.9), the variation of implied leverage with respect to the growth parameters also make intuitive sense. For example, since $r-\delta$ is the growth rate of spot gold, a higher growth rate would result in less risk to the gold miner, since the gold price S_t would rise more in the long run. On the other hand, a lower growth rate would result in greater risk to the gold miner, since the gold price would rise less in the long run. Therefore,

our model predicts that a positive shock to the permanent growth rate of the physical gold causes implied leverage to fall, while a negative shock causes implied leverage to rise, as our intuition suggests.

Another look at Figure 2 illustrates the dependence of the implied leverage on volatility parameter σ. From Proposition 3, under condition (2.3.9), higher volatility leads to higher betas when $(r-\delta)\gamma - r > 0$ and lower betas when $(r-\delta)\gamma - r < 0$. For example, for our choice of parameters, we have $(r-\delta)\gamma - r < 0$ and we see that when (2.3.9) is met, Figure 2 shows that $\beta(\sigma; S_t)$ is downward sloping. Thus, implies leverage falls with volatility as intuition would predict.

We note that Tufano (1996), the main chapter that analyzed the factors behind implied gold leverage, did not find any effect of gold price volatility on firm leverage. He originally predicted that implied leverage would decline with high volatility under a discounted cash flow model where the firm never hedges. In fact, not only were the coefficients statistically insignificant, but they often had even the wrong sign, suggesting that leverage would *increase* with volatility. However, our model explains this anomaly: simply changing the choice of γ for the firm can totally invert the relationship between volatility and firm leverage. For example, even if (2.3.9) is satisfied, we can still have $\frac{\partial \beta}{\partial \sigma} > 0$ in Proposition 3 if $(r-\delta)\gamma - r > 0$. Therefore, it's not surprising Tufano (1996) found no significant effect of gold volatility on implied leverage.

Thus, by appealing to a real options model we have managed to explain previous empirical results in the gold miner literature and understand several anomalies on what affects implied gold leverage. As expected, we find that implied leverage varies positively with fixed costs and negatively with gold prices. On the other hand, we show why capital structure and marginal mining costs are not very important for explaining gold miner implied leverage, since these variables are in practice typically overwhelmed by mining costs and gold price. Finally, we resolve an anomaly in the literature by demonstrating that gold price volatility can have both positive and negative effects on the firm's leverage, depending on the current

Security Name (Ticker)	Inception Date	Fee	Market Cap
SPDR Gold ETF	11/18/2014	0.4%	$ 36.00 B
Barrick Gold (ABX)	01/01/1985	–	$ 18.37 B
Gold Corp (GG)	04/01/1994	–	$ 11.20 B
Gold Miners ETF (GDX)	05/16/2006	0.52%	$ 9.62 B
Junior Gold Miners ETF (GDXJ)	11/10/2009	0.56%	$ 3.97 B

Table 1: Summary of stock and ETF data. Data used for our analysis is from max{11/18/2014, Inception Date} to 04/21/2017 unless otherwise noted. For the two ETFs, fee is total expense ratio as stated on the prospectus as of 10/28/2017.

market regime.

2.4 Factor Replication of Gold Miner Stocks

Motivated by the real option model of Section 2.3, we construct a model-free, dynamic portfolio that replicates the returns of gold miner equities using a combination of the physical gold, risk-free asset, and equity market portfolio. With this replicating portfolio and its relevant factor loadings, we have constructed a way to mine gold without digging.

2.4.1 Data

We examine the returns of several gold miner ETFs and large gold mining companies between the years 2006-2017. We restrict our sample to only US traded gold miner stocks and ETFs. The corresponding market portfolio index for each gold miner index is the Vanguard Total Stock Market Index.[3]

Table 1 describes the equity and gold price data. We have data for all stocks and ETFs dating back to at least 2009. The data is truncated at 2005, because that is the first date when GLD, the physical gold ETF began to trade. We chose the individual gold miner stocks by choosing the largest market cap gold miners who derived at least 50% of profits from mining gold. All ETFs and stocks are highly liquid, with a bid ask spread less than

[3]For example, see the composition of the ETF GDX: `https://screener.fidelity.com/ftgw/etf/goto/snapshot/portfolioComposition.jhtml?symbols=GDX`

5 bps and a market capitalization greater than $1 billion throughout the entire sampling period. Finally, we use the 3M LIBOR rate as the risk-free rate in our calculations. All price data was obtained from Quandl, but at the money implied volatility estimates for gold were taken from Bloomberg.

2.4.2 Constructing the Replicating Portfolio

Intuitively, gold miner returns should have significant correlation with both gold returns and the market returns. However, since Section 2.3 suggests that all gold miner stocks are related to real gold options, leverage with respect to gold price varies over time. Since firm leverage should increase when gold prices fall closer to production cost, a pooled regression would ignore the time series variation in firm leverage. Thus, it is not sensible to use a standard pooled regression over the whole sample space to estimate a firm's exposure to gold price as preferred under the asset pricing literature. On the other hand, since the (variable) price of gold is much more volatile than (fixed) production costs, the variation of firm leverage with respect to gold must vary substantially, even over short time periods. Therefore, we will must infer β_{GLD}, the firm's implied gold leverage, through short-window rolling regressions.

For notational simplicity, we fix a particular gold miner, or gold mining index j. We denote by $R_{t,j}$ the time series of returns of the gold miner, $R_{Mkt,t}$ the time series of returns of the equity market portfolio, $R_{GLD,t}$ the time series of returns of physical gold and r_{f_t} the risk free rate.[4] With this setup, the dynamic $\beta_{GLD,t,j}$ at time t for miner j can be inferred from the following rolling regressions:

$$R_{t,j} - r_{f_t} = \alpha_{t,j} + \beta_{Mkt,t,j}(R_{Mkt,t} - r_{f_t}) + \beta_{GLD,t,j}(R_{GLD,t} - r_{f_t}) + \epsilon_{t,j}, \qquad (2.4.1)$$

for all $t \in \{t-25, ..., t\}$. The OLS assumptions hold so that the noise terms, $\epsilon_{t,j}$, have mean zero, with $\mathbb{E}[\epsilon_{t,j}|R_{mkt,t}, R_{GLD,t}] = 0$ and $\epsilon_{t,j} \perp\!\!\!\perp \epsilon_{s,j}$ for $t \neq s$.

[4] Although we tried both regular and log returns, we found almost no difference in our regression results, so herein we report only regular returns.

We regress the excess returns of the gold miner on the excess returns of the equity market portfolio and the excess return of gold over a time period of length 25 business days going backwards from the time point t. Our regression uses exponential weightings with the decay parameter $\lambda = 0.95$ so as to weigh the closer time points more due to the time varying nature of $\beta_{GLD,t,j}$. The regression factor coefficients, $\alpha_{t,j}$, $\beta_{Mkt,t,j}$ and $\beta_{GLD,t,j}$ depend on the time t where the regression time series ends, and the gold miner equity j whose returns we are trying to explain. In particular, the gold coefficients $\beta_{GLD,t,j}$ represent an estimation of the instantaneous elasticity of the gold miner stock with respect to gold price. However, unlike the coefficients of (2.3.8), so far we place no constraints on β_{GLD} besides the standard OLS assumptions. Later in Section 2.5, we will show a way to combine the real options model of Proposition 1 with our regression estimates to produce model consistent and efficient estimations of time varying implied gold leverage.

Recall that the real options of Section 2.3 implies that a time-varying portfolio in physical gold would explain the returns of gold miner stocks. In addition, since gold miner stocks generally exhibit positive covariance with the stock market, we should observe a significant loading on the market portfolio as well. Therefore, if our model is correctly specified, then the average α should be zero, with positive β_{GLD} and β_{Mkt} coefficients. Note that while this procedure assumes that the replicating portfolio is dynamic with respect to the factor loadings, it does not assume a payoff or specific structural form for the real option we are trying to calibrate. That is why we consider the replicating portfolio construction to be "model-free."

Having calculated the localized factor loadings for each gold miner on physical gold, we are now ready to construct the replicating portfolio. From our model free formulation, under the assumption that $\alpha_{t,j} \equiv 0$, we expect that a portfolio with weights of $\beta_{GLD,t,j}$ in the GLD ETF, $\beta_{Mkt,t,j}$ in the market portfolio, and $1 - \beta_{GLD,t,j} - \beta_{Mkt,t,j}$ in the risk free asset should exactly replicate $R_{t,j}$, the return of the gold miner at time t. Of course, unless $R^2 \equiv 1$ exactly, we will not have perfect replication, only replication on average. Finally, we must lag our

Security Name (Ticker)	R^2	α	$\beta_{portfolio}$
Barrick Gold (ABX)	0.609360	-0.003494^{*}	0.895739^{**}
Goldcorp (GG)	0.626465	-0.003983^{*}	0.916772^{**}
Gold Miners ETF (GDX)	0.715839	-0.005844^{**}	0.874759^{**}
Junior Gold Miners ETF (GDXJ)	0.634395	-0.008139^{**}	0.821515^{***}

Table 2: Performance of the replicating portfolio constructed with weights $\beta_{GLD,t,j}$ and $\beta_{Mkt,j}$ at each time t for equity j on a monthly frequency. These factor loadings are obtained via the regression (2.4.1). The table shows the result of the two sided t-test for $\alpha_j \neq 0$ and $\beta_{portfolio,j} \neq 1$. Hull-white standard errors were used to calculate t-statistics. The symbols *, **, and *** indicate significance at the 10%, 5% and 1% levels respectively for each test.

regression coefficients by one time period to ensure that the portfolio construction method only uses information available at time t.

Thus, at time t, with $\Delta t = 1$ week, we form a portfolio which consists of weights

$$\omega_{t,j} = (\beta_{GLD,t-\Delta t,j}, \beta_{Mkt,t-\Delta t,j}, 1 - \beta_{GLD,t-\Delta t,j} - \beta_{Mkt,t-\Delta t,j})$$

in the physical gold, market portfolio, and risk-free asset respectively. At time $t + \Delta t$, the portfolio will have a mark-to-market return of

$$R_{t,j,portfolio} = \omega'_{t,j}(R_{t,GLD}, R_{t,Mkt}, r_{f_t}).$$

Furthermore, since the gold miner's dependence on the market portfolio (equity market beta) should not be time varying, we simply set the time average of the $\beta_{Mkt,j}$ coefficients at all times t, thereby removing the dependence on t. Having constructed the replicating portfolio, we can test its success by running the regression

$$R_{t,j} = \beta_{portfolio,j} R_{t,j,portfolio} + \alpha_j + \epsilon_{t,j}. \tag{2.4.2}$$

Table 2 shows the result of our regression analysis with respect to our replicating portfolio, while Figure 3 demonstrates the goodness of fit of our replicating portfolio model. First, we

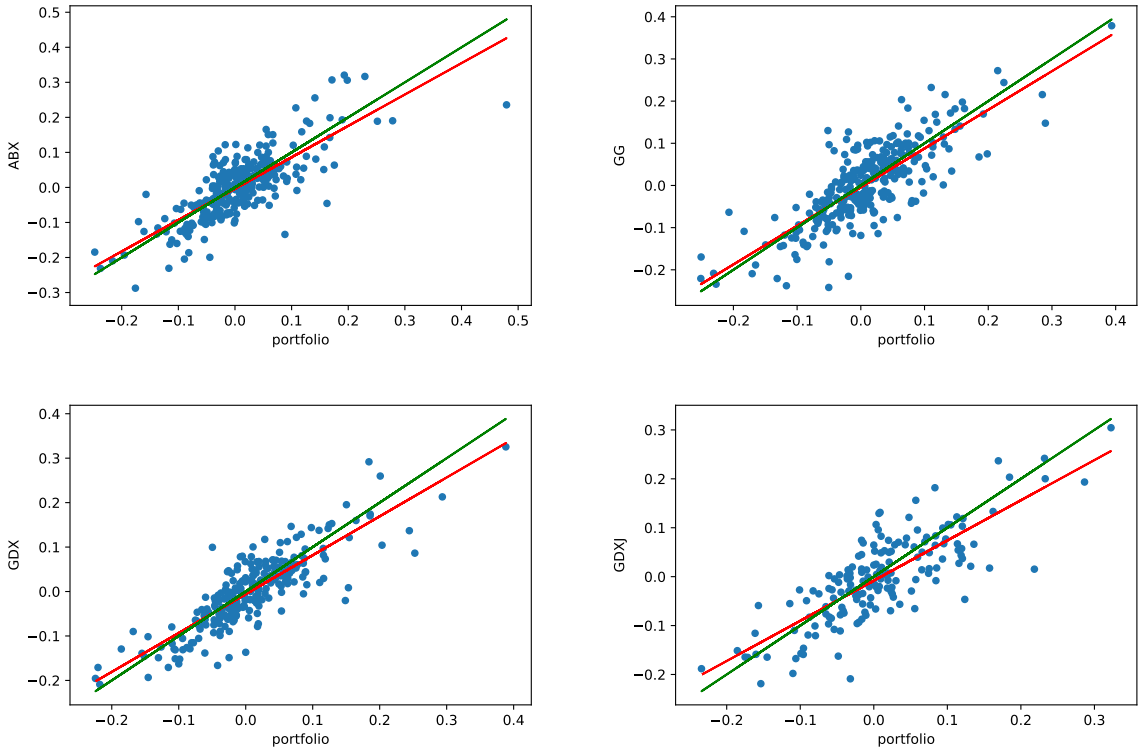

Figure 3: Plot of replicating portfolio returns (portfolio) vs gold miner equity returns (ticker). The red line represents the regression line estimated by (2.4.2) and the green line represents scenario of perfect replication (the line $f(x) = x$). The gold miners from left to right, top to bottom are ABX, GG, GDX, and GDXJ. The replicating portfolios are constructed by lagging the short-term $\beta_{GLD,t,j}$ and $\beta_{Mkt,j}$ coefficients by one week.

observe that about 65%-70% of the variance of gold miners in our sample can be explained by the returns of our replicating portfolio, which are spanned by two factors: gold and the market return. If our portfolio is successful, we would expect $\alpha \equiv 0$ and $\beta_{portfolio,j} \equiv 1$. Thus, we run the two sided t-test for $\alpha_j \neq 0$ and $\beta_{portfolio,j} \neq 1$. In fact, we discover that the α at the individual gold miner level are statistically insignificant, but at the ETF level, the α are consistently negative and significant, at a rate of about -0.58% per week. The portfolio level significance is most likely due to lower ETF volatility relative to that of single stocks, allowing for more precise point estimation. Furthermore, while the replicating portfolio should vary exactly one to one with the gold miner, we consistently find that the gold miners are less leveraged than the model might predict. In fact, we observe an average loading on

the portfolio of less than 0.90.

How can we explain the consistently negative α and low covariation with the replicating portfolio? Suppose that the firm owns a real option which they choose to exercise when they observe their stock covaries too much with gold prices. In practice, gold miners could buy put options, sell longer term futures or cut costs by firing workers and closing down mines. By exercising these options, the firm would in fact execute a regime change, so that the magnitude of the previously estimated implied leverage coefficient $\beta_{GLD,t,j}$ would become too large relative to the actual future $\beta_{GLD,t+\Delta t,j}$. Because the replicating portfolio cannot fully internalize this regime change for at least 25 business days (the length of our rolling training samples), the portfolio construction method would lead to portfolios which are too leveraged with respect to physical gold. However, hedging gold price risk is quite costly; if the managers do not have superior information about future gold prices then any hedging will result in a negative alpha penalty.

Figure 3 compares the difference between the anticipated relationship of full replication (green line) vs the actual performance of the replicating portfolio (red line). In particular, we find that the replicating portfolio declines moderately more than the actual gold miner during periods of negative gold returns, while the replicating portfolio significantly outperforms during periods of high gold prices. In other words, firms sacrifice large upward potential gains when gold prices gain in exchange for small relative gains when gold prices fall, suggesting that the cost of reducing leverage is paid through negative alpha relative to the replicating portfolio Finally, since gold has on average a positive return during the period under consideration, then the effects of holding and exercising these additional real options ends up generating a small negative alpha!

2.5 Estimating Model Parameters with Kalman Filter

In this section we present an application of our model, focusing on estimating the firm implied gold leverage parameters from the replicating portfolio for our model. In particular, we demonstrate a way to smooth the estimated dynamic factor loadings from Section 2.4 by estimating a Kalman Filter derived from the real options framework of Section 2.3.

So far, we have constructed a procedure to replicate the returns of gold miner equity prices, using only information which was available at the time of portfolio construction. Moreover, under the real options model, this portfolio should contain time-varying loadings on physical gold. Previously, we estimated these dynamic loadings using short-term rolling linear regressions. However, due to the low number of observations per rolling window, although estimation is consistent under OLS assumptions, the estimator on β_{GLD} has extreme variation. In this section, we demonstrate how under the real options model, the factor loadings follow a linear update rule, which allows us to smooth the OLS estimates with a Kalman Filter. Thus, by constraining the evolution of β_{GLD} to obey the real options model of Section 2.3, we obtain a more efficient estimator of the factor loadings.

Let S_t denote the gold price again, and assume we only have one gold miner stock. In order to analyze the implied gold leverage dynamics of gold miner stocks, we need to have an accurate estimate of the time series $\beta_{GLD,t} \equiv \beta(S_t)$, over $t \geq 0$. While our short rolling regressions can generate estimates of $\beta(S_t)$, the estimates are extremely noisy and vary quite substantially over even a single week. Therefore, we wish to extract the true $\beta(S_t)$ by estimating the noisy parameters $\mathbf{z}_{t_i} \equiv \beta(S_{t_i})$ with short-window rolling regressions. We do this by reframing our model within the context of the Extended Kalman Filter (see e.g. Brown and Hwang (1997) for a description of the Kalman Filter.)

Suppose that the true model for $\beta(S_t)$ follows (2.3.8). Discretizing the Ito process for

$\beta(S_t)$,

$$
\begin{aligned}
d\beta(S_t) &= \beta'(S_t)\left(dS_t - \beta\sigma^2 S_t dt\right), \\
\beta(S_{t_i}) &= \beta(S_{t_{i-1}}) + \beta'(S_{t_{i-1}}) \times \left(\Delta S_{t_i} - \beta(S_{t_{i-1}})\sigma^2 S_{t_{i-1}}\Delta t\right).
\end{aligned} \tag{2.5.1}
$$

At time t_i, the variables $\beta(S_{t_{i-1}})$, ΔS_{t_i}, $\beta(S_{t_{i-1}})$, and $S_{t_{i-1}}$ are all known. We take σ^2, the volatility of the gold price, as the implied volatility of an ATM 3M to maturity gold futures option and $\Delta t \equiv 1/252$. It remains to calculate $\beta'(S_{t-1})$. Applying Ito's Formula to $\beta(S)$ reveals

$$
\begin{aligned}
d\beta'(S_t) &= \beta(S_t)\beta'(S_t)\left(-2\frac{dS_t}{S_t} + \sigma^2(2\beta(S_t)+1)dt\right) - \sigma^2 S_t\left(\beta'(S_t)\right)^2 dt \\
\beta'(S_{t_i}) &= \beta'(S_{t_{i-1}}) + \beta(S_{t_{i-1}})\beta'(S_{t_{i-1}})\left(-2\frac{\Delta S_{t_i}}{S_{t_{i-1}}} + \sigma^2(2\beta(S_{t_{i-1}})+1)\Delta t\right) \\
&\quad - \sigma^2 S_{t_{i-1}}\left(\beta'(S_{t_{i-1}})\right)^2 \Delta t
\end{aligned}
$$

Thus, we can define a state vector $\mathbf{x}$, with white noise $\mathcal{N}(0, Q_{t_i})$ where

$$
\begin{aligned}
\mathbf{x}_{t_i} &= \left(\beta_{S_{t_i}}, \beta'(S_{t_i})\right)^T, \\
\mathbf{Q}_{t_i} &= \begin{pmatrix} S_{t_i}^2 & -2\beta(S_{t_i})S_{t_i} \\ -2\beta(S_{t_i})S_{t_i} & 4\beta(S_{t_i})^2 \end{pmatrix} \times \left(\beta'(S_{t_i})\right)^2 \sigma^2 \Delta t.
\end{aligned}
$$

In other words, we choose the betas and partials of betas with respect to the gold price as our state space $\mathbf{x}$. Each state evolves with error equal to the instantaneous quadratic covariation of the process $\mathbf{Q}$. Finally, the predicted update function $f(x)$ is given by (2.5.1).

Define the 2×2 covariance transition matrix, the 2×1 observation matrix, and the 1×1

observation error matrix as

$$\mathbf{F}_{t_i} = \begin{pmatrix} 1 - \beta'(S_{t_i})\sigma^2 S_{t_i}\Delta t & \Delta S_{t_i} - \beta(S_{t_i})\sigma^2 S_{t_i}\Delta t \\ \beta'(S_{t_i})\left(-2\frac{\Delta S_{t_i}}{S_{t_i}} + \sigma^2(4\beta(S_{t_i})+1)\Delta t\right) & 1 + \beta(S_{t_i})\left(-2\frac{\Delta S_{t_i}}{S_{t_i}} + \sigma^2(2\beta(S_{t_i})+1)\Delta t\right) \\ & -2\sigma^2 S_{t_i}\beta'(S_{t_i})\Delta t \end{pmatrix}$$

$\mathbf{H}_{t_i} = (1,0)^T$

$\mathbf{R}_{t_i} = \text{Standard Error}^2_{\beta_{GLD}}(t_i)$.

In other words, $\mathbf{F}$ is an updating matrix for the covariance matrix of errors, assuming our model and state space specification is correct. $\mathbf{H}$ reflects the fact that only $\beta(S_t)$ is observable through our short-window rolling regressions, while $\beta'(S_t)$ remains a latent variable. Finally, we choose the scalar measurement error $\mathbf{R}$ to be the standard error attached to the estimates of $\beta(S_t)$ from our rolling regressions (2.4.1). Thus, the Kalman Filter procedure is

Predict

$$\begin{aligned} \text{Predicted state estimate: } \hat{\mathbf{x}}_{t_i|t_{i-1}} &= f(\hat{\mathbf{x}}_{t_{i-1}|t_{i-1}}), \\ \text{Predicted covariance estimate: } \mathbf{P}_{t_i|t_{i-1}} &= \mathbf{F}_{t_{i-1}}\mathbf{P}_{t_{i-1}|t_{i-1}}\mathbf{F}^T_{t_{i-1}} + \boldsymbol{Q}_{t_{i-1}}, \end{aligned}$$

Update

$$\begin{aligned} \text{Innovation or measurement residual: } \tilde{\mathbf{y}}_{t_i} &= \mathbf{z}_{t_i} - \mathbf{H}^T_{t_i}\hat{\boldsymbol{x}}_{t_i|t_{i-1}}, \\ \text{Innovation (or residual) covariance: } \mathbf{S}_i &= \mathbf{H}^T_{t_i}\mathbf{P}_{t_i|t_{i-1}}\mathbf{H}_{t_i} + \boldsymbol{R}_{t_i}, \\ \textit{Near-optimal} \text{ Kalman gain: } \mathbf{K}_{t_i} &= \mathbf{P}_{t_i|t_{i-1}}\mathbf{H}_{t_i}\boldsymbol{S}^{-1}_{t_i}, \\ \text{Updated state estimate: } \hat{\mathbf{x}}_{t_i|t_i} &= \hat{\mathbf{x}}_{t_i|t_{i-1}} + \mathbf{K}_i\tilde{\boldsymbol{y}}_{t_i}, \\ \text{Updated covariance estimate: } \mathbf{P}_{t_i|t_i} &= \mathbf{P}_{t_i|t_{i-1}}(\mathbf{I} - \mathbf{H}_{t_i}\mathbf{K}^T_{t_i}), \end{aligned}$$

where $\mathbf{x}$ is the (possibly hidden) state variable, f is the state update equation, $\mathbf{Q}$ is the

covariance matrix of the state variables, $\mathbf{H}$ is the observation matrix, $\mathbf{F}$ is the covariance update matrix, and $\mathbf{R}$ is the estimation error, all of which as previously defined.

Having defined all the parameters of the Kalman Filter, we apply the filtering procedure at a daily frequency over the observed lifetime of our various ETFs and gold miner stocks (see Table 1 for a list of inception dates.) Figure 4 compares the improvement of the Kalman Filtered implied leverage time series and the simple moving average (SMA) smoothed time series over the raw regression coefficients. For the SMA model, we experimented with different moving time windows, settling on a window of 200 days so that the SMA coefficients have a similar degree of volatility as the filtered estimates. While we did experiment with shorter windows, we found that the resulting series was too similar to the original raw time series, necessitating longer smoothing windows for the SMA method.

First, note that the SMA coefficients are less volatile than the raw estimated parameters. While SMA gains in less volatility relative to the raw estimates, it loses in missing information to the filtered estimates. For example in mid-2013, gold prices fell and the implied leverage of gold mining firms rose to an all time high. The Kalman Filter captures the regime change in 2013 almost immediately, but the SMA model does not pick it up until the beginning of 2014. In addition, for GDX and GDXJ the SMA model misses a regime change in mid-2009 when gold prices rose while the Kalman Filter picks it up much faster. Therefore, while long window SMA smoothers are less complex and adequate substitutes during times of stable gold prices, the Kalman Filter outperforms when gold prices are more volatile, since it can capture instantaneous changes in implied leverage.

However, most of the time there is not a huge difference between the Kalman Filtered implied leverage coefficients and SMA smoothed parameters, as long as we use a long enough window. The main advantage of the Kalman Filter over simple smoothing methods is that it not only infers the true process for β_{GLD}, but it also preserves some volatility of our dynamic factor loadings. On the other hand, while the SMA procedure certainly is less complex and less prone to model risk, it requires a very long window to generate an estimate as smooth

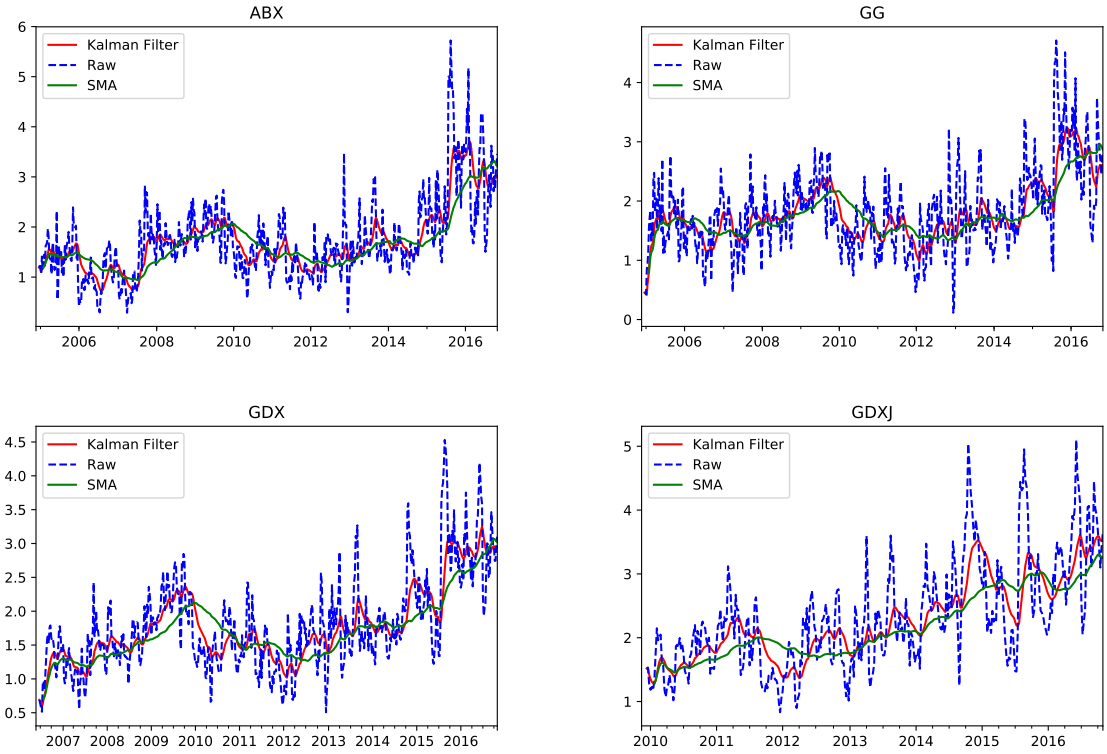

Figure 4: Plot of raw β_{GLD} vs Kalman Filtered β_{GLD} vs Simple Moving Average β_{GLD}. The Kalman Filter start end dates for each security were given by Table 1. We hold out 100-days of data to train the Kalman Filter initially. In addition, the SMA uses a moving window of 200 days. The time axis has been converted to weekly frequencies for illustration purposes due to the extreme variations in raw time series. The gold miners from left to right, top to bottom are ABX, GG, GDX, and GDXJ.

as the Kalman Filter's, leading to too much information loss and long lags in the estimates.

Overall, the main improvement of the filtering procedure is over the raw estimated parameters. Relative to the raw parameters, the filtered series has significantly less volatility and much more plausible values. For example, the maximum value for $\beta(S_t)$ in the unfiltered version for ABX exceeds 5.5, which is implausible since ABX has never displayed $5.5 \times \sigma_{GLD} \approx 60\%$ volatility in its entire trading lifetime! However, the maximum such value for the filtered series never exceeds 3.5, which is a much more reasonable estimate.

2.6 Testing Predictions for Gold Miners' Implied Leverage

In this section we analyze the accuracy of the predictions made by the real options model for gold miners as applied to our gold miner stock portfolio, focusing on our model's explanatory power of firm implied gold leverage. We perform an empirical test of our real options model by analyzing the effect of gold prices on firm leverage, using monthly observations of the filtered estimates for the $\beta(S_t)$ estimates. Overall, we find that the real options model can explain much of the time series variation of implied gold leverage, suggesting that gold miner stocks really do behave like real options on gold.

Having developed a method to robustly estimate the factor loadings themselves, we can now empirically investigate our model's predictions about how changes in gold prices affect firm leverage. In particular, recall that at each time t, we have inferred firm j's dependence on gold prices $\beta_{GLD,t,j}$ by carrying out a rolling, exponentially weighted regression (2.4.1). Now that we have an unbiased, smoothed estimate of the implied leverage parameters via the Kalman Filter, we can test how the firm leverage depends on gold prices, as our real options model would predict. Figure 5 illustrates this relationship for the four gold miner ETFs/stocks in our sample. Notice that in most circumstances, the relationship between physical gold prices and the firm implied gold leverage is quite muted, with β_{GLD} varying around some constant level. However, as the gold price declines past a critical level, firm price declines and leverage increases rapidly. Similarly, around this critical level, when the gold price increases, the firm price decreases and the leverage falls rapidly as well. Recall that Figure 2 predicts that the firm's implied gold leverage only becomes extremely sensitive around the critical gold price which pushes the firm close to default. Thus, these summary figures suggest that our real options model should have strong explanatory power for understanding gold miners' implied leverage.

While the general pattern between gold prices and firm implied leverage can be eyeballed

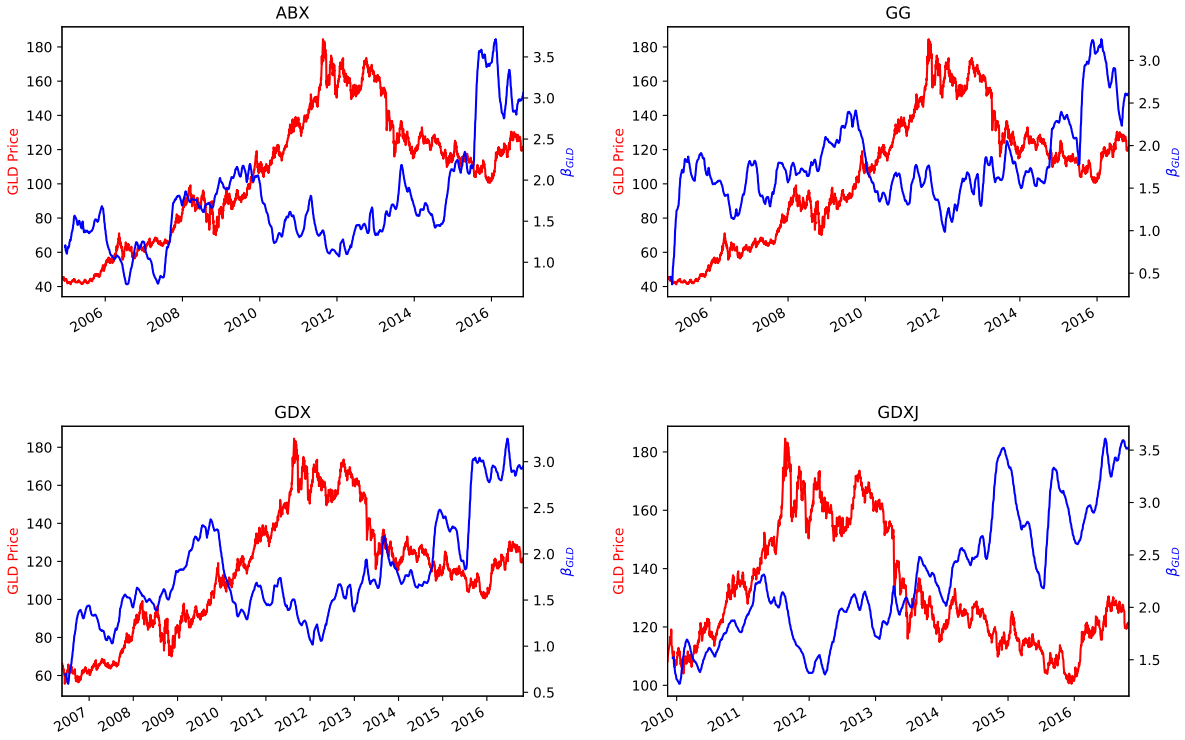

Figure 5: Plot of β_{GLD} vs Gold miner equity prices. The β_{GLD} coefficients shown have been smoothed by a Kalman Filter (see Section 2.5). The gold miners from left to right, top to bottom are ABX, GG, GDX, and GDXJ.

from Figure 5, we will need a detailed model to understand the precise relationship. Thus, in this section we test the proposition that the real options model can explain the drivers behind firm implied gold leverage. Equation (2.3.7) predicts a relationship between the estimated coefficients β_{GLD} and the corresponding equity and gold prices J_t and S_t respectively. Therefore, after some rearrangement, we have for each gold miner indexed by j the relationship

$$\begin{aligned} \ln \beta_{GLD,j,t} &= \gamma \ln S_t - \ln J_{t,j} + \gamma A, \\ \ln \beta_{GLD,j,t} &= \gamma_0 \ln S_t - \gamma_1 \ln J_{t,j} + \alpha_j + \epsilon_{t,j}, \end{aligned} \tag{2.6.1}$$

where the second equation specifies a regression to estimate the first relationship. In particular, we regress the gold price S_t, the gold miner equity price $J_{t,j}$ on the implied firm leverage

Security Name (Ticker)	R^2	γ_0	γ_1	α
Barrick Gold (ABX)	0.281607	0.257169**	−0.432529***	0.711987
Goldcorp (GG)	0.195562	0.327015**	−0.487025***	0.638916
Gold Miners ETF (GDX)	0.331800	0.228697**	−0.532948***	1.341798
Junior Gold Miners ETF (GDXJ)	0.292139	0.123082*	−0.284187**	1.828136

Table 3: Performance of real options model using monthly observations. Results from the regression (2.6.1). The tests for γ_1 are two-sided t-tests centered at -1, while the test for γ_0 are one-sided t-tests centered at zero. White standard errors are used to calculate t-statistics. The symbols *, **, and *** indicate significance at the 10%, 5% and 1% levels respectively. The tests for statistical significance with respect to α are omitted for brevity.

$\beta_{GLD,j,t}$, which was estimated using the Kalman Filter.

If gold miners were equivalent to real options on gold then, we should have $\gamma_0 > 0$ and $\gamma_1 = -1$. In other words, for every \$1 increase in the log stock price, its log implied gold leverage by 1. Furthermore, for every \$1 increase in the log gold price, the log implied leverage with respect to gold should increase by γ which is given by Theorem 2.3.2. In particular, the regression (2.6.1) represents a test of the real gold options model.

Table 3 displays the result of our regressions. The R^2 for the regressions is about 30%, suggesting a strong fit for our real options model. Although 30% may not seem very impressive at first, we note that in comparison Tufano (1996) used about a dozen firm level variables to estimate the firm's dependence on β_{GLD}, finding an average R^2 of only 19% per firm. Therefore without considering the impact of firm level decisions, our much sparser model has stronger explanatory power than the previous results in the literature. Unfortunately, our model is less interpretable since the two independent variables in our model (gold price and gold miner equity) are themselves highly correlated. Thus, while this regression can serve as a test for the real options model, it cannot dissect the factors' effects on the fluctuations of the leverage coefficients.

The main tests for the real options model are the two sided test $\gamma_1 \neq -1$ and the one sided test $\gamma_0 > 0$. We choose the one sided form, since in the real options model, we must have $\gamma_0 \geq 0$. In most of the regressions, we have $\gamma_0 > 0$ at the 5% significance level,

demonstrating that holding gold miner prices the same, then higher gold prices do in fact generate higher leverage coefficients. However, the junior gold miner ETF (GDXJ) has an insignificant coefficient on γ_0. Finally, the tests for $\gamma_1 \neq -1$ reject the null hypothesis for every single stock, with all the γ_1 coefficients being too small. Thus, a firm's dependence on gold prices is much smaller than the real options model suggests, since the β_{GLD} coefficients increase slower than one to one with the decline of log gold miner equity prices. This result confirms our previous analysis with the replicating portfolios, which finds that the gold miner equities are much less levered than their replicating portfolios would predict. In other words, since firms may have extra firm-level options such as mine closure, layoffs, or hedging with futures and options, their equity can become less volatile than the real option model suggests when gold prices decline.

If gold miner firms were just junior claims to gold inside a mine, then implied leverages should act similarly to that of a gold option. Although we find that modeling gold miner stocks as gold call options can explain over 30% of the implied leverage variation, ultimately gold prices alone are insufficient to explain local implied leverage. In particular, firm implied gold leverage is often much lower than the real options model would predict, likely because firms can dampen their volatility by exercising management level real options that are outside the market's observation. Furthermore, the real options model has a much worse fit for junior gold miners, likely because they are exposed to more idiosyncratic risks. However, our overall conclusion remains the same: gold mining stocks behave like real options on gold, albeit with significant idiosyncratic risk during periods of price declines.

2.7 Conclusion

This chapter provides both theoretical and empirical studies on the drivers of gold miner stock returns. By studying a real options model, we confirm the widely held practitioner's view that gold miner stocks behave more like options on gold rather than standard equities.

Our model can explain many anomalies in the literature about gold miners' returns by quantifying the main drivers behind the fluctuations in implied gold leverage.

Motivated by our theoretical results, we construct a dynamic replicating portfolio consisting of two factors - spot gold and the market portfolio - in order to explain gold miner equity returns. After decomposing the return into a market replicable component and an idiosyncratic component, we demonstrate first that the market replicable component has time varying loadings with respect to gold, but static loadings with respect to the equity market portfolio. Second, gold miner stock returns are consistently lower than our model predicts and covary less than expected relative to spot gold returns. Overall, our results suggest that firms hold real options allow the firm to hedge their exposure to gold prices during times of low prices, but these options come at the expense of lower average returns when gold prices recover.

For future research, a natural direction is to investigate if similar findings hold more generally by applying the same pricing model and estimation methodology to other commodity producers, such as oil, natural gas, agricultural products, and other precious metals. Other than working with the convenience yield model, it may be appropriate to consider mean-reverting models for some commodities and study the optimal production/investment strategies (Cortazar and Schwartz, 1997; Leung et al., 2014; Guo and Leung, 2017). Finally, our model can be applied to develop trading strategies that account for the factor loadings and alpha of gold miner equities, we can easily construct a market-neutral portfolio of gold miners to capture the idiosyncratic component of gold miner returns.

Chapter 3

Understanding the Returns of Commodity LETFs

Commodity exchange-traded funds (ETFs) are a significant part of the rapidly growing ETF market. They have become popular in recent years as they provide investors access to a great variety of commodities, ranging from precious metals to building materials, and from oil and gas to agricultural products. In this chapter, we analyze the tracking performance of commodity leveraged ETFs and discuss the associated trading strategies. It is known that leveraged ETF returns typically deviate from their tracking target over longer holding horizons due to the so-called volatility decay. This motivates us to construct a benchmark process that accounts for the volatility decay, and use it to examine the tracking performance of commodity leveraged ETFs. From empirical data, we find that many commodity leveraged ETFs underperform significantly against the benchmark, and we quantify such a discrepancy via the novel idea of *realized effective fee*. Finally, we consider a number of trading strategies and examine their performance by backtesting with historical price data.

3.1 Introduction

The advent of commodity exchange-traded funds (ETFs) has provided both institutional and retail investors with new ways to gain exposure to a wide array of commodities, including precious metals, agricultural products, and oil and gas. All commodity ETFs are traded on exchanges like stocks, and many have very high liquidity. For example, the SPDR Gold Trust ETF (GLD), which tracks the daily London gold spot price, is the most traded commodity ETF with an average trading volume of 8 million shares and market capitalization of US $31 billion in 2013.[1]

Within the commodity ETF market, some funds are designed to track a constant multiple of the daily returns of a reference index or asset. These are called leveraged ETFs (LETFs). An LETF maintains a constant leverage ratio by holding a variable portfolio of assets and/or derivatives, such as futures and swaps, based on the reference index. For example, the Dow Jones U.S. Oil & Gas Index (DJUSEN) or the Dow Jones U.S. Basic Materials Index (DJUSBM) and their associated ETFs track the stocks of a basket of commodities producers, as opposed to the physical commodity prices. On the other hand, most LETFs are based on total return swaps and commodity futures. The most common leverage ratios are ± 2 and ± 3, and LETFs typically charge an expense fee. Major issuers include ProShares, iShares, VelocityShares and PowerShares (see Table 4). For example, the ProShares Ultra Long Gold (UGL) seeks to return 2x the daily return of the London gold spot price minus a small expense fee. One can also take a bearish position by buying shares of an LETF with a negative leverage ratio. The ProShares Ultra Short Gold (GLL) is an inverse LETF that tracks -2x the daily return of the London gold fixing price. LETFs are a highly accessible and liquid instrument, thereby making them attractive instruments for traders who wish to gain leveraged exposure to a commodity without borrowing money or using derivatives.

For a long LETF, with a leverage ratio $\beta > 0$, the fund must add to a winning position in

[1] According to ETF Database website (http://www.etfdb.com/compare/volume).

a bull market to maintain a constant leverage ratio. On the other hand, during a bear market, the fund must sell its losing positions to maintain the same leverage ratio. Similar arguments can be made for short (or inverse) LETFs ($\beta < 0$). As a consequence, LETFs can potentially outperform β times its reference during periods of market trending. However, should the LETF exhibit high volatility but no significant movement in price over a period of time, the constant daily re-balancing would cause the fund to decline in value. Therefore, LETFs can be viewed as long momentum but short volatility, and the value erosion due to realized variance of the reference is called *volatility decay* (see Avellaneda and Zhang (2010); Cheng and Madhavan (2009); Dobi and Avellaneda (2012)). This raises the important question of how well do LETFs perform over a long horizon.

Since their introduction to the market, LETFs a number of criticisms from both practitioners and regulators.[2] Some are concerned that the returns of LETFs exhibit some discrepancies from the goals stated in their prospectuses. In fact, some issuers provide warnings that LETFs are unsuitable for long-term buy-and-hold investors.

Many existing studies focus on equity-based ETFs and their leveraged counterparts. For example, Avellaneda and Zhang Avellaneda and Zhang (2010) study the price behavior and discuss the volatility decay of equity LETFs in different sectors. They find minimal 1-day tracking errors among the most liquid equity ETFs. They explain that an equity LETF can replicate the leveraged returns of its reference through a dynamic portfolio consisting of the component equities.

In contrast, commodities are unique because the physical assets cannot be stored easily. As such, ETF issuers are required to replicate through either warehousing[3], which is very costly, and thus uncommon except for precious metals such as silver and gold, or trading futures with multiple counterparties (see Guedj et al. (2011)). Since the reference indices

[2]In 2009, the SEC and FINRA issued an alert on the risk of leveraged ETFs on `http://www.sec.gov/investor/pubs/leveragedetfs-alert.htm`.

[3]For more details on the issue of storage cost for commodity ETFs, we refer to the Morningstar Report: "An Ugly Side to Some Commodity ETFs" by Bradley Kay, August 19, 2009.

may represent the spot prices of physical commodities, futures-based commodity ETFs may fail to track their reference indices perfectly and their tracking performance is subject to the fluctuation and term structure of futures prices. On top of that, most commodity LETFs use over-the-counter (OTC) total return swaps with multiple counterparties to generate the required leverage ratios. The lower liquidity of OTC contracts and counterparty risk can contribute to additional tracking errors. As we show in this chapter, tracking errors can seriously affect the long-term fund performance of LETFs.

In a related work, Murphy and Wright Murphy and Wright (2010) perform a t-test based on 1-day returns to determine if any commodity LETF has a non-zero tracking error. They conclude that all LETFs have a very good daily tracking performance. However, they do not conduct the analysis over a longer horizon, or account for the volatility decay. There is also no discussion of trading strategies there. On the other hand, Guedj et al. Guedj et al. (2011) discuss the difficulties faced by an ETF provider in replicating a commodity index using futures. In particular, they point out that the term structure of futures may lead to large deviations between the ETF price and the spot price of a commodity.

In this chapter, we analyze the tracking performance of commodity leveraged ETFs. Through a series of regression analyses, we illustrate how the returns of commodity LETFs deviate from the reference returns multiplied by the leverage ratio over different holding periods. In particular, the average tracking error tends to turn more negative over a longer horizon and for higher leveraged ETFs. With in mind that realized variance of the reference can erode the LETF value, we examine the over/under-performance of LETFs with respect to a benchmark that incorporates the effect of volatility decay. From empirical data, we find that many commodity leveraged ETFs in our study underperform significantly against the benchmark, and we quantify such a discrepancy by introducing the *realized effective fee*. Finally, we consider a static trading strategy that involves shorting two LETFs with leverage ratios of different signs, and study its performance and dependence on the realized variance of the reference. We find that the resulting portfolio is always long realized variance both

LETF	Reference	Underlying	Issuer	β	Fee	Inception
SLV	SLVRLN	Silver Bullion	iShares	1	0.50%	04/21/2006
AGQ	SLVRLN	Silver Bullion	ProShares	2	0.95%	12/01/2008
ZSL	SLVRLN	Silver Bullion	ProShares	-2	0.95%	12/01/2008
USLV	SPGSSIG	Silver Bullion	VelocityShares	3	1.65%	10/13/2011
DSLV	SPGSSIG	Silver Bullion	VelocityShares	-3	1.65%	10/14/2011
GLD	GOLDLNPM	Gold Bullion	iShares	1	0.40%	11/18/2004
UGL	GOLDLNPM	Gold Bullion	ProShares	2	0.95%	12/01/2008
GLL	GOLDLNPM	Gold Bullion	ProShares	-2	0.95%	12/01/2008
UGLD	SPGSGCP	Gold Bullion	VelocityShares	3	1.35%	10/13/2011
DGLD	SPGSGCP	Gold Bullion	VelocityShares	-3	1.35%	10/14/2011
IYE	DJUSEN	Oil & Gas	iShares	1	0.48%	06/12/2000
DDG	DJUSEN	Oil & Gas	ProShares	-1	0.95%	06/10/2008
DIG	DJUSEN	Oil & Gas	ProShares	2	0.95%	01/30/2007
DUG	DJUSEN	Oil & Gas	ProShares	-2	0.95%	01/30/2007
DBO	DBOLIX	WTI Crude Oil	PowerShares	1	0.75%	01/05/2007
UCO	DJUBSCL	WTI Crude Oil	ProShares	2	0.95%	11/24/2008
SCO	DJUBSCL	WTI Crude Oil	ProShares	-2	0.95%	11/24/2008
UWTI	SPGSCLP	WTI Crude Oil	VelocityShares	3	1.35%	02/06/2012
DWTI	SPGSCLP	WTI Crude Oil	VelocityShares	-3	1.35%	02/06/2012
IYM	DJUSBM	Building Materials	iShares	1	0.48%	06/12/2000
SBM	DJUSBM	Building Materials	ProShares	-1	0.95%	03/16/2010
UYM	DJUSBM	Building Materials	ProShares	2	0.95%	01/30/2007
SMN	DJUSBM	Building Materials	ProShares	-2	0.95%	01/30/2007

Table 4: A summary of the 23 LETFs studied in this chapter, arranged by commodity type and then leverage. Notice that the non-leveraged (1x) ETFs have the smallest expense fees, and LETFs with higher absolute leverage ratios, $|\beta| \in \{2, 3\}$, tend to have higher expense fees. Finally, notice that higher β LETFs are much more recent additions to the market.

theoretically and empirically, but is also exposed to the tracking errors associated with the two LETFs. We also backtest the strategy through examining its empirical returns over rolling periods.

The rest of the chapter is organized as follows. In Section 3.2, we analyze the returns of commodity LETFs over different holding periods and illustrate horizon dependence of tracking errors. In Section 3.3, we use a benchmark process that incorporates the realized variance of the reference to study the over/under-performance of each LETF. In Section 3.4, we discuss a static trading strategy and backtest using historical data. Section 3.5 concludes the chapter and points out a number of directions for future research.

3.2 Analysis of Tracking Error

We first compare the returns of LETFs and their reference indices. For every ETF, we obtain its closing prices and reference index values from Bloomberg for the period December 2008-May 2013. We then calculate the n-day returns from $n = \{1, 2, \ldots, 30\}$ using disjoint successive periods (e.g. the return over days 1-30 then returns over days 31-60 for 30-day returns). Let L_t be the price of an LETF and S_t be the reference index value at time t. For a given leverage ratio β, we compare the log-returns of the LETF to β times the log-returns of the corresponding reference index. This leads us to define the n-day tracking error at time t by

$$Y_t^{(n)} = \ln \frac{L_{t+n\Delta t}}{L_t} - \beta \ln \frac{S_{t+n\Delta t}}{S_t}, \tag{3.2.1}$$

where Δt represents one trading day. We explore the empirical distribution of the n-day tracking error, and then analyze the effect of holding horizon on the magnitude of tracking errors. We remark there are alternative ways to define tracking errors for ETFs. For example, one can consider the difference in relative returns as opposed to log-returns, or the root mean square of the daily differences (see Mackintosh and Lin (2010b)).

3.2.1 Regression of Empirical Returns

We conduct a regression between log-returns of the LETF and its reference index based on the linear model:

$$\ln \frac{L_t}{L_0} = \hat{\beta} \ln \frac{S_t}{S_0} + \hat{c} + \epsilon,$$

where $\epsilon \sim N(0, \sigma^2)$ is independent of the reference index value S_t, $\forall t \geq 0$. In other words, we run an ordinary least square 1-variable regression between the log-returns for every fixed horizon of n days. Then, we increase the holding period from 1 to 30 days, and observe how the regression coefficients vary.

We display the regression results in Figures 6 through 9 for log-returns over periods of

1, 5, 10, and 20 days. To avoid dependence among returns, we use disjoint time intervals to calculate returns. For example, we use $\frac{S_{20}}{S_0}, \frac{S_{40}}{S_{20}} \ldots$ and $\frac{L_{20}}{L_0}, \frac{L_{40}}{L_{20}} \ldots$ for 20-day log-returns as the inputs for the regression.

In Figure 6, the regression coefficient $\hat{\beta}$ for DIG ($\beta = 2$, oil & gas) increases from 2 to 2.1 as the holding period lengthens from 1 to 20 days. Although the coefficient of determination R^2 is close to 99% for up to 20 days, it is highest for 1-day returns. In Figure 7 for DUG ($\beta = -2$, oil & gas), one again observes $\hat{\beta}$ increasing, and R^2 decreasing. For DUG ($\beta = -2$, oil & gas), as n varies from 1 to 20, $\hat{\beta}$ increases from -2 to -1.66. As a result, this implies that DIG ($\beta = 2$, oil & gas) effectively gains leverage as the holding time increases, while DUG ($\beta = -2$, oil & gas) loses leverage compared to the advertised fund β.

On the other hand, UGL ($\beta = 2$, gold) and GLL ($\beta = -2$, gold) exhibit very different return behaviors. In Figure 8 the R^2 for UGL ($\beta = 2$, gold) is surprisingly worst for the shortest holding period of 1 day, whereas it increases to 95% over a holding period of 20 days. In Figure 9 for GLL ($\beta = -2$, gold), the R^2 increases from 35% to 96% when holding the fund from 1 to 20 days. Furthermore, the estimators $\hat{\beta}$ for UGL ($\beta = 2$, gold) and GLL ($\beta = -2$, gold) both slowly approach their advertised $\beta = \pm 2$. The variation of $\hat{\beta}$ for DIG ($\beta = 2$, oil & gas) and UGL ($\beta = 2$, gold) over different holding periods is summarized in Figure 10.

We observe that LETFs that track an illiquid reference, such as the gold bullion index GOLDLNPM, tend to have more tracking errors than those tracking a liquid index, such as the oil & gas index DJUSEN. The oil & gas commodity LETFs involve exchange-traded futures which are liquid proxy to the spot price. The gold and silver bullion LETFs consist of OTC total return swaps. The difficulty and higher costs replication using swaps, as well as infrequent (typically daily) update of the swaps' mark-to-market values can weaken the fund's tracking ability. For example, the 1-day regressions of UGL and GLL ($\beta = \pm 2$, gold) yield R^2 values less than 40%, while DIG and DUG ($\beta = \pm 2$, oil & gas) have 1-day R^2 values of over 90%. On the other hand, full physical replication yields the greatest R^2, with

examples of the non-leveraged gold and silver ETFs, GLD and SLV, respectively. Hence, the replication strategy can significantly affect a fund's tracking errors. A more precise understanding of the effectiveness of swaps, futures, and other replication strategies requires the full holdings history from the ETF provider, which is not publicly available at all times.[4]

In addition, the LETFs we studied have an increasingly negative constant coefficient $\hat{c}$ as the holding time increases. For example, over a holding period of 20-days, DUG ($\beta = -2$, oil & gas) has a 3% decay on returns compared to β times its reference index. We would expect this phenomenon, however, since the LETF would need to buy high and sell low, while the reference investor would simply hold his securities. Therefore, the longer the LETF is held, the more likely the fund will underperform against β times the reference index. As we will see in Section 3.3, the constant coefficient $\hat{c}$ depends on two factors, the expense fee charged by the issuer as well as the realized variance of the reference index.

Hence, with this simple linear model for LETF prices, we have observed that although LETFs safely replicate β times the reference over short holding periods, they begin to exhibit negative tracking error and deviations in their leverage ratios β as the holding time increases. Furthermore, we see that LETFs which attempt to track illiquid spot prices perform much more poorly than expected. We conclude that more factors must be considered when modeling LETF returns.

3.2.2 Distribution of Tracking Errors

As defined in (3.2.1), the tracking error is the difference between the LETF's log-return and the corresponding multiple of its reference index's log-return. In this section, we examine the distribution of the tracking error. This provides a picture of the LETF's efficiency in its stated goal of replicating the leveraged return of a reference index.

For the 23 LETFs in Table 5, we compute the mean μ and standard deviation σ for the

[4]For a detailed snapshot of the holdings for a proshares ETF, please see `http://www.proshares.com/funds/{XYZ}_daily_holdings.html` where $\{XYZ\}$ is the ETF ticker.

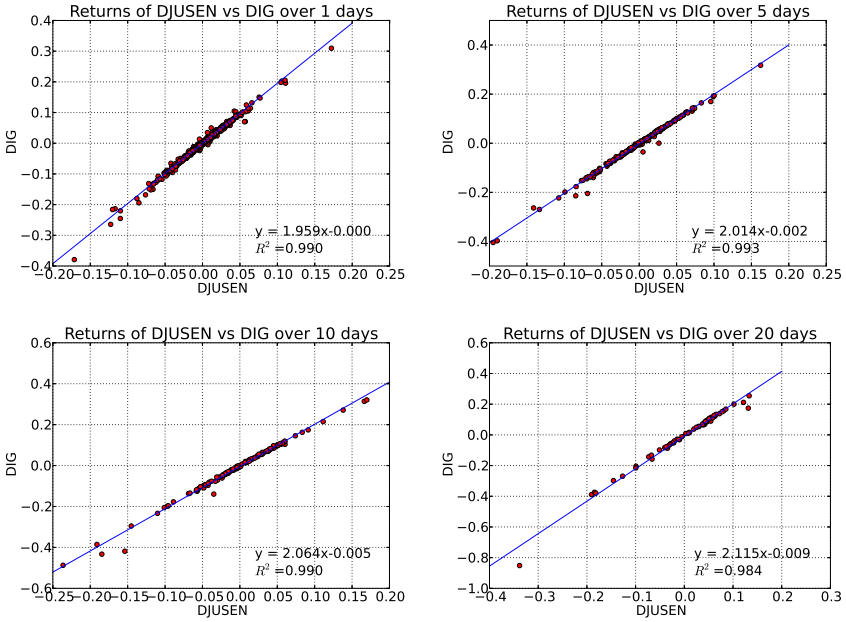

Figure 6: From top left to bottom right: regression of DJUSEN-DIG ($\beta = 2$, oil & gas) 1, 5, 10, 20-day log-returns. We consider disjoint periods from December 2008 to May 2013.

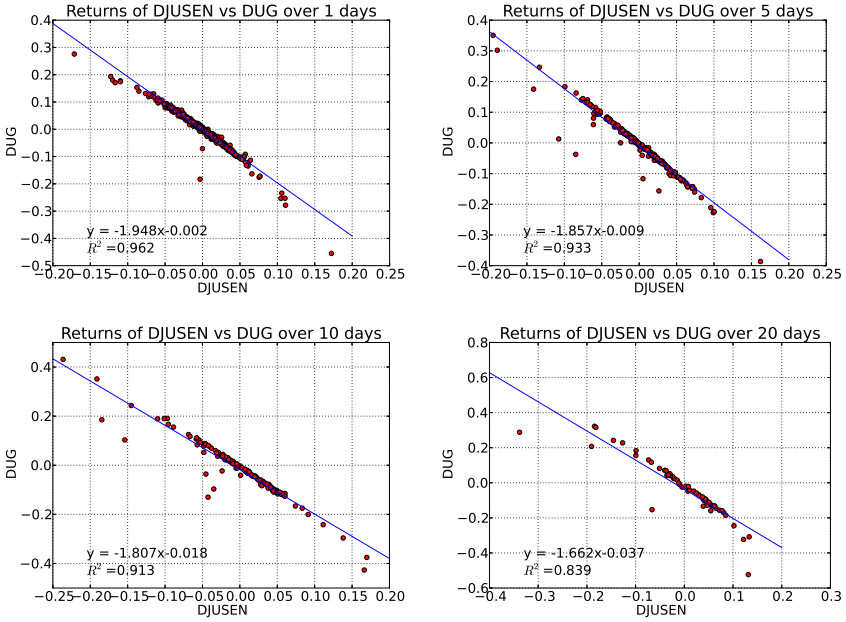

Figure 7: From top left to bottom right: regression of DJUSEN-DUG ($\beta = -2$, oil & gas) 1, 5, 10, 20-day log-returns. We consider disjoint periods from December 2008 to May 2013.

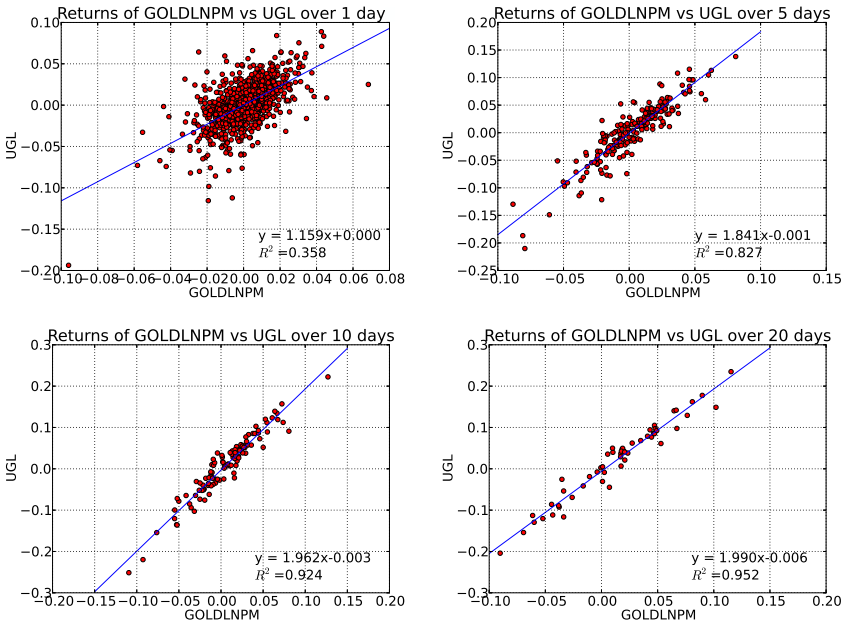

Figure 8: From top left to bottom right: regression of GOLDLNPM-UGL ($\beta = 2$, gold) 1, 5, 10, 20-day log-returns. We consider disjoint periods from December 2008 to May 2013.

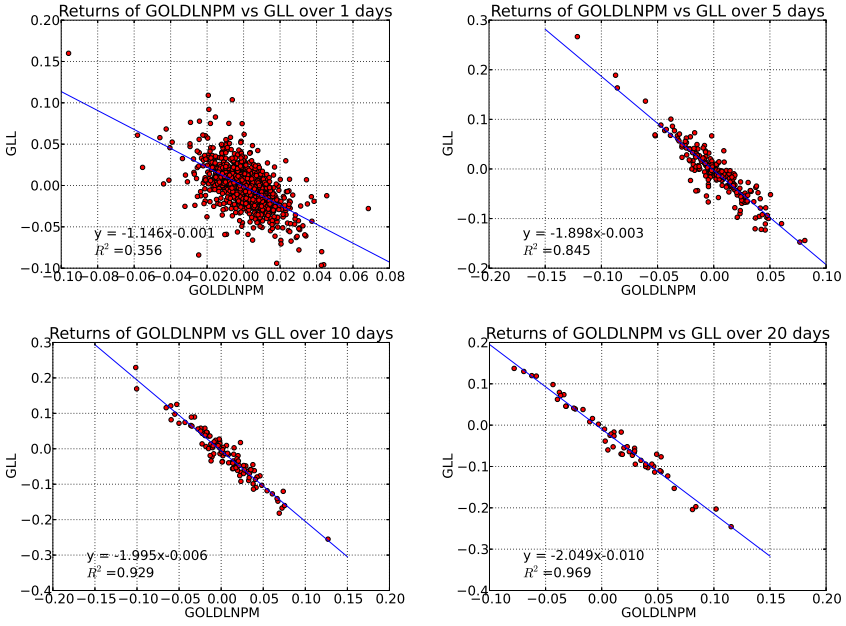

Figure 9: From top left to bottom right: regression of GOLDLNPM-GLL ($\beta = -2$, gold) 1, 5, 10, 20-day log-returns. We consider disjoint periods from December 2008 to May 2013.

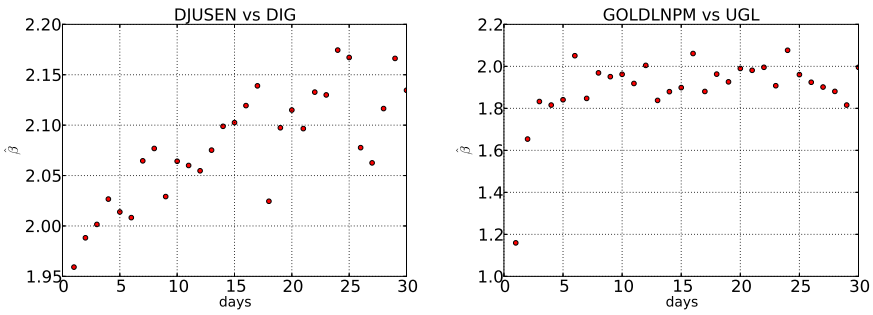

Figure 10: The estimated $\hat{\beta}$ from the regressions for DJUSEN-DIG ($\beta = 2$, oil & gas), and GOLDLNPM-UGL ($\beta = 2$, gold).

LETF	**Underlying**	β	μ	σ
SLV	Silver Bullion	1	0.0000	0.0302
AGQ	Silver Bullion	2	-0.0009	0.0539
ZSL	Silver Bullion	-2	-0.0022	0.0543
USLV	Silver Bullion	3	-0.0014	0.0231
DSLV	Silver Bullion	-3	-0.0027	0.0237
GLD	Gold Bullion	1	0.0000	0.0128
UGL	Gold Bullion	2	-0.0003	0.0221
GLL	Gold Bullion	-2	-0.0005	0.0221
UGLD	Gold Bullion	3	-0.0006	0.0134
DGLD	Gold Bullion	-3	-0.0010	0.0139
IYE	Oil & Gas	1	0.0000	0.0049
DDG	Oil & Gas	-1	-0.0008	0.0118
DIG	Oil & Gas	2	-0.0005	0.0044
DUG	Oil & Gas	-2	-0.0018	0.0087
DBO	WTI Crude Oil	1	0.0000	0.0070
UCO	WTI Crude Oil	2	-0.0006	0.0135
SCO	WTI Crude Oil	-2	-0.0016	0.0132
UWTI	WTI Crude Oil	3	-0.0008	0.0147
DWTI	WTI Crude Oil	-3	-0.0017	0.0178
IYM	Building Materials	1	0.0000	0.0020
SBM	Building Materials	-1	-0.0004	0.0065
UYM	Building Materials	2	-0.0005	0.0062
SMN	Building Materials	-2	-0.0022	0.0149

Table 5: Mean μ and standard deviation σ of the 1-day tracking error by commodity.

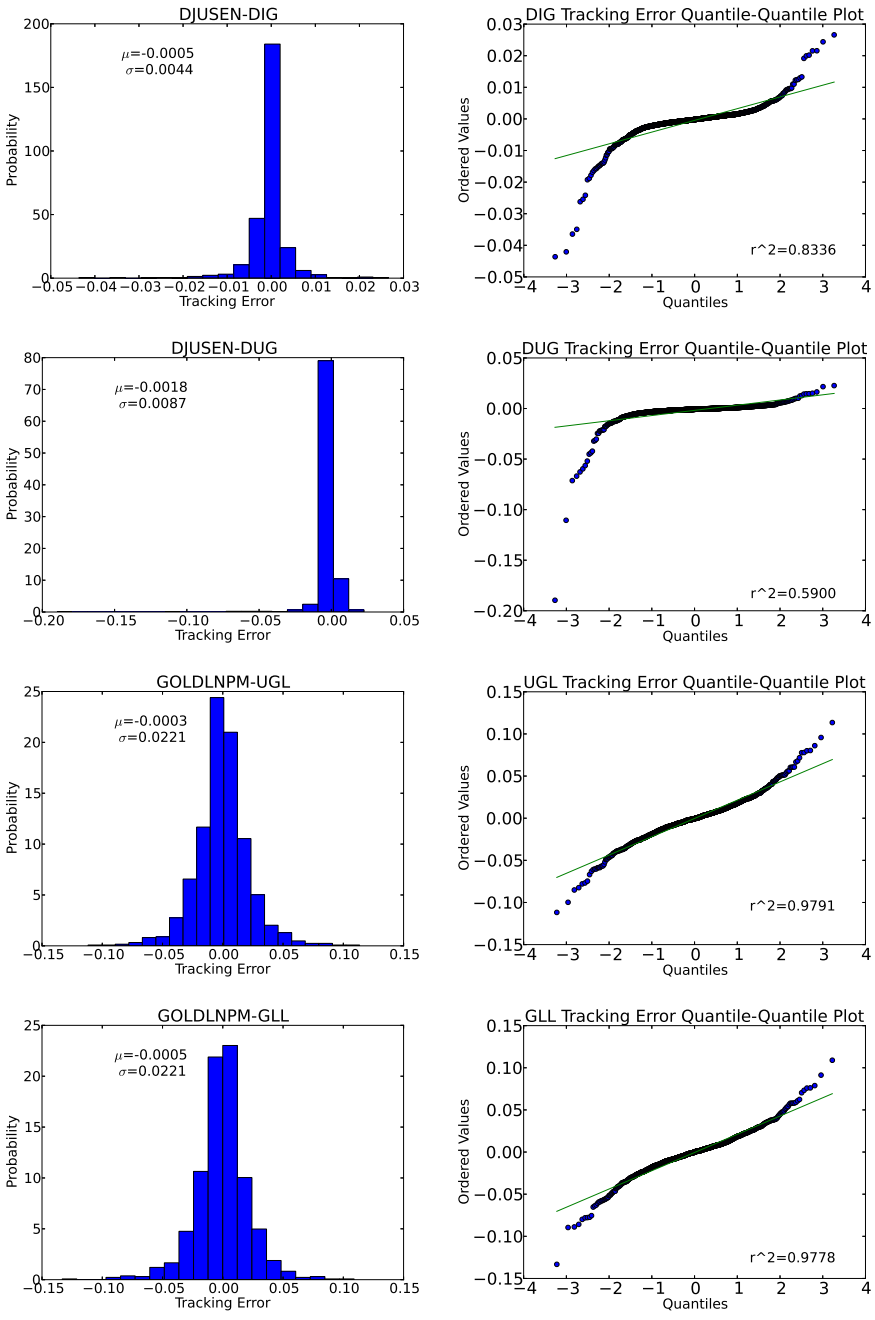

Figure 11: Histograms and QQ plots of 1-day tracking errors for DIG, DUG ($\beta = \pm 2$, oil & gas); UGL, GLL ($\beta = \pm 2$, gold) from top to bottom.

tracking errors using available price data during the period Dec 2008 to May 2013. For all these funds, the mean 1-day tracking error has $\mu \approx 0$, ranging from 0% to -0.27%. Therefore, all these LETFs on average successfully replicate the stated multiple β of the daily reference return, with a slight negative bias. In fact, many LETFs even continued to replicate returns over periods as long as 10 days. However, as the holding time increases, the average tracking error grows more negative, so that the LETF in fact underperforms its intended goal over longer holding periods (see Figure 11).

Interestingly, the tracking errors for the silver and gold LETFs (AGQ, ZSL ($\beta = \pm 2$, silver); UGL, GLL ($\beta = \pm 2$, gold)) in Table 5 have σ several magnitudes higher than μ. For example, AGQ ($\beta = 2$, silver) has a tracking error σ of 5% compared to a μ of 0.01%. In other words, these four LETFs, while they might track their references well on average, may also exhibit positive and negative deviations over 1-day holding periods as well. These observations are consistent with the regressions in Figures 8 and 9, where UGL and GLL ($\beta = \pm 2$, gold) show significant 1-day tracking errors. On the other hand, the non-leveraged gold and silver bullion ETFs, GLD and SLV, have almost no tracking error $\sigma \approx 0$, because they hold the underlying bullion according to their prospectuses. Since many investors use these ETFs to gain leveraged exposure to commodities, they should be aware of the large variance of the associated tracking errors.

In Figure 11, we show the histogram for the tracking error for each ETF along with a quantile-quantile plot to illustrate the distribution. For DIG and DUG ($\beta = \pm 2$, oil & gas), the quantile-quantile plot shows that the tracking error distribution is not quite normal, and has a large negative tail, so that the commodity LETF tracking error is negatively biased even for the shortest possible holding period of one day. On the other hand, for UGL, GLL ($\beta = \pm 2$, gold) the distribution appears to be normal with R^2 close to 98%. However, as noted in Table 5, the tracking errors for UGL and GLL ($\beta = \pm 2$, gold) also have a very large variance.

Next, we examine the horizon effect of tracking errors. Figure 12 indicates that higher

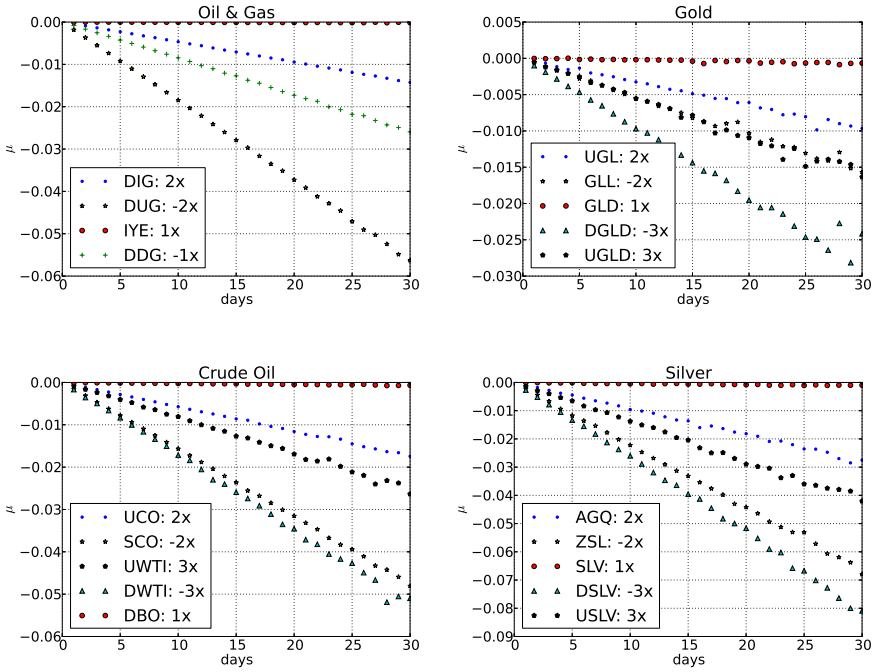

Figure 12: A plot of no. of days vs the mean tracking error arranged by commodities tracked. From top left to bottom right: US Oil & Gas, Gold, Crude Oil,and Silver. As the holding period increases, the average tracking error becomes more negative as well.

leveraged ETFs tend to have more negative average tracking errors, which appear to be decreasing linearly over longer holding periods. In addition, negative leveraged LETFs have a more negative average tracking error than their positive counterparts. For example, in Figure 12, GLL ($\beta = -2$, gold) has a lower slope than UGL ($\beta = 2$, gold) even though they have the same absolute value of leverage ratio $|\beta|$. Furthermore, with few exceptions,the average tracking error is most negative when $\beta = -3$ followed by $\beta = 3, -2, 2, -1, 1$. Thus, there is a higher holding horizon punishment for buying short than long LETFs.

Our analysis of the tracking error distribution reveals several characteristics of the tracking error defined in (3.2.1). Over a very short holding period, most LETFs perform close to their objectives stated in their prospectuses. Nevertheless, the realized tracking error varies over time, and can be positive or negative. For gold and silver LETFs, the tracking error is more volatile. Moreover, the magnitude of the mean tracking error depends heavily on the

β of the LETF, with bear LETFs suffering a higher penalty than bull LETFs.

3.3 Incorporating Realized Variance into Tracking Error Measurement

As is well known in the industry (see Avellaneda and Zhang (2010); Cheng and Madhavan (2009)), the price dynamics of an LETF depends on the realized variance of the reference index. This leads us to incorporate the realized variance in measuring the performance of an LETF. We run a regression analysis based on empirical LETF and reference prices that incorporates the realized variance as an independent variable. We then derive a realized effective fee associated with each LETF and analyze the realized price behavior relative to a theoretical benchmark to better quantify the over/under-performance.

3.3.1 Model for the LETF Price

Let S_t be the price of the reference index, and L_t be the price of the LETF at time t. Also denote f as the expense rate, r as the interest rate and β as the leverage ratio. Assume the reference asset follows the SDE

$$\frac{dS_t}{S_t} = \mu_t dt + \sigma_t dW_t, \quad t \geq 0, \tag{3.3.1}$$

with stochastic drift $(\mu_t)_{t\geq 0}$ and volatility $(\sigma_t)_{t\geq 0}$. For our analysis herein, we assume a general diffusion framework, but do not need to specify a parametric model. Many well-known models, including the CEV, Heston, and exponential Ornstein-Uhlenbeck models, fit within the above framework.

A long β-LETF L can be constructed through a dynamic portfolio. Specifically, the portfolio at time t consists of the cash amount $\$\beta L_t$ invested in the reference index S_t, while $\$(\beta - 1)L_t$ is borrowed at the positive risk free rate r. As a result, the LETF satisfies the

SDE

$$dL_t = L_t\beta\frac{dS_t}{S_t} - L_t((\beta-1)r + f)dt.$$

Solving the SDE, the log-return of the LETF is given by

$$\ln\frac{L_t}{L_0} = \beta\ln\frac{S_t}{S_0} + \frac{\beta-\beta^2}{2}V_t + ((1-\beta)r - f)t, \tag{3.3.2}$$

where

$$V_t = \int_0^t \sigma_s^2 ds$$

is the realized variance of S accumulated up to time t. Therefore, under this general diffusion model, the log-return of the LETF is proportional to the log-return of the reference index by a factor of β, but also proportional to the variance by a factor of $\frac{\beta-\beta^2}{2}$. The latter factor is negative if $\beta \notin (0,1)$, which is true for every LETF traded on the market. Also, the expense fee f reduces the return of the LETF.

Our regression analysis will focus on testing the functional form (3.3.2). We observe from (3.3.2) that the functional form of L_t in terms of S_t and V_t holds for any parametric model within the diffusion framework in (3.3.1). Considering the daily LETF returns, we set $\Delta t = \frac{1}{252}$ as one trading day. Let R_t^S be the daily return of the reference index at time t. At any time t, the n-day log-returns of an LETF follows

$$\ln\frac{L_{t+n\Delta t}}{L_t} = \beta\ln\frac{S_{t+n\Delta t}}{S_t} + \frac{\beta-\beta^2}{2}V_t^{(n)} + ((1-\beta)r - f)n\Delta t, \tag{3.3.3}$$
$$V_t^{(n)} = \sum_{i=0}^{n-1}(R_{t+i\Delta t}^S - \bar{R}_t{}^S)^2, \quad \bar{R}_t{}^S = \frac{1}{n}\sum_{i=0}^{n-1} R_{t+i\Delta t}^S.$$

This serves as a benchmark process for our subsequent analysis.

3.3.2 Regression of Empirical Returns

The log-return equation (3.3.3) suggests a regression with two predictors: the log-returns and the realized variance of the reference over n-days. This results in the linear model

$$\ln \frac{L_t}{L_0} = \hat{\beta} \ln \frac{S_t}{S_0} + \hat{\theta} V_t + \hat{c} + \epsilon,$$

where $\hat{c}$ is a constant intercept to be determined, and $\varepsilon \sim N(0, \sigma^2)$ is independent of $(S_t)_{t \geq 0}$.

In Table 6, we summarize the estimated $\hat{\theta}$ from our regression with holding periods of 30 days. Again, we use price data from disjoint periods to calculate returns. The realized variance is calculated using the inter-period returns (30 days). The choice of 30-day periods gives us sufficient points to compute the realized variance while providing enough disjoint periods during the period Dec 2008-May 2013 to perform a regression. A longer price history would certainly have helped in balancing this tradeoff, but all these commodity LETFs were introduced only in the past five years.

Our empirical analysis confirms several aspects of our theoretical model in (3.3.2) and provides explanations in cases where there is discrepancy. The theoretical value of θ according to (3.3.2) is given by $\frac{\beta - \beta^2}{2}$. Table 6 shows that the estimator $\hat{\theta}$ is typically in the neighborhood of θ, its theoretical value. For example, SCO ($\beta = -2$, crude oil) has $\hat{\theta} = 2.93$ versus a theoretical θ of 3. In addition, the non-leveraged ETFs all have $\hat{\theta}$ close to 0, suggesting that realized variance does not play an important role in its price process, as predicted. However, some LETFs have $\hat{\theta}$ diverging significantly from θ. For example, the $\hat{\theta}$ for UGL ($\beta = 2$, gold) differs from its theoretical value by a factor of 114% even with a regression R^2 of 99%.

We attribute the deviation of $\hat{\theta}$ from θ in our regression to the collinearity effect of the two predictors ($\ln \frac{S_t}{S_0}$ and V_t). Of course $\ln \frac{S_t}{S_0}$ and V_t cannot be independent observations, since V_t depends on the price path process of S_t, the reference index. In general, the reference returns and the realized variance are negatively correlated. When the realized variance is high, it is likely the reference has suddenly dropped in value. When the realized variance is

LETF	**Underlying**	β	$\hat{\theta}$	θ	r^2	$r^2_{x\|y}$	$r^2_{y\|x}$
SLV	Silver Bullion	1	0.11	0	0.9799	0.9503	0.0078
AGQ	Silver Bullion	2	-1.31	-1	0.9885	0.9751	0.3892
ZSL	Silver Bullion	-2	-3.27	-3	0.9995	0.9988	0.7514
USLV	Silver Bullion	3	-2.24	-3	0.9995	0.9988	0.7514
DSLV	Silver Bullion	-3	-6.94	-6	0.9994	0.9989	0.9654
GLD	Gold Bullion	1	-0.14	0	0.9898	0.9791	0.0064
UGL	Gold Bullion	2	-2.44	-1	0.9934	0.9867	0.2900
GLL	Gold Bullion	-2	-0.96	-3	0.9914	0.9828	0.0417
UGLD	Gold Bullion	3	-2.38	-3	0.9982	0.9955	0.6355
DGLD	Gold Bullion	-3	-6.26	-6	0.9846	0.9685	0.0809
IYE	Oil & Gas	1	-0.06	0	0.9988	0.9965	0.1905
DDG	Oil & Gas	-1	-0.99	-1	0.8866	0.7662	0.2342
DIG	Oil & Gas	2	-1.11	-1	0.9996	0.9989	0.9498
DUG	Oil & Gas	-2	-3.31	-3	0.9884	0.9769	0.8873
DBO	WTI Crude Oil	1	-0.02	0	0.9992	0.9981	0.0035
UCO	WTI Crude Oil	2	-1.15	-1	0.9987	0.9972	0.7747
SCO	WTI Crude Oil	-2	-2.93	-3	0.9987	0.9975	0.9619
UWTI	WTI Crude Oil	3	-2.14	-3	0.9974	0.9939	0.6218
DWTI	WTI Crude Oil	-3	-7.25	-6	0.9974	0.9939	0.6218
IYM	Building Materials	1	0.03	0	0.9996	0.9987	0.0495
SBM	Building Materials	-1	-0.98	-1	0.9970	0.9920	0.5446
UYM	Building Materials	2	-1.10	-1	0.9997	0.9993	0.9380
SMN	Building Materials	-2	-3.59	-3	0.9613	0.9221	0.5301

Table 6: $\hat{\theta}$ vs. θ, estimated from 30-day multi-variable regression of returns, with a partial correlation table. $r^2_{y|x}$ stands for the marginal predictive power of adding the realized variance (y) into the model, holding constant the predictive power of the reference index returns (x). Similar definition for $r^2_{x|y}$. Data from Dec 2008-May 2013.

low, it usually implies a period of steady positive growth for the reference. Thus, the multicollinearity effect is responsible for shifting predictive power among the different predictor variables. In order to measure the magnitude of the collinearity effect and the contribution of each correlated predictor variable, we compute the coefficients of partial determination for our regression model.

The factor $r^2_{y|x}$ which measures the marginal predictive power of adding the realized variance into the model. As $r^2_{y|x}$ increases, $\hat{\theta}$ becomes closer to θ, suggesting a larger dependence of LETF returns on realized variance during holding periods of high volatility. For example, for the 3 LETFs DIG ($\beta = 2$, oil & gas), SCO ($\beta = -2$, crude oil), and UYM ($\beta = 2$, building materials) all have $r^2_{y|x}$ over 90%. Their estimated $\hat{\theta}$ is similarly very close to the theoretical θ, never differing by more than 10%. However, for non-leveraged ETFs, the realized variance has minimal added predictive power in the model. For those ETFs, we observe $\hat{\theta} \approx 0$. For example, SLV ($\beta = 1$, silver), GLD ($\beta = 1$, gold), and DBO ($\beta = 1$, crude oil) all have $r^2_{y|x} \approx 0$, and they subsequently have $\hat{\theta} \approx 0$. In addition, $r^2_{x|y}$, which is the marginal predictive power of adding the log-returns of the reference into our regression model, is always very high, indicating that the log-returns of the reference affect the LETF prices the most, but that the realized variance is still important for predictive power, especially when leverage and the holding period is high.

3.3.3 Realized Effective Fee

In Figure 13, we show three empirical price paths: the LETF log-returns, the benchmark process defined in (3.3.2), and β times the reference index log-returns. As we can see, the value erosion due to realized variance (volatility decay) starts to play a significant role in determining LETF prices as the holding time increases. The path associated with β times the reference log-returns dominates the LETF log-returns after about 1 month of holding. After about 1 year, the benchmark which incorporates volatility decay more closely models the empirical LETF log-returns. For example, after 6 months of holding, SCO ($\beta = -2$,

crude oil) diverges from β times the reference, illustrating the effects of volatility decay.

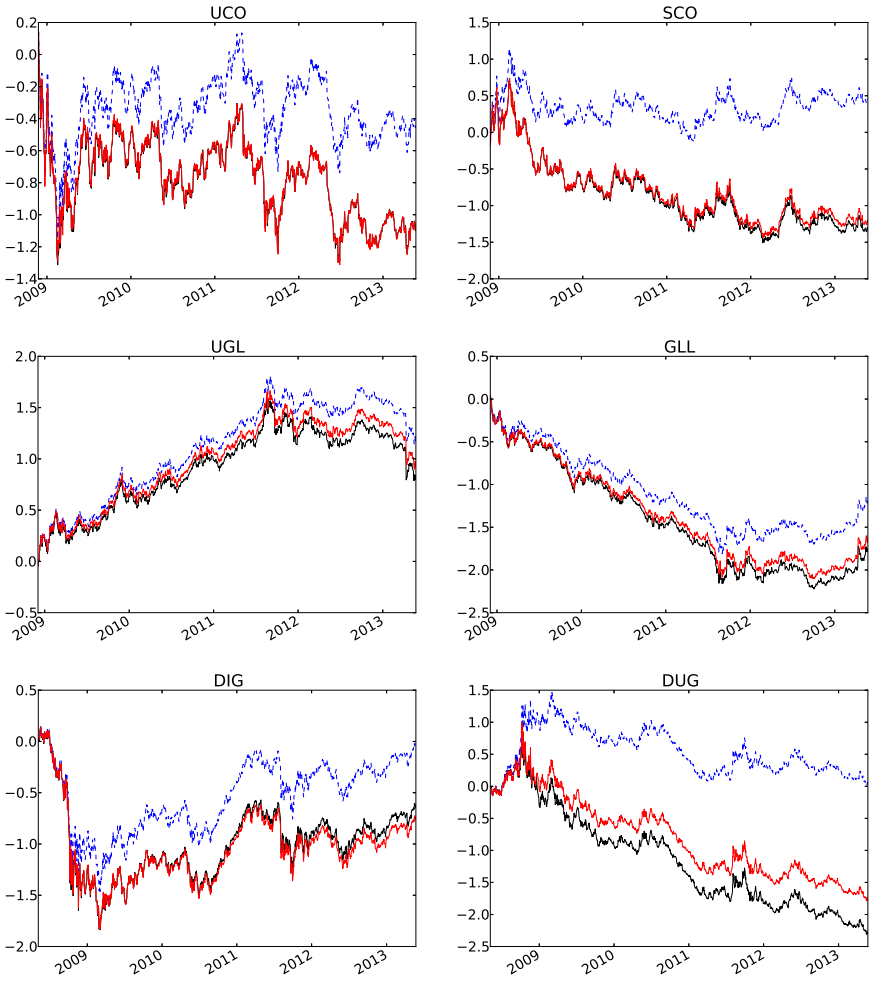

Figure 13: Cumulative empirical log-returns of the LETF (solid dark) vs benchmark (solid light) and β times reference (dashed light), from Dec 2008-May 2013. From top left to bottom right: UCO, SCO (crude oil); UGL, GLL (gold); DIG, DUG (building materials). UCO, UGL, and DIG have $\beta = 2$ while SCO, GLL, and DUG have $\beta = -2$.

However, there are also some strong deviations from the predictions given by the benchmark, which compound as the holding time increases. This causes the LETF to underperform even after the volatility decay is accounted for. For example, DUG's ($\beta = -2$, oil & gas) empirical returns begin to trail its benchmark significantly around 2009. Therefore, the volatility decay cannot explain all the LETF underperformance.

We are therefore motivated to quantify the over/under-performance of the LETFs after

observing deviations from the benchmark in Figure 13. We introduce the concept of *realized effective fee* (REF) as the effective deduction rate charged by the LETF provider over the frictionless dynamic portfolio from which the LETF is constructed in Section 3.3.1. For a holding interval $[0, t]$, the corresponding REF is defined by

$$\hat{f}_t = (1-\beta)r - \frac{\ln \frac{L_t}{L_0} - \beta \ln \frac{S_t}{S_0} - \frac{\beta-\beta^2}{2} V_t}{t}. \tag{3.3.4}$$

Since for each LETF, L_t, S_t, V_t, β, and r are all known, we can calculate the REF $\hat{f}_t$ for any LETF over a given holding period $[0, t]$ using historical prices. We remark that the REF, which is indexed by time t, depends on the selected holding horizon.

LETF	**Underlying**	β	**Prospectus Fee** (bps)	**Realized Effective Fee** (bps)
SLV	Silver Bullion	1	50	96
AGQ	Silver Bullion	2	95	524
ZSL	Silver Bullion	-2	95	567
USLV	Silver Bullion	3	165	93
DSLV	Silver Bullion	-3	165	504
GLD	Gold Bullion	1	40	48
UGL	Gold Bullion	2	95	343
GLL	Gold Bullion	-2	95	406
UGLD	Gold Bullion	3	135	139
DGLD	Gold Bullion	-3	135	521
IYE	Oil & Gas	1	48	50
DDG	Oil & Gas	-1	95	953
DIG	Oil & Gas	2	95	-142
DUG	Oil & Gas	2	95	1134
DBO	WTI Crude Oil	1	75	56
UCO	WTI Crude Oil	2	95	84
SCO	WTI Crude Oil	-2	95	321
UWTI	WTI Crude Oil	3	135	3
DWTI	WTI Crude Oil	-3	135	549
IYM	Building Materials	1	48	11
SBM	Building Materials	-1	95	456
UYM	Building Materials	2	95	-204
SMN	Building Materials	-2	95	1625

Table 7: Comparison of the official fee for the LETF charged on the fund prospectus and the REF calculated using 5 years of price data (December 2008-May 2013) for the LETF and reference (see (3.3.4)). We set $r = 69.1$ bps, the annualized LIBOR rate.

In many cases, the REF is seen to be much larger than the fund's advertised fee, indicating significant underperformance. Out of the 23 commodity LETFs, 2 have negative implied costs, so that the fund overperforms by the end of the five year period Dec 2008 to May 2013. If the REF exceeds the advertised fee, then the investor effectively pays an extra price for the opportunity to invest in the LETF. As a general trend, the bear LETFs tend to charge higher REFs than bull LETFs with the same magnitude of leverage $|\beta|$. For example, USLV ($\beta = 2$, silver) has a REF of 93 bps, while DSLV ($\beta = -2$, silver) has an REF of 504 bps over the period Dec 2008-May 2013. The two highest REFs correspond to DUG ($\beta = -2$, oil & gas) and SMN ($\beta = -2$, building materials), whose REFs are 1134 bps and 1625 bps respectively. Figure 13 illustrates that DUG ($\beta = -2$, oil & gas) drastically underperforms the benchmark, thereby realizing a high REF. Notice that in both cases, however, DUG and SMN's bull counterparts DIG ($\beta = 2$, oil & gas) and UYM ($\beta = 2$, building materials) respectively)display a negative REF, indicating overperformance during the same period. It is possible that as the reference trends upwards for a long period of time, the bear LETF will underperform, while the bull LETF will overperform.

3.4 A Static LETF Portfolio

Taking advantage of the volatility decay, a well-known trading strategy used by practitioners involves shorting a $\pm\beta$ pair of LETFs with the same reference, as discussed in Avellaneda and Zhang (2010); Leung and Santoli (2013); Mackintosh and Lin (2010a); Mason et al. (2010). Since the LETFs have opposite daily returns on the same reference index, the portfolio has very little exposure to the reference as long as the holding period is sufficiently short. With this strategy, the volatility decay can help generate profit, which is the intuition of many practitioners. However, the portfolio is exposed to risk during periods of low volatility and high trending, as well as tracking errors. In this section, we describe an extension of this trading strategy by allowing the positive and negative leverage ratios to differ. We determine

the portfolio weights to approximately eliminate the dependence on the reference. We show that the resulting portfolio is long volatility. For a number of LETF pairs, we find from empirical data that on average the strategy is profitable with enormous tail risk.

We now construct a weighted portfolio which is short the LETF with leverage ratio $\beta_+ > 0$ and short another LETF with leverage ratio $\beta_- < 0$. We emphasize that both LETFs having the same reference, but that β_+ and $|\beta_-|$ may differ. We hold fraction $\omega \in (0,1)$ of the portfolio in the β_+-LETF and $(1-\omega)$ of the portfolio in the β_--LETF. At time T, the normalized return from this strategy is

$$\mathcal{R}_T = 1 - \omega \frac{L_T^+}{L_0^+} - (1-\omega)\frac{L_T^-}{L_0^-}. \tag{3.4.1}$$

Applying (3.3.2), $\mathcal{R}_T$ admits the expression

$$\mathcal{R}_T = 1 - \omega \left(\frac{S_T}{S_0}\right)^{\beta_+} \exp\left(\Gamma_T^+\right) - (1-\omega)\left(\frac{S_T}{S_0}\right)^{\beta_-} \exp\left(\Gamma_T^-\right), \tag{3.4.2}$$

where

$$\Gamma_T^{\pm} = \frac{\beta_\pm - \beta_\pm^2}{2} V_T + ((1-\beta_\pm)r - f_\pm)T,$$

Here, $\beta_\pm$ and $f_\pm$ are the respective leverage ratios and fees of the two LETFs in the portfolio defined in (3.4.1). Over a short holding period such that $\frac{L_T}{L_0} \approx 1$, one can pick an appropriate weight ω^* to approximately remove the dependence of $\mathcal{R}_T$ on S_T.

Proposition 4. *Select the portfolio weight $\omega^* = \frac{-\beta_-}{\beta_+ - \beta_-}$. For $\frac{L_T}{L_0} \approx 1$, the return from this strategy is given by*

$$\mathcal{R}_T = \frac{-\beta_-\beta_+}{2} V_T - \frac{\beta_-}{\beta_+ - \beta_-}(f_+ - f_-)T + (f_- - r)T. \tag{3.4.3}$$

Proof. For $\frac{L_T}{L_0} \approx 1$, we can substitute for $\frac{L_T}{L_0}$ with $\ln \frac{L_T}{L_0} + 1$ in (3.4.1). Then, we set $\omega = \omega^*$ and apply (3.3.2) to conclude (3.4.3). □

(β_+, β_-)	ω^*	$\frac{-\beta_-\beta_+}{2}$
$(1,-1)$	$1/2$	$1/2$
$(1,-2)$	$2/3$	1
$(1,-3)$	$3/4$	$3/2$
$(2,-1)$	$1/3$	1
$(2,-2)$	$1/2$	2
$(2,-3)$	$3/5$	3
$(3,-1)$	$1/4$	$3/2$
$(3,-2)$	$2/5$	3
$(3,-3)$	$1/2$	$9/2$

Table 8: Table of (β_+, β_-) pairs vs ω^* the weight of the β_+ portfolio, and $\frac{-\beta_-\beta_+}{2}$ the dependence of the strategy on V_t (see Prop. 4).

The return (3.4.3) corresponding to portfolio weight ω^* reflects a linear dependence on the realized variance. In particular, the coefficient $\frac{-\beta_-\beta_+}{2}$ is strictly positive, so the strategy is effectively long volatility (V_T). Also, as it does not depend on S_T, the ω^* portfolio is Δ-*neutral* as long as the reference does not move significantly. In Table 8, we summarize the coefficient of V_T and the weighted portfolio $(\omega^*, 1-\omega^*)$ for different combinations of leverage ratios. Note that as long as $\beta_+ = -\beta_-$, we end up with the portfolio weight $\omega^* = \frac{1}{2}$. Also, the coefficient $\frac{-\beta_-\beta_+}{2}$ exceeds or equals to 1 except for the pair $(\beta_+, \beta_-) = (1,-1)$, and it is largest for the pair $(\beta_+, \beta_-) = (3,-3)$.

We now backtest the ω^* strategy from Prop. 4 as follows. For each LETF pair, we short \$0.5 of the β_+-LETF and \$0.5 of the β_--LETF with $\beta_+ = -\beta_- = 2$ and hold the position for some time T. The normalized return $\mathcal{R}_T$ depends on the relative weights on the long/short-LETFs but not the absolute cash amounts. More generally, one can also test the strategy with different $\beta_\pm$ and ω^*.

Dividing the price data from Dec 2008-May 2013 into n-day rolling (overlapping) periods, we calculate the returns from the strategy over each period. For every n-day return, we compare against the realized variance over the same period. This is illustrated in Figure 14. As a theoretical benchmark, we also plot $\mathcal{R}_T$ in (3.4.3) as a linear function. Each point (dot) on the plots represents a 5-day return, but over rolling periods the returns are

not independent. In other words, the lines in Figure 14 are not generated by regression but taken from (3.4.3). We choose (3.4.3) as a benchmark because it is expected to hold *pathwise* as long as $\frac{L_T}{L_0} \approx 1$ with negligible tracking error.

We can observe from Figure 14 that the returns exhibit positive dependence on the realized variance (V_T). In particular, for the energy pairs (DIG-DUG ($\beta = \pm 2$, oil & gas) and UCO-SCO ($\beta = \pm 2$, crude oil)), the returns tend to be very positive when the realized variance is high. This is because the strategy captures the volatility decay as profit. Nevertheless, there is also a visible amount of noise in the returns deviating from the linear dependence on V_T, especially for the gold and silver pairs (UGL-GLL ($\beta = \pm 2$, gold) and AGQ-ZSL ($\beta = \pm 2$, silver), respectively). This can be partly attributed to tracking errors from both LETFs in the portfolio. Also, the ω^*-strategy loses its Δ-neutrality if the reference moves significantly.

While this portfolio is expected to be Δ-neutral (with respect to the reference index) for small reference movements, in reality the strategy is also short-Γ. One way to see this is through Figure 15 that plots the returns against the reference index returns. Common to all four LETF pairs, when the reference return is either very positive or negative, the return of the ω^*-strategy tends to be negative. As a theoretical benchmark, we also plot the normalized return equation (3.4.2) which applies even for large reference movements.

In contrast to the energy pairs, the gold and silver pairs yield very noisy returns. This is consistent with our earlier observations from our regressions in Figures 8 and 9. For instance, both UGL and GLL ($\beta = \pm 2$, gold) show substantial tracking errors over short periods such as 5 days, and their regressed leverage ratios differ from the stated ones. On the other hand, the DIG and DUG ($\beta = \pm 2$, oil & gas) regressions in Figures 6 and 7 reflect much less tracking errors.

Furthermore, Figure 16 shows that as the holding time increases, the returns from the ω^* strategy increases as well. The performance is best for the energy pairs UCO-SCO ($\beta = \pm 2$, crude oil) and DIG-DUG ($\beta = \pm 2$, oil & gas), but more subdued for the bullion pairs

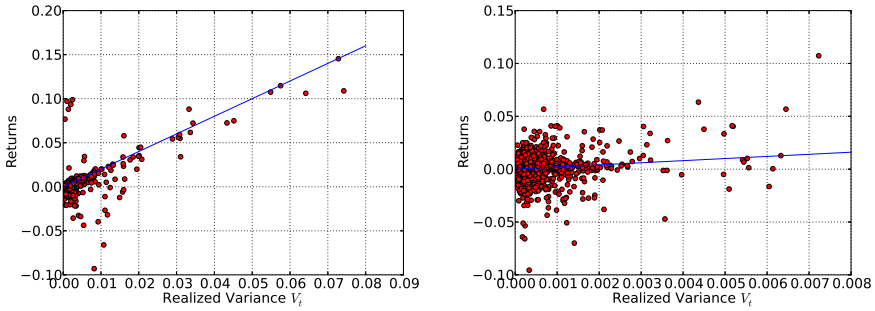

(a) DJUSEN-DIG-DUG

(b) GOLDLNPM-UGL-GLL

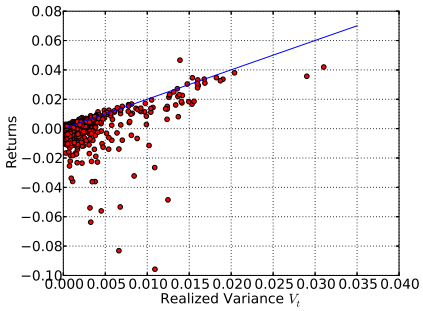

(c) DJUBSCL-UCO-SCO

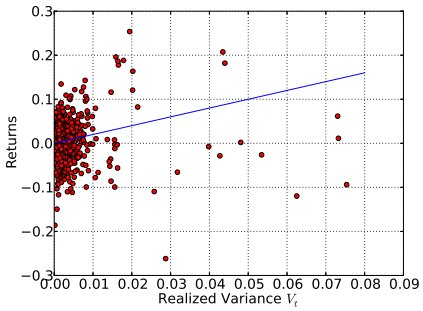

(d) SLVRLN-AGQ-ZSL

Figure 14: Plot of trading returns vs realized variance for a double short strategy over 5-day rolling holding periods, with $\beta_\pm = \pm 2$ for each LETF pair. We compare with the empirical returns (circle) from the ω^* strategy with the predicted return (solid line) in Prop. 4. Trading pairs are DIG-DUG (oil & gas), UGL-GLL (gold), UCO-SCO (crude oil), AGQ-ZSL (silver).

UGL-GLL ($\beta = \pm 2$, gold) and AGQ-ZSL ($\beta = \pm 2$, silver). However, over longer holding periods, the ω^* portfolio may lose its Δ-neutral status, thereby generating more risk as well. Although average returns from the ω^* strategy are positive, one is subject to enormous tail risk, which increases with the holding time of the static portfolio. In order to ensure that we do not subject ourselves to excessive tail risk, we should not only be sure of a high volatility environment, but we must also adjust the holding time to account for the extra risk associated with time horizon of returns.

Figure 17 gives another perspective of the ω^* strategy's dependence on realized variance. It shows the time series of the 30-day rolling returns along with the realized variance of the reference index from Dec 2008 to May 2013. We see that when the realized variance

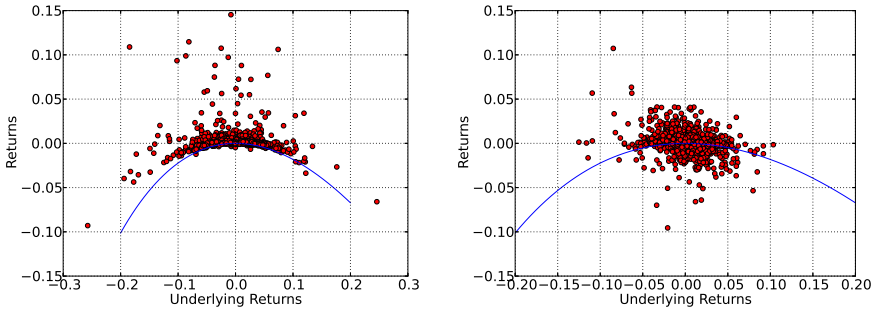

(a) DJUSEN-DIG-DUG

(b) GOLDLNPM-UGL-GLL

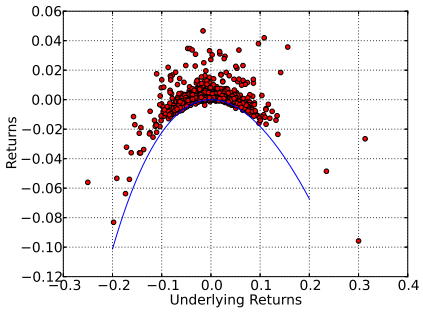

(c) DJUBSCL-UCO-SCO

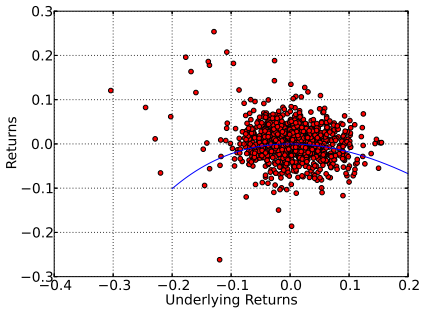

(d) SLVRLN-AGQ-ZSL

Figure 15: Plot of returns of reference index vs trading returns for a double short strategy over 5-day rolling, holding periods. $\beta_{\pm} = \pm 2$ for each LETF pair. We compare the empirical returns from our trading strategy (dark solid circle) with the predicted dependence on reference returns according to (3.4.2), using $\Gamma_T^{\pm} = 0$ (light solid line). Trading pairs are DIG-DUG (oil & gas), UGL-GLL (gold), UCO-SCO (crude oil), AGQ-ZSL (silver).

increases sharply, the strategy returns also spike sharply. For example, when DJUSEN index realized variance spikes, the DIG-DUG ($\beta = \pm 2$, oil & gas) trading pair accumulates a 30% return over a single 30-day holding period. However, when realized variance is subdued over a period of time, the ω^* returns may turn quite negative as well.

In summary, the double-short trading strategy studied herein is profitable on average, but it is commodity specific and subject to enormous tail risk, as seen from empirical prices. The strategy's profitability depends strongly on a high volatility from the reference index. Although longer holding times tend to enhance the average return, they also enormously increase the horizon risk. According to these findings, this strategy appears to be appealing

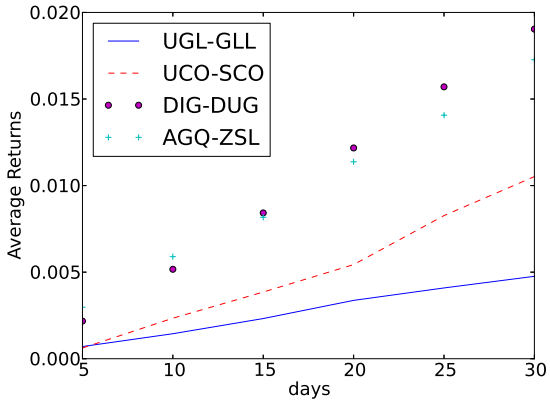

Figure 16: Average returns from a double short trading strategy by commodity pair over no. of days holding period. $\beta_{\pm} = \pm 2$ for each LETF pair. Trading pairs are DIG-DUG (oil & gas), UGL-GLL (gold), UCO-SCO (crude oil), AGQ-ZSL (silver).

only during times of high volatility in the reference index.

3.5 Concluding Remarks

The ETF market has continued to grow in quantity and diversity, especially in the past five years. For both investors and regulators, it is very important to understand and quantify the risks involved with various ETFs. In this chapter, we have focused on commodity ETFs and their leveraged counterparts. We find that the LETF returns tend to deviate significantly from the corresponding multiple of the reference returns as the holding horizon lengthens. To study the performance of an LETF, we have applied a new benchmark process that accounts for the realized variance of the underlying. We find that many commodity LETFs still diverge, typically negatively, from this benchmark over time. These empirical observations motivate us to illustrate the over/under-performance of an LETF via the concept of realized expense fee. Based on the funds and the time periods we have studied, most commodity LETFs effectively charge significantly higher expense fees than stated on their prospectuses.

In view of LETFs' common pattern of value erosion over time, one well-known trading strategy in the industry involves statically shorting both long and short LETFs in order to

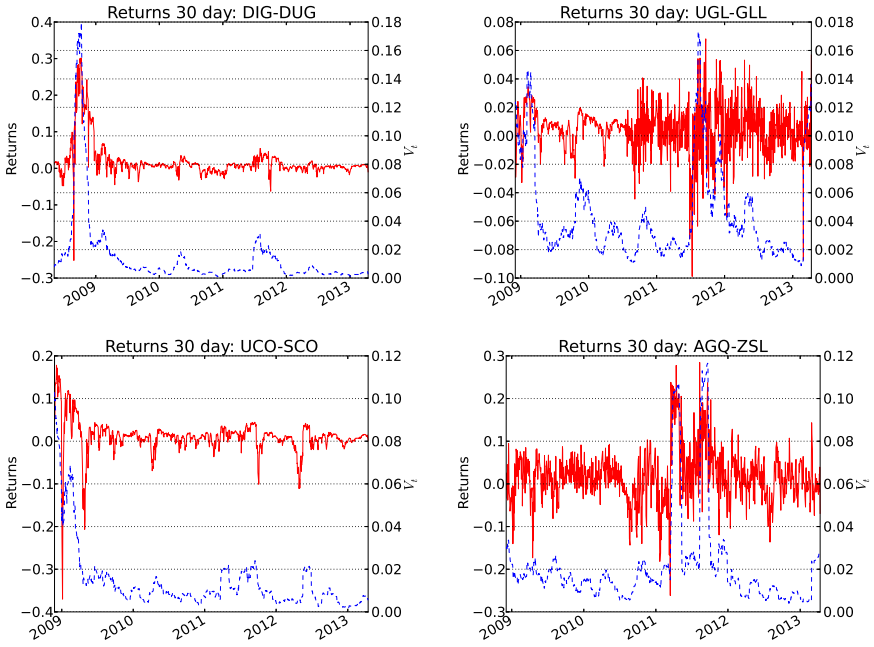

Figure 17: Time series of returns for a double short strategy over 30-day rolling, holding periods, with $\beta_{\pm} = \pm 2$ for each LETF pair. Notice how during the periods of greatest volatility the double short strategy has the greatest return. Trading pairs are DIG-DUG (oil & gas), UGL-GLL (gold), UCO-SCO (crude oil), AGQ-ZSL (silver).

capture the volatility decay as profit. We systematically study an extension of this strategy that is applicable to LETF pairs with different asymmetric leverage ratios. We analytically derive the specific weights in the LETFs so that the resulting portfolio is approximately Δ-neutral, but short-Γ as well. This strategy can potentially be quite profitable but its return can be negatively impacted by tracking errors generated by the LETFs and large movements of the reference index. These two factors both depend on the holding horizon. This should motivate future research on the horizon risk for LETF strategies. To this end, Leung and Santoli Leung and Santoli (2013) study the admissible holding horizon and leverage ratio given a risk constraint. The recent chapters Leung and Li (2015); Naylor et al. (2011); Triantafyllopoulos and Montana (2009) examine the dynamics of price spreads between ETF pairs, for example, gold vs. silver.

Our analysis herein does not assume a parametric stochastic volatility model for the underlying. It is of practical interest to investigate the price behavior of LETF under a number of well-known stochastic volatility models, such as the Heston and SABR models. On top of LETFs, there are also options written on these funds. This gives rise to the question of consistent pricing of LETF options across leverage ratios (see Ahn et al. (2012); Leung and Sircar (2012)). Finally, models that capture the connection between LETFs and the broader financial market would be very useful for not only traders and investors, but also regulators.

Chapter 4

Non-convergence of Agricultural Futures

This chapter studies the market phenomenon of non-convergence between futures and spot prices in the grains market. We postulate that the positive basis observed at maturity stems from the futures holder's timing options to exercise the shipping certificate delivery item and subsequently liquidate the physical grain. In our proposed approach, we incorporate stochastic spot price and storage cost, and solve an optimal double stopping problem to give the optimal strategies to exercise and liquidate the grain. Our new models for stochastic storage rates lead to explicit no-arbitrage prices for the shipping certificate and associated futures contract. We calibrate our models to empirical futures data during the periods of observed non-convergence, and illustrate the premium generated by the shipping certificate.

4.1 Introduction

Standard no-arbitrage pricing theory asserts that spot and futures prices must converge at expiration. Nevertheless, during 2004-2009 traders observed significantly higher expiring futures prices for corn, wheat, and soybeans on the CBOT compared to the spot price of

the physical grains. As shown in Figure 18, the unprecedented differential between cash and futures prices reached its apex in 2006, where at the height of the phenomenon, CBOT corn futures had surpassed spot corn prices by almost 30%! In the literature, Adjemian et al. (2013) and Aulerich et al. (2011) reported that on July 1, 2008, the price for a July 2008 CBOT wheat futures contract closed at \$8.50 per bushel. On the other hand, the corresponding cash price in the Toledo, Ohio delivery market was only \$7.18 per bushel, a price differential of \$1.32/bu (+15%). Irwin et al. (2009) first coined the term "non-convergence" for this phenomenon of observed positive premium, which recurred persistently from 2004 onwards. According to their study, "performance has been consistently weakest in wheat, with futures prices at times exceeding delivery location cash prices by \$1.00/bu, a level of disconnect between cash and futures not previously experienced in grain markets."

However, a small difference between expiring futures and cash prices does not necessarily imply a market failure. Before expiration, futures and cash prices may differ due to the convenience yield, storage costs, or financing costs. Upon expiration, if cash prices are lower/higher than futures prices, then arbitrageurs may profit from trading simultaneously in the spot and futures markets. If sufficient numbers of arbitrageurs engage in these trades, they will drive cash and futures prices to convergence at expiration. In fact, the futures expiration date and delivery date may also differ. After the last trade date, the exchange contacts the longest outstanding long who is notified of his obligation to undertake delivery. Before the month's end, the delivery instrument is then exchanged at the settlement price between long and short parties. Therefore, since the delivery process does not occur immediately after the last trade date, cash and futures prices might still differ by a spread called the *basis*. In this chapter, we use the following definition for the basis:

$$\text{basis} = \text{futures price - spot price.}$$

Figure 18 displays the basis time series associated with the expiring futures on soybeans and

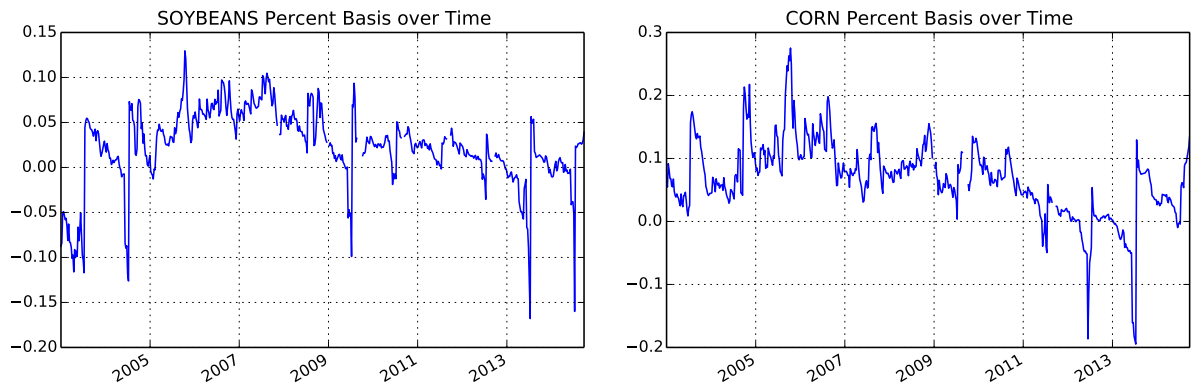

Figure 18: Time series of basis for soybeans (left) and corn (right) futures. During 2004-2009, the expiring futures price tends to be significantly higher than the spot price.

corn.

Since the short party may choose the location and time to deliver, Biagini and Bjork (2007) posit that futures price should be biased below the spot price on the last trade date. However, their theoretical model would yield the opposite of the empirical observations in the grain markets. In fact, the positive basis in the CBOT grain markets between 2004-2009 were too large to have been caused by the small inefficiencies of the delivery process. This motivates us to investigate the factors that drive the non-convergence phenomenon.

In order to explain the positive premium, one must turn to embedded *long-side* options in the futures. Long-side options in futures markets depend totally on the idiosyncrasies of each commodity's exchange traded structure. The survey chapter by Carmona and Coulon (2013) demonstrates the appropriate model for a commodity varies highly depending on storability, instantaneous utility, and alternatives. At expiration, a CBOT agricultural futures contract does not deliver the physical grains but an artificial instrument called the *shipping certificate* that entitles its holder to demand loading of the grains from a warehouse at any time. Before exercising the option to load, the holder must pay a fixed storage fee to the storage company,[1] as stipulated in the certificate. Since the storage capacity of grain elevators is

[1]Only a small number of storage companies that have contracts with the futures exchange are allowed to issue shipping certificates. They are also called the regular firms in the industry.

limited and expensive, the number of grain elevators is fixed to a minimum necessary to efficiently carry out transfers of grain from one transport system to another.[2] Thus, like a fractional-reserve banking system, shipping certificates alleviate the congestion of grain elevators by only keeping enough grain on hand to satisfy instant withdrawal demand. A detailed explanation on the structure of the shipping certificate market can be found in Aulerich et al. (2011) and Garcia et al. (2014).

In this chapter, our storage differential hypothesis posits that when the certificate storage rate is sufficiently low, investors will pay a premium for the certificate over the spot grain in order to save on storage cost over time, resulting in non-convergence of futures and spot prices. When the storage cost of the certificate is set lower than the true storage cost paid by the regular firm, the regular firm will cease to issue the unprofitable shipping certificates. Since shipping certificates can only be issued by a set number of regular firms with limited inventories, the market cannot issue certificates with lower fixed storage rates to keep the market flowing. Instead, since the supply of certificates remains fixed, the value of existing shipping certificates will be bid up in the secondary market, resulting in a premium over the spot price. On the other hand, during periods where the certificate storage rate is set much higher than the market storage rate, the certificate should not command any premium over the spot because agents would exercise and store at the lower market rate. Therefore, as shown by Aulerich et al. (2011), large quantities of certificates remaining unredeemed under the storage differential hypothesis becomes a strong predictor of non-convergence. In fact, in 2009 under mounting evidence that storage differentials were responsible for non-convergence, the CBOT raised the certificate storage rate for wheat, after which non-convergence decreased significantly.[3] This observation is consistent with our findings in this chapter.

Let us point out an alternative explanation for non-convergence even though it is not

[2] See http://www.cmegroup.com/rulebook/CBOT/II/11/11.pdf

[3] http://www.cftc.gov/idc/groups/public/@aboutcftc/documents/file/reportofthesubcommitteeonconve.pdf

the approach in this chapter. The speculator hypothesis for non-convergence postulates that large *long* positions held by commodity index traders (CITs) have made it impossible for arbitrageurs to carry sufficient grain forward to drive terminal prices to convergence (see Tang and Xiong (2012) an example of the effects of excess speculation). While the speculator hypothesis is plausible, empirical studies by Garcia et al. (2014) and Irwin et al. (2011) found no evidence that rolling or initiation of large positions by index funds had contributed to an expansion of the basis. In this chapter, we illustrate mathematically how the non-convergence phenomenon can arise under rational no-arbitrage models with stochastic storage rates.

We propose two new models that incorporate the stochasticity of the market storage rate and capture the storage option of the shipping certificate by solving two optimal timing problems, namely, to exercise the shipping certificate and subsequently liquidate the physical grain. First, we propose the Martingale Model whereby the spot price minus storage cost is a martingale while the stochastic storage rate follows an Ornstein-Uhlenbeck (OU) process. In addition, we present a second model in which the stochastic storage rate is a deterministic function of the spot price that follows an exponential OU (XOU) process. Among our results, we provide explicit prices for the shipping certificate, futures prices, and the basis size under a two continuous-time no-arbitrage pricing models with stochastic storage rates. By examining the divergence between expiring futures prices and corresponding spot prices, we derive the timing option generated by the differential between the market storage rate and the constant storage rate stipulated in the shipping certificate, which explains the non-convergence phenomenon in agricultural commodity markets. We also fit our model prices to market data and extract the numerical value of the embedded timing option.

The rest of the chapter is organized as follows. Section 4.2 reviews the literature on the subject of non-convergence for agricultural futures. In Section 4.3, we discuss a martingale spot price model with an OU stochastic storage rate, and derive the certificate price as well as the optimal exercise and liquidation timing strategies. In Section 4.4, we analyze a shipping certificate valuation model with a local stochastic storage rate and an exponential OU spot

price. Section 4.5 concludes. Proofs are provided in the Appendix.

4.2 Related Studies

The long history of the theory of storage dates back to Kaldor (1939) who argued that the future price should reflect the spot price plus storage cost via a no-arbitrage relationship. Johnson (1960) proposed an extension of Kaldor's model which related inventories and hedging motivations to the intersection of futures and spot markets. However, in order to account for possibly backwardated futures curves, Brennan (1958) and Working (1949) developed the notion of a stochastic convenience yield, a fictitious dividend that accrues to the commodity holder, but not the futures holder. Furthermore, Fama and French (1987) and Gorton et al. (2012) found plenty of empirical evidence for the theory of storage by examining inventories data. These authors not only created a theoretical basis for understanding commodity spot and futures prices, but also empirically demonstrated the validity of the theory of storage over a century.

Much of the literature on embedded options in futures contracts studies the short-side options which *lower* the futures price below the spot price. For example, Hranaiova et al. (2005) estimate the values of the delivery option, which allows the short to choose the location of cheapest delivery. In addition, Biagini and Bjork (2007) compute model-free futures prices for the short-side timing option. In contrast, our models explain how the futures price can be *higher* than the spot price at maturity. Our proposed approach contributes to the theory of storage as it provides a new link between the futures and spot markets through the storage cost differential and the associated timing option. In a related study, Hinz and Fehr (2010) consider the impact of storage cost constraints on commodity options, but their model cannot account for backwardated futures curves or non-convergence.

Aulerich et al. (2011) consider an alternative model in which non-convergence reflects the value of an exchange option due to the scarcity of shipping certificate. They incorporate

a long-side option but not stochastic or differential storage rates. The exchange option explanation is unsatisfactory because the exchange option is universal to all commodity futures, while the non-convergence phenomenon is observed only in the grain markets. Our approach identifies different storage rates between the certificate and real world as the driver for non-convergence at maturity. Finally, instead of using a closed-form approximation for the certificate price, we derive the explicit value of the shipping certificate under different stochastic storage rate models.

The storage differential hypothesis is supported by several recent studies. Garcia et al. (2014) and Adjemian et al. (2013) set up a discrete-time model and give conditions for the number of shipping certificates in the market at equilibrium. While they identified the difference between the market and certificate storage rates as the crucial factor for non-convergence, they did not compute the value of the shipping certificate. In this chapter, we derive and compute explicitly the prices of the futures and shipping certificate, and provide the necessary and sufficient conditions for non-convergence. Furthermore, our approach requires only the existence of the shipping certificate and no-arbitrage condition, and does not have specific assumptions on the characteristics of market agents and their interaction.

The core mathematical problem within our stochastic storage models is an optimal double stopping problem driven by a mean-reverting process. To this end, we adapt to our problem the results developed by Leung et al. (2015) that study the optimal entry and exit timing strategies when the underlying is an OU process. Other mean-reverting processes can also be used to model the market storage rate so long as the corresponding optimal double stopping problem can be solved analytically; see, e.g. Leung and Li (2015) and Leung et al. (2014) for the cases with an exponential OU and Cox-Ingersoll-Ross (CIR) underlying, respectively, and related applications to futures trading in Leung and Li (2016) and Leung et al. (2016).

4.3 Martingale Model with Stochastic Storage

We now discuss a futures pricing model for a single grain type, with the spot price process $(S_t)_{t\geq 0}$. The cost of physical storage is stochastic, represented by the rate process $(\delta_t)_{t\geq 0}$. The spot price satisfies

$$dS_t = (rS_t + \delta_t)dt + \sigma S_t dW_t, \tag{4.3.1}$$

where r is the positive risk-free rate, σ is the volatility parameter of spot grain, and W is a standard Brownian motion under the risk-neutral measure $\mathbb{Q}$. In this model, we assume that the commodity is continuously traded, with units of the commodity constantly being sold to pay the flat storage rate. Hence, the discounted spot price S_t *net* storage cost, i.e. $M_t := e^{-rt}S_t - \int_0^t \delta e^{-ru}du$, $t \geq 0$, is a $\mathbb{Q}$-martingale.

Note that δ_t is the *net* storage cost, which is the true storage cost minus the convenience yield associated with owning the physical grain. Furthermore, the storage rate δ_t is quoted in \$/bushel, and not as a proportion of the commodity price. In the standard treatment of storage rates, agents pay a proportion of the commodity price S_t per bushel i.e. $\delta_t = cS_t$. However, since empirical storage rates are quoted in \$/bushel and not as a percentage of the crop, our specification of a flat storage rate δ_t is realistic and amenable for empirical analysis. One can view the storage rate δ_t as a negative dividend rate on the commodity which the commodity holder pays but the futures holder does not. In our model, the storage cost δ_t follows an Ornstein-Uhlenbeck (OU) process

$$d\delta_t = \kappa(\nu - \delta_t)dt + \zeta d\widetilde{W}_t, \tag{4.3.2}$$

where $\widetilde{W}$ is a standard Brownian motion under $\mathbb{Q}$, and is independent of W. The parameter κ dictates the speed of mean-reversion for δ_t, ν is the average value of δ_t, and ζ is the volatility of the storage rate δ_t. The parameters are required to satisfy the condition $2\kappa \geq \zeta$. The filtration $\mathbb{F} \equiv (\mathcal{F}_t)_{t\geq 0}$ is generated by $(S_t)_{t\geq 0}$ and $(\delta_t)_{t\geq 0}$. We let $\mathcal{T}$ be the set of all

$\mathbb{F}$-stopping times, and $\mathcal{T}_{s,u}$ be the set of $\mathbb{F}$-stopping times bounded by $[s,u]$.

At time T, the T-futures contract expires, and the long party receives the shipping certificate. This certificate is perpetually lived and gives the holder an option to load out the grain anytime, but the holder pays a constant storage rate $\widehat{\delta}$ before exercising this option. Note that $\widehat{\delta}$ is a flat rate quoted in the futures contract, and thus must be positive. Since the certificate holder does not possess the physical grain, and thus, cannot derive any convenience yield from it. After exercising, the certificate holder then stores at the market rate δ_t until he chooses to liquidate the grain. We allow δ_t to be possibly negative to account for the convenience yield. The fixed costs, c_1 and c_2 respectively, are incurred upon exercising and liquidation of the grain.

The value of the shipping certificate can be obtained by solving two optimal timing problems. First, suppose the agent has exercised at time $t \geq \tau$. The agent selects the optimal time to liquidate the grains by solving[4]

$$J(S_t, \delta_t) = \sup_{\eta \in \mathcal{T}_{t,\infty}} \mathbb{E}\left[e^{-r(\eta - t)}\left(S_\eta - c_2\right) - \int_t^\eta \delta_u e^{-r(u-t)} du | \mathcal{F}_t\right].$$

Working backward in time, the value function J now serves an input for the optimal exercise problem. The agent receives the shipping certificate at time T, and selects the optimal time $\tau \geq T$ to exercise the grains. Therefore, the agent's value function at time T is

$$V(S_T, \delta_T) = \sup_{\tau \in \mathcal{T}_{T,\infty}} \mathbb{E}\left[e^{-r(\tau - T)}\left(J(S_\tau, \delta_\tau) - c_1\right) - \int_T^\tau \widehat{\delta} e^{-r(u-T)} du | \mathcal{F}_T\right]. \tag{4.3.3}$$

Economically, we interpret J as the liquidation value of the commodity for an individual who optimally times storage, and V as the price of the certificate (for an individual who can choose between storage rates). Furthermore, since $T = \tau = \eta$ is always a valid stopping time

[4]Throughout this chapter, the shorthand notation "sup" stands for "ess sup". All computations in this chapter are assumed to be under $\mathbb{Q}$, the risk-neutral measure.

for (4.3.3), we must have

$$V(S_T, \delta_T) \geq S_T - c_1 - c_2.$$

In the absence of transaction costs, the shipping certificate is valued higher than the grain itself, and thus the certificate can be considered a long-side option. The value of the long-side option is quantified with the basis: if T is the maturity of a futures contract, then the basis $w(S_T, \delta_T)$ is the difference between futures and cash prices at maturity

$$w(S_T, \delta_T) = V(S_T, \delta_T) - S_T. \tag{4.3.4}$$

As the shipping certificate, not the spot grain, is the true delivery instrument, the price $F(t, S_t, \delta_t; T)$ of a futures contract expiring at T satisfies the model-free price

$$F(t, S_t, \delta_t; T) = \mathbb{E}[V(S_T, \delta_T)|\mathcal{F}_t], \qquad t \leq T. \tag{4.3.5}$$

From this representation, it follows that the expiring futures price equals the certificate price $F(T, S_T, \delta_T; T) = V(S_T, \delta_T)$.

Intuitively, the agent decides to liquidate when the spot price is sufficiently high. On the other hand, the agent may decide to exercise for two reasons: first if the spot price is sufficiently high, and second if the storage rate δ_t is sufficiently low relative to the certificate rate $\widehat{\delta}$. In the first case, the agent exercises and liquidates (i.e. $\tau^* = \eta^*$), and in the second case, he exercises the shipping certificate but holds the commodity for longer, thus taking advantage of the lower storage rate δ_t until the eventual liquidation.

The stochastic storage rate δ_t is a crucial factor for non-convergence. Indeed, if we instead consider the simple constant storage rate ($\delta_t \equiv \delta$), then the certificate pricing problem (4.3.3)

simplifies to

$$V(S_T,\delta_T)=\sup_{\tau\in\mathcal{T}_{T,\infty}}\sup_{\eta\in\mathcal{T}_{\tau,\infty}}\mathbb{E}\left[e^{-r(\eta-T)}S_\eta-\int_T^\tau(\widehat{\delta}-(c_1+c_2)r)e^{-r(u-T)}du\right.$$
$$\left.-\int_\tau^\eta(\delta-c_2r)e^{-r(u-T)}du|\mathcal{F}_T\right]-c_1-c_2. \tag{4.3.6}$$

By inspecting the value function in (4.3.6), we see that at every time t, the agent effectively has a choice between paying the storage rate $\widehat{\delta}-(c_1+c_2)r$ and the storage rate $\delta-c_2r$. In other words, the agent will immediately lock in the lesser of the two rates. If $\delta-\widehat{\delta}\leq-c_1r$, then the agent exercises immediately at expiration ($\tau^*=T$). On the other hand, if $\delta-\widehat{\delta}>-c_1r$, then the agent liquidates immediately after uploading ($\eta^*=\tau^*$). We recognize instantly that under the assumption of constant storage rates at least one stopping time (τ^* or η^*) is trivial. Either the agent exercises immediately, or he liquidates after exercising. In particular, this fact does not depend at all on the realized path of S. Therefore, a constant storage rate model is insufficient since the shipping certificate is never used for storing the grain for a non-trivial period of time. Since certificate holders empirically store and exercise in a multitude of competitive markets, we must consider a stochastic storage rate δ_t in all our models.

In order to solve for J and V under the dynamics (4.3.1) and (4.3.2), we need to study an ODE. Define the differential operator $\mathcal{L}\equiv\mathcal{L}^{a,b,c}$ by

$$\mathcal{L}=a(b-x)\frac{d}{dx}+\frac{1}{2}c^2\frac{d^2}{dx^2}, \tag{4.3.7}$$

with the generic parameters (a,b,c) with $a,c>0$ and $b\in\mathbb{R}$. This is the infinitesimal generator associated with an OU process. In turn, the ODE

$$\mathcal{L}f(x)-rf(x)=0$$

has the two general classical solutions (see e.g. Borodin and Salminen (2002))

$$H(x;a,b,c) = \int_0^\infty v^{\frac{r}{a}-1} e^{\sqrt{\frac{2a}{c^2}}(x-b)v - \frac{v^2}{2}} dv, \tag{4.3.8}$$

$$G(x;a,b,c) = \int_0^\infty v^{\frac{r}{a}-1} e^{\sqrt{\frac{2a}{c^2}}(b-x)v - \frac{v^2}{2}} dv. \tag{4.3.9}$$

Direct differentiation yields that $H'(x) > 0$, $H''(x) > 0$, $G'(x) < 0$ and $G''(x) > 0$. Hence, both $H(x)$ and $G(x)$ are strictly positive and convex, and they are, respectively, strictly increasing and decreasing. Without ambiguity in this section, we denote $H(\delta) \equiv H(\delta;\kappa,\nu,\zeta)$ and $G(\delta) \equiv G(\delta;\kappa,\nu,\zeta)$ in this section. Alternatively, the functions F and G can be expressed as

$$H(x;a,b,c) = \exp\left(\frac{a}{2c^2}(x-b)^2\right) D_{-r/a}\left(\sqrt{\frac{2a}{c^2}}(b-x)\right),$$
$$G(x;a,b,c) = \exp\left(\frac{a}{2c^2}(x-b)^2\right) D_{-r/a}\left(\sqrt{\frac{2a}{c^2}}(x-b)\right).$$

Here, the function $D_\cdot$ is also known as parabolic cylinder function or Weber function, whose properties are elaborated in detail by Erdelyi and Tricom (1953). The functions F and G will play a crucial role in the solutions for V and J.

Proposition 5. *Under the Martingale Model in* (4.3.1) *and* (4.3.2)*, we have:*

1. *After the shipping certificate is exercised, it is optimal to never liquidate the grain, and the value function $J(S_t,\delta_t) = S_t$, for $t \geq T$.*

2. *The value of the shipping certificate is given by*

$$V(S_t,\delta_t) = S_t + \frac{1}{\kappa+r}\left(\delta_t - \frac{H(\delta_t)}{H'(\delta^*)} - \widehat{\delta} + \frac{\kappa(\nu-\widehat{\delta})}{r}\right)\mathbf{1}\{\delta_t \geq \delta^*\} - c_1\mathbf{1}\{\delta_t < \delta^*\}, \tag{4.3.10}$$

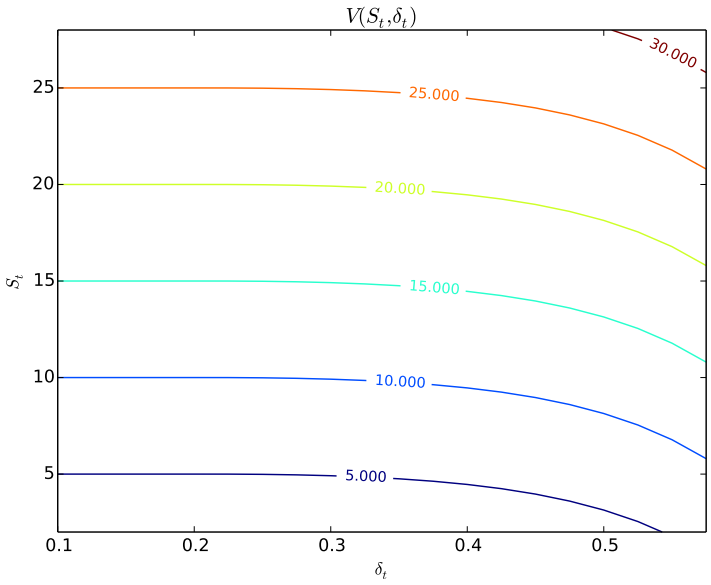

Figure 19: The shipping certificate price $V(S_t, \delta_t)$ as a function of spot price S_t and market storage rate δ_t. Parameters are $r = 0.03$, $c_1 = 0$, $c_2 = 0$, $\kappa = 0.3$, $\zeta = 0.2$, $\nu = 0.07$, $\widehat{\delta} = 0.06$. The optimal exercise level is $\delta^* = 0.21$.

for $t \geq T$, where the unique optimal exercise threshold δ^* solves the equation

$$\delta^* = \frac{H(\delta^*)}{H'(\delta^*)} - c_1(\kappa + r) + \widehat{\delta} - \frac{\kappa(\nu - \widehat{\delta})}{r}. \tag{4.3.11}$$

The optimal exercise and liquidation strategies are respectively given by

$$\tau^* = \inf\{\, t \geq T : \delta_t \leq \delta^* \,\}, \qquad \textit{and} \qquad \eta^* = \infty.$$

We observe from (4.3.10) that the shipping certificate value is separable in terms of the terminal spot price S_T and market storage rate δ_T at time T. As we can see in Figure 19, the shipping certificate price $V(S_T, \delta_T)$ is increasing in both S_T and δ_T, and always dominates S_T. When the market storage rate δ_T is below the critical level δ^* at time T, the shipping certificate price is equal to the spot price S_T, implying an immediate exercise by the holder. In this model, the non-convergence or basis is determined by the market storage rate δ_T since

the exercise and liquidation strategies do not depend on S_T at all.

In fact, the basis is roughly proportional to both the present value of the storage differential $\delta_T - \widehat{\delta}$ and the present value of the the average storage differential $\nu - \widehat{\delta}$. If $\delta_t < \widehat{\delta}$, then the value of the certificate decreases because it is currently cheaper to store at the real rate vs the certificate rate. Furthermore, if $\nu < \widehat{\delta}$, then the average storage rate is lower than the certificate rate, so the value of the shipping certificate decreases. This model explicitly states that agent must consider both the long-run storage differential $\nu - \widehat{\delta}$ and the immediate storage differential $\delta_T - \widehat{\delta}$ in choosing his exercise strategy δ^*. In particular, when we set the parameters $\zeta = 0$, $\kappa = 0$ and $\nu = \delta$, the problem reduces to the case with a constant market storage rate. In this case, the optimal exercise level becomes $\delta^* = \widehat{\delta} - c_1 r$, and the basis is completely linearly proportional to the storage differential $\delta - \widehat{\delta}$. After exercising the shipping certificate and thus receiving the grain, there is no benefit to sell the grain early ($\eta^* = \infty$). This is due to the martingale property of the spot price.

According to Proposition 5, the critical level δ^* determines the time τ^* to exercise the shipping certificate, and thus, plays a role in the non-convergence of the futures at maturity. Indeed, the higher the critical level δ^*, the more likely the agent will exercise the shipping certificate at maturity, resulting in zero non-convergence. In contrast, a low δ^* implies a high likelihood of non-convergence at maturity. In fact, when $c_1 = 0$, the basis $w(S_T, \delta_T) > 0$ if and only if $\delta_T > \delta^*$.

Furthermore, the conditional probability that a T-futures contract expires with a strictly positive basis is given by

$$\mathbb{Q}(w(S_T, \delta_T) > 0 | \mathcal{F}_t) = 1 - \Phi\left(z^*_{t,T}\right), \tag{4.3.12}$$

where

$$\begin{aligned} z^*_{t,T} &= \frac{\delta^* - \bar{\nu}_{t,T}}{\bar{\zeta}_{t,T}}\,, \\ \bar{\nu}_{t,T} &= \delta_t e^{-\kappa(T-t)} + \nu(1 - e^{-\kappa(T-t)})\,, \\ \bar{\zeta}^2_{t,T} &= \frac{\zeta^2}{2\kappa}\left(1 - e^{-2\kappa(T-t)}\right)\,, \end{aligned} \tag{4.3.13}$$

and Φ is the standard normal cdf. In particular, the probability of a strictly positive basis depends solely on the current storage rate δ_t and the long run parameters of $(\delta_t)_{t\geq 0}$. This probability is completely independent of the realization S_t at any time t, or its driving parameters r and σ! Furthermore, since non-convergence at maturity is undesirable behavior, we would like to know precisely how the parameters of our model affect δ^*. Differentiating (4.3.11) with respect to $\widehat{\delta}$, c_1, and ν, respectively, we obtain the sensitivity in each of these parameters.

$$\frac{d\delta^*}{d\widehat{\delta}} = h(\delta^*)\left(1 + \frac{\kappa}{r}\right) \geq 0, \quad \frac{d\delta^*}{d\nu} = -h(\delta^*)\frac{\kappa}{r} \leq 0, \quad \frac{d\delta^*}{dc_1} = -h(\delta^*)\left(\kappa + r\right) \leq 0 \tag{4.3.14}$$

where we have defined

$$h(\delta^*) := \frac{H'(\delta^*)^2}{H(\delta^*)H''(\delta^*)} \geq 0.$$

The function h is positive because H is positive, increasing, and convex. Therefore, we deduce the properties of the optimal exercise threshold δ^*.

Corollary 1. *Under the Martingale Model defined in* (4.3.1) *and* (4.3.2)*, the optimal stopping threshold δ^* is increasing with respect to $\widehat{\delta}$, but decreasing with respect to ν and c_1.*

Having solved the certificate pricing problem, we proceed to examine how the storage optionality propagates to futures prices. At time T, the agent will exercise if storage rate δ_T is lower than the critical level δ^*. Therefore, a higher δ^* increases the chance an agent will

exercise the shipping certificate immediately upon the futures expiration. A higher certificate storage rate $\widehat{\delta}$ increases δ^* and hence lowers the probability of non-convergence. On the other hand, a higher average storage rate ν increases the probability of non-convergence. This occurs due to the incentive to store in the cheaper market: if the certificate storage rate is higher (resp. lower) than the market rate, then the agent will exercise sooner (resp. lower).

When calculating the derivatives in (4.3.14), the magnitude of each derivative is roughly proportional to κ, the rate of mean reversion of the storage rate δ_t. Indeed, as κ increases, the long run effect of ν dominates, acting as an amplifier on δ^*. Therefore, under higher κ, if the storage differential $\nu - \widehat{\delta}$ is positive, the basis increases more, whereas if $\nu - \widehat{\delta}$ is negative, the basis increases less. Intuitively, since the value c_1 increases the agent's cost to exercise, it is expected, as seen in (4.3.14), that δ^* is decreasing in c_1. Lastly, after exercising, the agent's liquidation timing η^* is trivial, so the liquidation cost c_2 does not affect the exercise level δ^*.

Next, we compute the futures price using the shipping certificate price given in Proposition 5. It follows from the property of the OU process that $\delta_T|\delta_t$ is normally distributed with parameters $\bar{\nu}_{t,T}$ and $\bar{\zeta}_{t,T}$ which are given in (4.3.13). Following the definition in (4.3.5), the futures price is given by

$$\begin{aligned} F(t, S_t, \delta_t; T) = \quad & \mathbb{E}\left[S_T|\mathcal{F}_t\right] + \frac{1}{\kappa + r}\mathbb{E}\left[\left(\delta_T - \frac{H(\delta_T)}{H(\delta^*)} - \widehat{\delta} + \frac{\kappa(\nu - \widehat{\delta})}{r}\right)\mathbf{1}\{\delta_T \geq \delta^*\}|\mathcal{F}_t\right] \\ & - c_1\mathbb{Q}(\delta_T < \delta^*|\mathcal{F}_t)\,. \end{aligned}$$

By computing the conditional truncated expectations of S_T and δ_T, we obtain an explicit formula for the futures price.

Corollary 2. *Under the Martingale Model defined in* (4.3.1) *and* (4.3.2)*, the grain futures price is given by*

$$\begin{aligned} F(t,S_t,\delta_t;T) = \quad & e^{r(T-t)}\left[S_t+\frac{\nu}{r}\left(1-e^{-r(T-t)}\right)+\frac{\delta_t-\nu}{\kappa+r}\left(1-e^{-(\kappa+r)(T-t)}\right)\right] \\ & +\frac{1}{\kappa+r}\left[\bar{\nu}_{t,T}+\frac{\phi\left(z^*_{t,T}\right)}{1-\Phi\left(z^*_{t,T}\right)}\bar{\zeta}_{t,T}-\int_{z^*_{t,T}}^{\infty}\frac{H(\bar{\nu}_{t,T}+\bar{\zeta}_{t,T}u)}{H'(\delta^*)}\phi(u)du\right. \\ & \left.+\left(\frac{\kappa(\nu-\widehat{\delta})}{r}-\widehat{\delta}\right)\left(1-\Phi\left(z^*_{t,T}\right)\right)\right]-c_1\Phi\left(z^*_{t,T}\right), \qquad t\le T, \end{aligned} \tag{4.3.15}$$

where $z^*_{t,T}$, $\bar{\nu}_{t,T}$ *and* $\bar{\zeta}_{t,T}$ *are given in* (4.3.13)*, and* ϕ *and* Φ *are the standard normal pdf and cdf respectively.*

We note that like the shipping certificate prices, futures prices can be separated into an expectation that depends on S_t and another involving δ_t. Despite the separation, since δ_t appears in the diffusion for S_t, the two stochastic factors are not independent. The futures price encapsulates a number of components: (i) the risk-neutral expectation of the future spot price; (ii) expected future basis $w(S_T,\delta_T)$ (see (4.3.4)); and (iii) expected future exercise cost c_2. Thus, by accounting for the expected future basis resulting from the storage differential $\delta_t-\widehat{\delta}$, the futures price for all $t\le T$ in a market with shipping certificates carries a premium over the price of a futures contract that delivers just the grain at time T. We therefore demonstrate that anticipated future storage differentials can impact current futures prices, including the contracts that are far from expiry.

With an understanding on the theoretical behavior of grain futures prices under the Martingale Model, we now calibrate to empirical data, and discuss the results and economic implications. We obtain futures prices from 2004-2011 for CBOT corn, wheat and soybeans contracts using Bloomberg terminal. We obtain spot prices from 2004-2011 for CBOT corn,

wheat, and soybeans from an average of daily sale prices of several Illinois grain depots.[5] We also obtain the empirical certificate storage rate $\widehat{\delta}$, quoted in $\$/bushel$, from the CBOT website.[6,7] For the interest rate in our model, we use the 3-month LIBOR rate observed on the same date. There are several quoted prices for spot grain, differing only in the quality of the grain. This quality option allows the short to choose the grade he wishes to deliver, subject to some prior fixed conversion multiplier of the settlement price. In order to obtain a single series of spot prices, for every time t we use the then cheapest-to-deliver price as the spot price for grain.

Recall that the basis $w(S_T, \delta_T)$ is the premium of the certificate price $V(T, S_T)$ over the spot price S_T. at time T. On the day $t = 0$, we have the empirical futures prices $(F_k)_{k=0}^N$ with maturities $(T_k)_{k=0}^N$, and a known spot price $F_0 = S_0$; we seek a model-consistent futures curve $\mathbf{F}_k(\nu, \kappa, \zeta, \delta_0)$ for $k = 0, 1, \ldots, N$ which best fits the empirical futures prices, given model parameters (ν, κ, ζ) and δ_0, with the model futures prices given in (4.3.15). Under this setup, the best fit calibrated futures curve $\mathbf{F}_k^*$ for $k = 0, 1, \ldots, N$ minimizes the sum of squared errors (SSE) between the empirical futures curve and the model futures curve. Furthermore, the best-fit parameters are defined to be $(\nu^*, \kappa^*, \zeta^*, \delta_0^*)$ the model parameters which achieve the best fit futures curve. The other exogenous parameters $(r, S_t, \widehat{\delta}, c_1, c_2)$ are directly determined via contract specifications. Precisely, the calibrated parameters and the resulting futures curve are found from

$$(\nu^*, \kappa^*, \zeta^*, \delta_0^*) = \underset{\nu,\kappa,\zeta,\delta_0}{\arg\min} \sum_{k=0}^{N} (F_k - \mathbf{F}_k(\nu, \kappa, \zeta, \delta_0))^2$$

$$\mathbf{F}_k^* = \vec{\mathbf{F}}(\nu^*, \kappa^*, \zeta^*, \delta_0^*) \qquad k = 0, 1, \ldots N.$$

[5] http://www.farmdoc.illinois.edu/MARKETING/INDEX.ASP

[6] http://www.cmegroup.com/rulebook/CBOT/II/n/m.pdfwhere$(n,m)\in\protect\T1\textbraceleft(10,10),(11,11),(14,14)\protect\T1\textbraceright.$

[7] As a result of the certificate rate $\widehat{\delta}$ increase in 2009, the size of the empirical basis became smaller afterward. However, a large strictly positive basis can still manifest in the future if the market storage rate δ_t is significantly higher than the new certificate rate $\widehat{\delta}$.

In Figure 20, we calibrate the Martingale Model to the corn futures prices on two dates selected to show two characteristically different futures curves. On the left panel, the futures curve is downward sloping. With the expiring futures price and spot price being \$3.17 and \$2.81, respectively, a positive basis is observed. Intuitively, given that the current market storage rate is higher than the certificate rate ($\delta_0^* > \widehat{\delta}$), the agent thus prefers the certificate storage rate over the market rate and will wait to exercise the certificate, resulting in a positive basis. The current storage rate δ_0^* is also higher than the estimated long-run storage rate ν^*. Therefore, the model suggests that in the long run, a convenience yield will dominate, leading to a downward sloping futures curve. In contrast, the right panel also reflects a positive basis, but the futures curve is upward sloping.

Figure 21 displays the calibrated futures curves under the Martingale Model for wheat on two dates when the futures market is in backwardation and contango, respectively. Again, non-convergence is observed on each of these two dates as the expiring futures price dominates the spot price. On the left panel, the futures curve is upward sloping while the right panel shows that the futures curve is downward sloping. In this case, the current market storage rate satisfies $\delta_0^* > \widehat{\delta}$, so it is optimal for the agent to continue to store at the lower certificate storage rate. Hence, the value of the associated timing option to exercise the shipping certificate yields a positive basis.

In addition, we consider the differences between the model futures curve and the futures curve generated without considering the timing options. To be precise, let the 'no certificate' futures price $\psi(t, S_t, \delta_t; T)$ be

$$\begin{aligned} \psi(t, S_t, \delta_t; T) &= \mathbb{E}[S_T|\mathcal{F}_t], \\ &= e^{r(T-t)}\left[S_t + \frac{\nu}{r}\left(1 - e^{-r(T-t)}\right) + \frac{\delta_t - \nu}{\kappa + r}\left(1 - e^{-(\kappa+r)(T-t)}\right)\right]. \end{aligned} \tag{4.3.16}$$

This follows from direct calculations and resembles the first line of (4.3.15). In Figure 20, we plot the values of $\psi(0, S_0, \delta_0^*; T_i)$ for $i = 0 \ldots N$, using the same fitted parameters from our

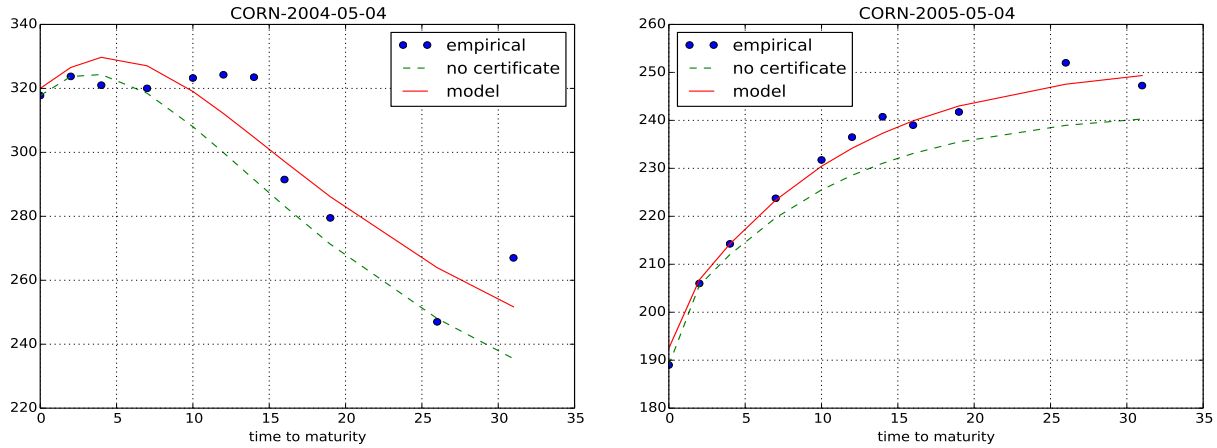

Figure 20: Calibrating the Martingale Model to empirical corn futures prices. The x-axis is time to maturity in months and the y-axis is the price of a bushel of corn in *cents*. The 'no certificate' curve is taken from equation (4.3.16). We use the fitted parameters from the 'model' curve as inputs for the 'no certificate' curve to illustrate the premium. Fitted parameters: (left) $\nu^* = -0.48$, $\kappa^* = 0.0015$, $\zeta^* = 0.0161$, and $\delta_0^* = 1.2532$; (right) $\nu^* = 0.832$, $\kappa^* = 0.021$, $\zeta^* = 0.428$, and $\delta_0^* = 0.782$. Other parameters are $r = 0.017$, $S_0 = \{282, 167\}$ (cents), $\widehat{\delta} = 0.55$, and $c_1, c_2 = 0$.

model $(\nu^*, \kappa^*, \zeta^*, \delta_0^*)$ and the constraint that $S_t = F_0$, the empirical terminal futures price. In other words, we ignore the data on spot grain prices, so there is initially zero basis, as would be the case under physical delivery, as opposed to receiving the shipping certificate upon expiration. As expected, the model futures prices with shipping certificate dominate the those without one, for all maturities. As seen in Figure 20, the premium of the shipping certificate over the spot as the delivery item tends to be higher for longer maturities. Finally, the Martingale Model fits both backwardated and upward-sloping futures curves well.

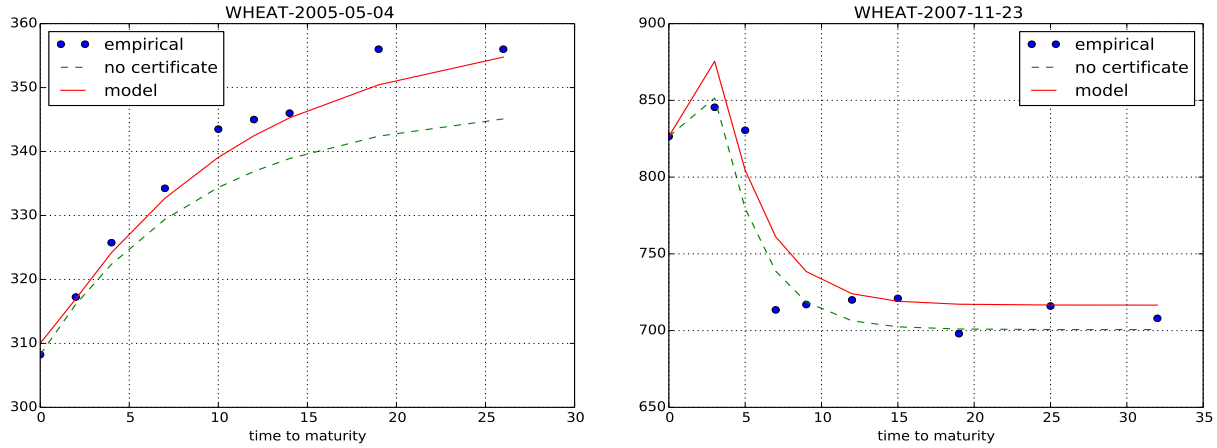

Figure 21: Calibrating the Martingale Model to empirical wheat futures prices. The x-axis is time to maturity in months and the y-axis is the price of a bushel of wheat in *cents*. The 'no certificate' curve is taken from equation (4.3.16). Fitted parameters: (left) $\nu^* = 0.91$, $\kappa^* = 0.035$, $\zeta^* = 0.14$, and $\delta_0^* = 0.871$; (right) $\nu^* = -0.22$, $\kappa^* = 0.0032$, $\zeta^* = 0.61$, and $\delta_0^* = 1.44$. We use the fitted parameters from the 'model' curve as inputs for the 'no certificate' curve to illustrate the premium. Other parameters are $r = 0.017$, $S_0 = \{273, 772\}$ (cents), $\widehat{\delta} = 0.55$, and $c_1, c_2 = 0$.

Commodity	Average Basis (pre)	Max Basis (pre)	Average Basis (post)	Max Basis (post)
Corn	9.11%	27.52%	2.54%	13.50%
Soybeans	4.31%	12.96%	0.89%	5.61%
Wheat	1.32%	14.10%	-0.97%	7.05%

Table 9: Basis summary during 2004-2014 before (pre) and after (post) CBOT introduced new certificate policies to facilitate convergence in the corn, soybeans, and wheat futures markets. For corn and soybeans futures, the policy changed in in January 2011. For wheat contracts, a variable storage rate policy was introduced in July 2010. For comparison across commodities, the basis here is computed in percentage at expiration according to [(futures price/spot price)-1]$\times$100%.

Our model postulates that the non-convergence occurs when the market storage rate is significantly higher than the certificate storage rate. Therefore, if the two rates are brought into alignment, we expect that the basis to diminish. Indeed, after years of high basis, the two exchanges, CBOT and KCBOT, enacted a series of reforms on the wheat futures to address the non-convergence phenomenon. During February 2009 to May 2011, both exchanges instituted a one-time hike in the formerly constant storage rates, and subsequently adopted a *variable* certificate storage rate for all wheat contracts, thus better aligning the certificate and market storage rates. For corn and soybeans, the exchanges merely raised the constant certificate storage rates once in Jan 2011. According to (4.3.12), these policy changes would decrease the likelihood of non-convergence. In Table 9, we compare the average basis before and after the policy implementation for each commodity. The average basis decreased by 6.57% for corn, 3.42% for soybeans, and 2.29% for wheat, suggesting that the effectiveness of changing the certificate storage rate. In fact, the study by Aulerich and Hoffman (2013) finds that introducing a variable certificate storage rate can significantly reduce non-convergence.[8]

[8]See also the CME Group report, "The Impact of Variable Storage Rates on Liquidity of the Deferred Month CBOT Wheat Futures" in 2010.

4.4 Local Stochastic Storage Model

We now consider an alternative to the Martingale Model. Since the commodity cannot necessarily be continuously traded, the market is incomplete, and one can specify a non-martingale evolution for the commodity price under the no-arbitrage risk-neutral measure. Commodities have the unique property that production can be increased or decreased in response to high or low prices, respectively. In addition, commodities can be consumed through production of end-goods (for example, turning corn into ethanol). In times of scarcity, production will increase to lower prices; in times of surplus, production will decrease while consumption continues to increase prices. Thus, the production and consumption process unique to commodities imply a mean-reverting price structure as suggested by Deaton and Laroque (1996).

Hence, we propose an exponential OU (XOU) model for the spot price. Under the risk-neutral measure $\mathbb{Q}$, the log-spot price of the grain, denoted by $U_t = \log S_t$, follows the OU process

$$dU_t = \alpha(\mu - U_t)dt + \sigma dW_t, \tag{4.4.1}$$

where W is standard Brownian motion under $\mathbb{Q}$, μ is the long-run mean, α is the rate of mean reversion, and σ is the volatility of the log-spot price. We impose the further regularity condition that $\sigma < \sqrt{2\alpha}$.

The market rate of storage δ_t is locally determined by the spot price through

$$\delta_t = \beta U_t + \gamma. \tag{4.4.2}$$

We typically set the coefficient $\beta \geq 0$ so that the storage cost increases linearly with the log-price of the commodity, with a possibly flat storage rate $\gamma > 0$. In summary, we have described a local stochastic storage approach, whereby the market storage rate in (4.4.2) is a function of the stochastic spot price that follows the exponential OU model in (4.4.1).

Henceforth, we shall refer it as the XOU Model.

Denote by $\mathbb{G} \equiv (\mathcal{G}_t)_{t\geq 0}$ the filtration generated by the log-spot price $(U_t)_{t\geq 0}$. Also, let $\mathcal{S}$ be the set of all $\mathbb{G}$-stopping times, and $\mathcal{S}_{s,u}$ the set of $\mathbb{G}$-stopping times bounded by $[s,u]$. Note that δ_t is a function of U_t, the optimal liquidation problem is given by

$$J(U_t) = \sup_{\eta\in\mathcal{S}_{t,\infty}} \mathbb{E}\left[e^{-r(\eta-t)}\left(\exp(U_\eta) - c_2\right) - \int_t^\eta \delta_u e^{-r(u-t)}du|\mathcal{G}_t\right],$$

which applies after the shipping certificate is exercised at time τ. The optimal timing problem to exercise the shipping certificate is given by

$$V(U_T) = \sup_{\tau\in\mathcal{S}_{T,\infty}} \mathbb{E}\left[e^{-r(\tau-T)}\left(J(U_\tau) - c_1\right) - \int_T^\tau \widehat{\delta} e^{-r(u-T)}du|\mathcal{G}_T\right].$$

Since the shipping certificate serves as the delivery item instead of the actual grain, the futures price $F(t,U_t;T)$ at t for the contract expiring at T is given by

$$F(t,U_t;T) = \mathbb{E}[V(U_T)|\mathcal{G}_t].$$

We now denote the operator from (4.3.7) by $\mathcal{L} \equiv \mathcal{L}^{\alpha,\mu,\sigma}$, which is the infinitesimal generator for the OU process U. To solve for the certificate price and the agent's optimal policy, we solve the ODE

$$\mathcal{L}f(u) - rf(u) = 0,$$

which has the general solutions, $H(u;\alpha,\mu,\sigma)$ and $G(u;\alpha,\mu,\sigma)$, where $\mathcal{L}$, H, and G are defined in (4.3.7), (4.3.8) and (4.3.9). In this section, without ambiguity, we denote $H(u) \equiv H(u;\alpha,\mu,\sigma)$ and $G(u) \equiv G(u;\alpha,\mu,\sigma)$, both of which will play a role in the solution for J and V.

Proposition 6. *Under the XOU Model defined in* (4.4.1) *and* (4.4.2)*:*

1. *The liquidation value is given by*

$$J(u) = \begin{cases} AH(u) - \frac{1}{\alpha+r}\left[\beta u + \gamma + \frac{\alpha(\beta\mu+\gamma)}{r}\right] & \text{if } u < u^*, \\ e^u - c_2 & \text{if } u \geq u^*. \end{cases} \tag{4.4.3}$$

2. *The certificate price is given by*

$$V(u) = \begin{cases} e^u - c_1 - c_2 & \text{if } u > \overline{u}^{**}, \\ BH(u) + CG(u) - \frac{\widehat{\delta}}{r} & \text{if } \underline{u}^{**} \leq u \leq \overline{u}^{**}, \\ AH(u) - \frac{1}{\alpha+r}\left[\beta u + \gamma + \frac{\alpha(\beta\mu+\gamma)}{r}\right] - c_1 & \text{if } u < \underline{u}^{**}, \end{cases} \tag{4.4.4}$$

where

$$\begin{aligned} A &= \frac{e^{u^*} + \frac{\beta}{\alpha+r}}{H'(u^*)}\,, \\ B &= \frac{e^{\overline{u}^{**}} G'(\underline{u}^{**}) - \left(AH'(\underline{u}^{**}) - \frac{\beta}{\alpha+r}\right) G'(\overline{u}^{**})}{H'(\overline{u}^{**})G'(\underline{u}^{**}) - H'(\underline{u}^{**})G'(\overline{u}^{**})}\,, \\ C &= \frac{e^{\overline{u}^{**}} H'(\underline{u}^{**}) - \left(AH'(\underline{u}^{**}) - \frac{\beta}{\alpha+r}\right) H'(\overline{u}^{**})}{H'(\underline{u}^{**})G'(\overline{u}^{**}) - H'(\overline{u}^{**})G'(\underline{u}^{**})}\,, \end{aligned}$$

and the optimal thresholds u^*, $\overline{u}^{**}$ and $\underline{u}^{**}$ satisfy the equations:

$$\begin{aligned} AH(u^*) - \frac{1}{\alpha+r}\left[\beta u^* + \gamma + \frac{\alpha(\beta\mu+\gamma)}{r}\right] &= e^{u^*} - c_2\,, \\ BH(\overline{u}^{**}) + CG(\overline{u}^{**}) - \frac{\widehat{\delta}}{r} &= e^{\overline{u}^{**}} - c_1 - c_2\,, \\ BH(\underline{u}^{**}) + CG(\underline{u}^{**}) - \frac{\widehat{\delta}}{r} &= AH(\underline{u}^{**}) - \frac{1}{\alpha+r}\left[\beta \underline{u}^{**} + \gamma + \frac{\alpha(\beta\mu+\gamma)}{r}\right] - c_1. \end{aligned}$$

The optimal exercise and liquidation times, respectively, are given by

$$\tau^* = \inf\{\, t \geq T : U_t \leq \underline{u}^{**} \;\; or \;\; U_t \geq \overline{u}^{**} \,\},$$
$$\eta^* = \inf\{\, t \geq \tau^* : U_t \geq u^* \,\}.$$

The liquidation value $J(u)$ is entirely determined by the critical level u^* at which the agent will sell the physical grain. When the log-spot price U_t surpasses u^*, both the storage cost δ_t and spot price S_t will be high. Since the asset price is mean-reverting, intuitively there is a potential advantage to early liquidation before the asset reverts back to a lower value. In the holding region $\{u < u^*\}$ corresponding to low spot prices, the agent pays the present value of the storage rate $\beta u + \gamma$, and the present value of the average storage rate $\beta\mu + \gamma$. The conflict between increasing spot prices and higher storage rates, both of which are driven by U_t, determines when the agent liquidates. Thus, both instantaneous storage rates and the long-run storage rates affect the certificate price.

On the other hand, the certificate value $V(u)$ is determined by *two* stopping levels: the optimal exercise threshold $\underline{u}^{**}$ and the optimal liquidation threshold $\overline{u}^{**}$. When the spot price surpasses $\overline{u}^{**}$, the agent exercises *and* liquidates to take advantage of temporarily higher spot prices, while avoiding higher storage rates. On the other hand, when the spot price decreases below $\underline{u}^{**}$, the agent exercises but does *not* liquidate, because he wants to take advantage of a temporarily lower storage rate, storing in the real market at rate δ_t instead of at the certificate rate $\widehat{\delta}$. Recall that due to our specification of the optimal stopping times η^* and τ^*, the stopping levels satisfy $\overline{u}^{**} \geq u^* \geq \underline{u}^{**}$.

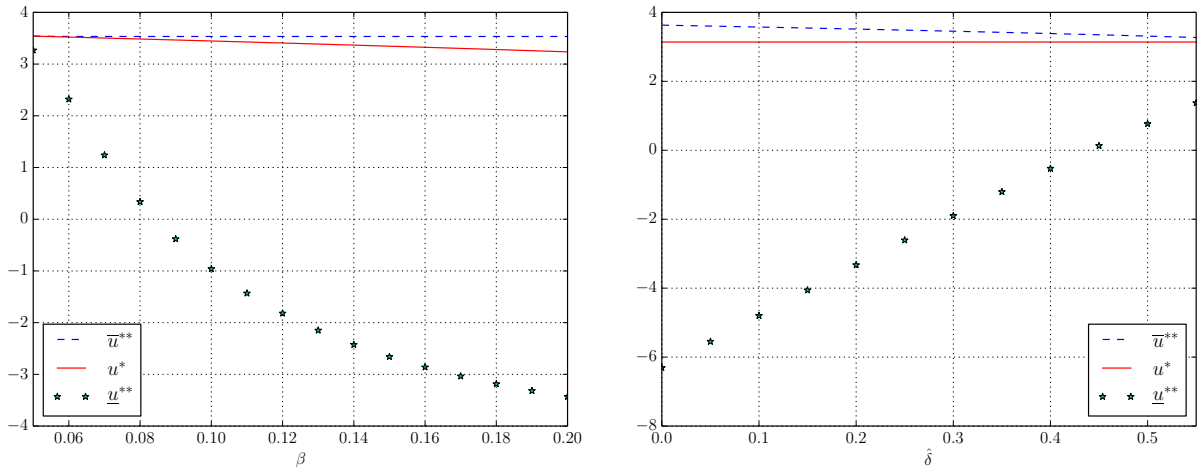

Figure 22: Optimal stopping levels for $[\underline{u}^{**}, u^*, \overline{u}^{**}]$, with default parameters $r = 0.03$, $U_t = \log 5$, $\gamma = 0$, $\widehat{\delta} = 0.2$, $\beta = 0.08$, $c_1 = 0$, $c_2 = 0$, $\mu = \log 30$, $\alpha = 0.1$, $\sigma = 0.2$. We vary the parameters β and $\hat{\delta}$ respectively in these plots.

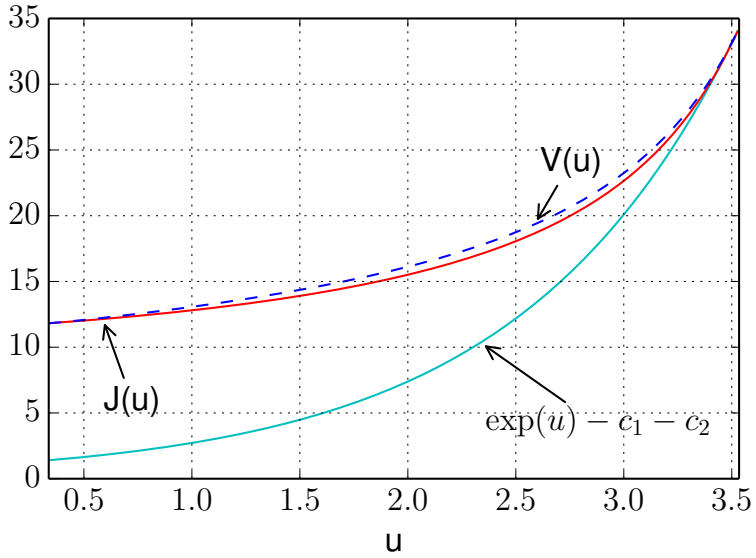

Figure 23: Immediate value $\exp(u) - c_1 - c_2$, liquidation value $J(u)$, and certificate price $V(u)$. The optimal stopping levels are given by $\underline{u}^{**} = 0.337$, $u^* = 3.485$, $\overline{u}^{**} = 3.534$. Parameters are $r = 0.03$, $\gamma = 0$, $\widehat{\delta} = 0.17$, $\beta = 0.10$, $c_1 = 0$, $c_2 = 0$, $\mu = \log 30$, $\alpha = 0.1$, $\sigma = 0.2$.

Figure 22 further illustrates the dependence of the three stopping levels $[\underline{u}^{**}, u^*, \overline{u}^{**}]$ on the parameters β and $\widehat{\delta}$. As β increases, the gap between $\underline{u}^{**}$ and $\overline{u}^{**}$ increases, so does the basis. However, as $\beta \to 0$, the market storage rate goes to 0 in this example, inducing the agent to exercise as soon as the futures expires and store in the real market. Consequently, the region $\{\underline{u}^{**}, \overline{u}^{**}\}$ for holding the certificate vanishes, which also means that all three thresholds, $\underline{u}^{**}, u^*$, and $\overline{u}^{**}$ converge to the same value representing the optimal level to liquidate the grain. A similar pattern is observed when the certificate storage rate $\widehat{\delta}$ increases since the agent will again be incentivized to exercise the shipping certificate immediately to store in the real market.

Figure 23 also reflects the relationship among the certificate price, liquidation value, and payoff from immediate exercise and liquidation. Note that

$$V(u) \geq J(u) \geq \exp(u) - c_1 - c_2,$$

i.e. the shipping certificate price dominates the liquidation value, which convexly dominates the immediate exercise value. The liquidation value is significantly higher than the immediate exercise value, especially as $u \to -\infty$. The value of $J(u)$ does not decrease as much as the immediate exercise value. Because the asset is mean reverting and the optionality is perpetual, the asset value is almost guaranteed to be eventually profitable. In this model, the ability to choose between two rates of storage adds merely a modest basis to the liquidation value. With the parameters in Figure 22, the maximum percent difference between $V(u)$ and $J(u)$ is 12.57%.

Recall that the basis $w(U_t)$ is defined as the difference between certificate and spot prices at maturity. As we established from a model-free argument, the basis $w(U_t) \geq 0$. Therefore, a positive basis occurs when the agent chooses a strategy which is different than exercising and liquidating ($\eta^* > \tau > T$). In this scenario, the agent either waits to exercise because storage rates are too high to exercise and spot prices are too low to liquidate, or he has

exercised to take advantage of lower storage prices but the spot price is too low to liquidate. In our model the probability of non-convergence depends completely on $\overline{u}^{**}$. In particular, if $c_1 = 0$ and $c_2 = 0$, then the basis $w(U_T) > 0$ iff $U_T < \overline{u}^{**}$. Thus, the probability that there is a strictly positive basis at time t for a contract maturing at $T \geq t$ is

$$\mathbb{Q}\left(w(U_T) > 0 \,|\, \mathcal{G}_t\right) = \Phi\left(\frac{\overline{u}^{**} - \bar{\mu}_{t,T}}{\bar{\sigma}_{t,T}}\right),$$

where

$$\begin{aligned} \bar{\mu}_{t,T} &= U_t e^{-\alpha(T-t)} + \mu(1 - e^{-\alpha(T-t)}), \\ \bar{\sigma}^2_{t,T} &= \frac{\sigma^2}{2\alpha}(1 - e^{-2\alpha(T-t)}). \end{aligned} \tag{4.4.5}$$

Finally, in order to calibrate our model for empirical analysis, we derive futures prices by taking an expectation of the certificate prices.

Under the OU model, the conditional log spot price $U_T|U_t$ is normally distributed with parameters $\bar{\mu}_{t,T}$ and $\bar{\sigma}_{t,T}$ given in (4.4.5). The result then follows from computing the associated conditional truncated expectations:

$$\begin{aligned} F(t, U_t; T) = \quad & \mathbb{E}\left[\left(e^{U_T} - c_1 - c_2\right)\mathbf{1}\{U_T > \overline{u}^{**}\}|U_t\right] \\ & + \mathbb{E}\left[\left(BH(U_T) + CG(U_T) - \frac{\widehat{\delta}}{r}\right)\mathbf{1}\{\underline{u}^{**} \leq U_T \leq \overline{u}^{**}\}|U_t\right] \\ & + \mathbb{E}\left[\left(AH(u) - \frac{1}{\alpha + r}\left[\beta U_T + \gamma + \frac{\alpha(\beta\mu + \gamma)}{r}\right] - c_1\right)\mathbf{1}\{U_T < \underline{u}^{**}\}|U_t\right] \end{aligned}$$

Corollary 3. *The futures price $F(t, U_t; T)$ under the XOU Model defined in* (4.4.1) *and* (4.4.2) *is given by*

$$
\begin{aligned}
F(t,U_t;T) = \quad & \exp\left(\bar{\mu}_{t,T}+\frac{\bar{\sigma}_{t,T}^2}{2}\right)\frac{\Phi\left(\bar{\sigma}_{t,T}-\overline{z}_{t,T}^{**}\right)}{1-\Phi\left(\overline{z}_{t,T}^{**}\right)}-(c_1+c_2)\left(1-\Phi\left(\overline{z}_{t,T}^{**}\right)\right)\\
&+\int_{\underline{z}_{t,T}^{**}}^{\overline{z}_{t,T}^{**}}(BH(\bar{\mu}_{t,T}+\bar{\sigma}_{t,T}v)+CG(\bar{\mu}_{t,T}+\bar{\sigma}_{t,T}v))\phi(v)dv\\
&-\frac{\widehat{\delta}}{r}\left(\Phi\left(\overline{z}_{t,T}^{**}\right)-\Phi\left(\underline{z}_{t,T}^{**}\right)\right)+\int_{-\infty}^{\underline{z}_{t,T}^{**}}AH(\bar{\mu}_{t,T}+\bar{\sigma}_{t,T}v)dv\\
&-\frac{\beta}{\alpha+r}\left(\bar{\mu}_{t,T}-\frac{\phi\left(\underline{z}_{t,T}^{**}\right)}{\Phi\left(\underline{z}_{t,T}^{**}\right)}\bar{\sigma}_{t,T}\right)-\left(\frac{\gamma}{\alpha+r}+\frac{\alpha(\beta\mu+\gamma)}{r(\alpha+r)}+c_1\right)\Phi\left(\underline{z}_{t,T}^{**}\right),
\end{aligned}
$$

where

$$
\overline{z}_{t,T}^{**}=\frac{\overline{u}^{**}-\bar{\mu}_{t,T}}{\bar{\sigma}_{t,T}},\qquad \underline{z}_{t,T}^{**}=\frac{\underline{u}^{**}-\bar{\mu}_{t,T}}{\bar{\sigma}_{t,T}},
$$

and $\bar{\mu}_{t,T}$, *and* $\bar{\sigma}_{t,T}$ *are defined in* (4.4.5).

We calibrate our model futures curve to empirical corn, wheat and soybeans data and consider the accuracy and economic implications. Refer to Table 9 for details of each contract's specification. Consider the futures curve at time $t=0$. Recall that the best-fit futures curve can be defined in the following manner. Let the futures prices at time T_k be F_k, for maturity times $(T_k)_{k=0}^N$, with $F_0=\exp(U_0)=S_0$, so the futures price at $T_0=0$ is just the market quoted settlement price. Denote the model futures curve generated at time T_k by the parameters $(\beta,\gamma,\mu,\alpha,\sigma)$ be denoted $\mathbf{F}_k(\beta,\gamma,\mu,\alpha,\sigma)$.

The best fit futures curve $\mathbf{F}_k^*$ for $k=0,1,\ldots,N$ minimizes the weighted sum of squared errors (SSE) between the empirical futures curve and the model futures curve at time t. Furthermore, the best-fit parameter is defined to be $(\beta^*,\gamma^*,\mu^*,\alpha^*,\sigma^*)$ the model parameters which achieve the best fit futures curve. The other exogenous parameters $(r,U_t,\widehat{\delta},c_1,c_2)$ are

directly determined via contract specifications (see Table 9).

$$(\beta^*, \gamma^*, \mu^*, \alpha^*, \sigma^*) = \underset{\beta,\gamma,\mu,\alpha,\sigma}{\arg\min} \sum_{k=0}^{N} (F_k - \mathbf{F}_k(\beta, \gamma, \mu, \alpha, \sigma))^2$$

$$\mathbf{F}_k^* = \mathbf{F}_k(\beta^*, \gamma^*, \mu^*, \alpha^*, \sigma^*) \qquad k = 0, 1, \ldots, N.$$

The *corn* futures curves calibrated from the XOU Model are illustrated in Figure 24. We have selected the two dates to illustrate two characteristically different futures curves. On the left panel, the futures curve that is upward sloping. With the expiring futures price and spot price being 317 and 281 (cents), respectively, a positive basis is observed. The current storage rate $\delta_0^* = 106.00$, and the long run storage rate $\beta^*\mu^* + \gamma^* = 89.55$ are both higher than the certificate rate $\widehat{\delta}$. This storage rate spread leads to the positive basis, while the long run storage rate anticipates a future basis. Furthermore, the current spot price $U_0 > \mu^*$, which indicates that the spot price will likely fall in the future, and results in a downward-sloping futures curve. On the right panel, the futures curve is upward sloping and the basis is more modest. The spot price current satisfies $U_0 < \mu^*$, so the spot price is expected to rise in the future, generating a more contango futures curve.

In Figure 25, we see the results of our empirical calibration under the XOU model for *wheat* on two dates. The left panel shows a basis of around 12%, and the futures curve is upward sloping. The current storage rate $\delta_0^* = 67.21$, and the long run storage rate $\beta^*\mu^* + \gamma^* = 69.84$ are both higher than the certificate rate $\widehat{\delta}$. Therefore, the current storage rate leads to a positive basis, while the long run storage rate anticipates a future basis. Furthermore, the current spot price $U_0 < \mu^*$, which indicates that the spot price will likely rise in the future, and results in an upward-sloping futures curve. In Figure 25 (right), the basis is more modest at 5%, while the futures curve is downward sloping. The current storage rate $\delta_0^* = 60.71$, is higher than the certificate storage rate, but the long run storage rate $\beta^*\mu^* + \gamma^* = 53.87$ is lower than the certificate rate $\widehat{\delta}$. Therefore, the current storage rate generates a smaller positive basis, while the long run storage rate anticipates little to no

basis on the futures curve. Furthermore, the current spot price is higher than the estimated long-run mean ($U_0 > \mu^*$), and the backwardated futures curve reflects the anticipation that the spot price will decrease in the future. This is consistent with the model's mean-reverting dynamics for the spot price.

In addition, we consider the differences between the model futures curve and the futures curve generated without considering the timing options. To be precise, let the 'no certificate' futures curve $\psi(t, U_t, \delta_t; T)$ be

$$\begin{aligned}\psi(t, U_t; T) &= \mathbb{E}[S_T|\mathcal{G}_t] \\ &= \exp\left(e^{-\alpha(T-t)}U_t + \mu(1 - e^{-\alpha(T-t)}) + \frac{\sigma^2}{4\mu}(1 - e^{-2\alpha(T-t)})\right), \qquad (4.4.6)\end{aligned}$$

which can be found in (Leung et al., 2016, Sect. 2.2). In Figure 25, we plot the futures curve, described by $\psi(0, U_0; T_i)$ for $i = 0 \dots N$, using the same fitted parameters from our model $(\mu^*, \alpha^*, \sigma^*)$ and the initial assumption that $\exp(U_0) = F_0$, the empirical terminal futures price. In other words, for the no-certificate case, we take the expiring futures price to be the spot price, and ignore the entire spot grain market prices. The last assumption means there is initially zero basis, as would be the case when physical grain is the delivery item.

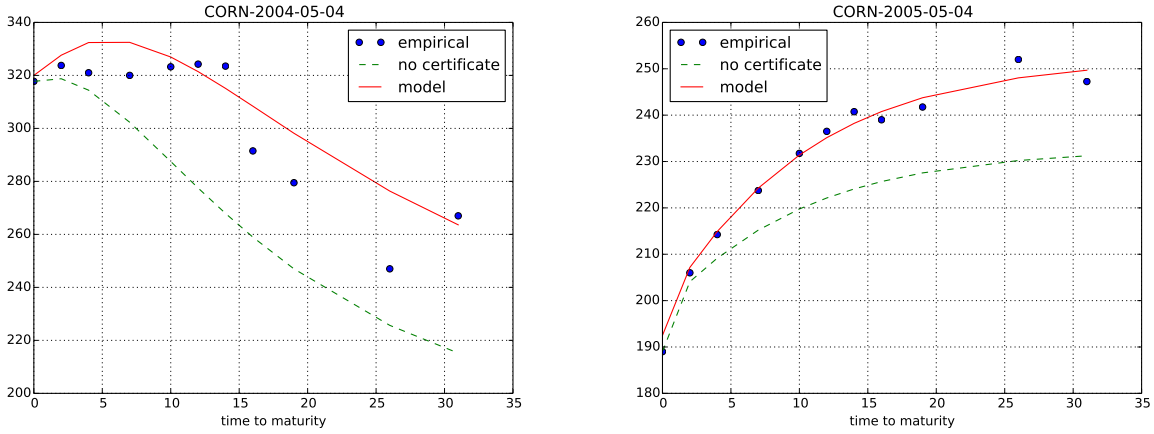

Figure 24: Calibrating the XOU Model to the empirical corn futures prices. The x-axis is time to maturity in months and the y-axis is the price of a bushel of corn in *cents*. The 'no certificate' curve is taken from equation (4.4.6). We use the fitted parameters from the 'model' curve as inputs for the 'no certificate' curve to illustrate the premium. Fitted parameters: (left) $\beta^* = 16.12$, $\gamma^* = 15.08$ $\mu^* = 4.62$, $\alpha^* = 0.058$, and $\sigma^* = 0.40$. Fitted parameters for the rightmost panel are $\beta^* = 10.75$, $\gamma^* = 15.10$, $\mu^* = 5.52$, $\alpha^* = 0.10$, and $\sigma^* = 0.12$. Other parameters are $r = 0.017$, and (in cents) $S_0 = \exp(U_0) = \{281, 167\}$, $\delta_0^* = 106$, $\widehat{\delta} = 55$ and $c_1, c_2 = 0$.

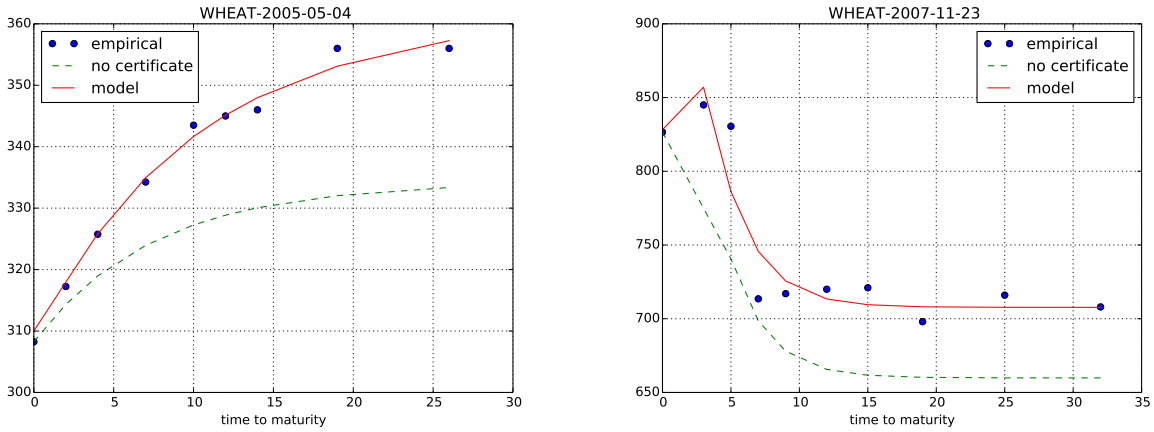

Figure 25: Calibrating XOU model with local storage to the empirical wheat futures curve. The x-axis is time to maturity in months and the y-axis is the price of a bushel of wheat in *cents*. The 'no certificate' curve is taken from equation (4.4.6). We use the fitted parameters from the 'model' curve as inputs for the 'no certificate' curve to illustrate the premium. Fitted parameters: (left) $\beta^* = 9.98$, $\gamma^* = 11.22$ $\mu^* = 5.83$, $\alpha^* = 0.08$, and $\sigma^* = 0.14$. Fitted parameters for the rightmost panel are $\beta^* = 7.13$, $\gamma = 14.16$, $\mu^* = 5.90$, $\alpha^* = 0.38$, and $\sigma^* = 0.91$. Other parameters are $r = 0.017$, $U_t = \{5.61, 6.65\}$, $\widehat{\delta} = 55$ and $c_1, c_2 = 0$.

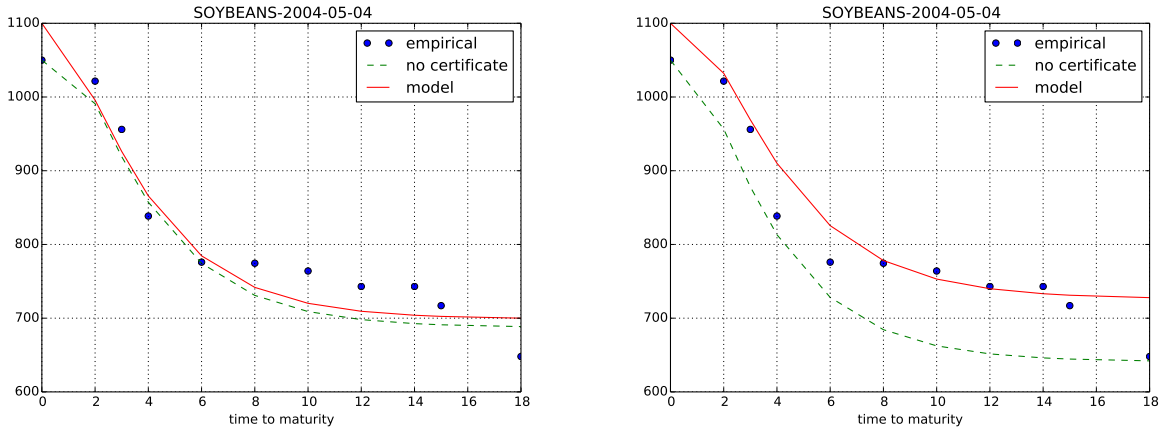

Figure 26: Calibrating the Martingale Model (left) and the XOU Model (right) to the empirical soybeans futures curve. The x-axis is time to maturity in months and the y-axis is the price of a bushel of wheat in *cents*. The 'no certificate' curve is taken from equations (4.3.16) and (4.4.6) respectively. The fitted parameters from the 'model' curve are used as inputs for the 'no certificate' curve to illustrate the premium. Fitted parameters: (left) $\nu^* = -0.44$, $\kappa^* = 0.023$, $\zeta^* = 0.92$, and $\delta_0^* = 1.42$; (right) $\beta^* = 11.88$, $\gamma^* = 9.97$, $\mu^* = 5.91$, $\alpha^* = 0.035$, and $\sigma^* = 0.95$. Other parameters are $r = 0.017$, $S_t = 1004.25$, $\widehat{\delta} = 55$ and $c_1 = c_2 = 0$.

As shown earlier, the model prices of futures of all maturities with a shipping certificate dominate the respective contracts without one due to the timing options embedded in the shipping certificate. Furthermore, the difference increases as the futures maturity lengthens, indicating that the storage option exerts a more significant price impact over a longer period of time. In summary, we have shown that the timing options in a shipping certificate are a crucial component to explain the positive basis. As we have seen, the exponential OU model is able to capture forward anticipative behaviors of the basis and account for both backwardated and upwards-sloping futures curves.

We close this section by comparing the empirical calibrations of the Martingale Model and the XOU Model in Figure 26. While both models are equally capable of estimating the immediate basis and fitting the empirical futures prices, the value of the timing option embedded in the shipping certificate is significantly higher under the XOU Model than the Martingale Model. This can be seen from the spread between the 'model' curve (shipping certificate delivery) and the 'no certificate' curve (physical spot delivery) plotted on both

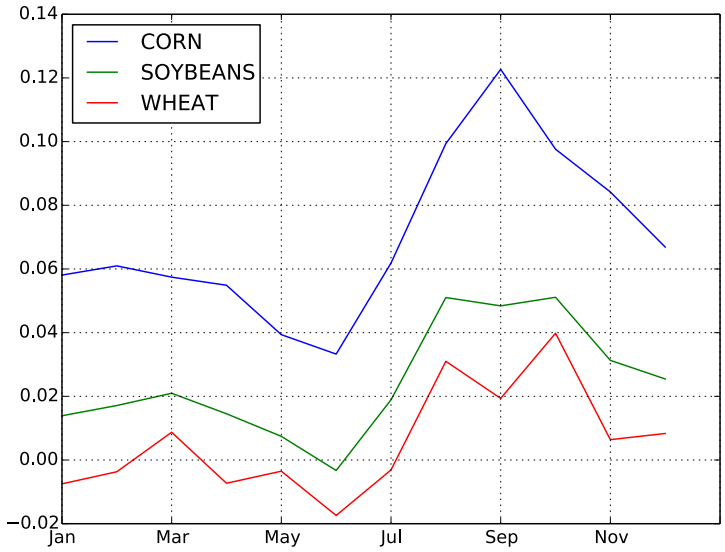

Figure 27: Seasonality of the average basis for corn, soybeans, and wheat during 2004–2010. The basis is highest during the harvest months (August-October) as storage rates are high due to grain silo capacity constraint. For instance, the average basis for soybeans exceeds 12% in September. From February to June, the basis tends to be smaller since the storage costs are lower due to empty grain silos before the next harvest begins.

panels. The 'no certificate' curve generated from the Martingale Model is much closer to the fitted 'model' curve, whereas a visibly larger gap is observed in the XOU Model. Intuitively, the XOU Model tends to propagate the basis forward as the market storage rate is assumed to be positively correlated with the spot price, but the Martingale Model assumes an independent stochastic (per bushel) storage rate. Therefore, the two models possess distinct features that address different market conditions, and have different implications to futures prices with longer maturities.

4.5 Concluding Remarks

We have demonstrated that the timing option embedded in the shipping certificate for grains leads to terminal non-convergence of futures and cash prices. The shipping certificate, by allowing its owner to choose the cheaper of two possible storage rates, therefore commands a premium over the physical grain itself. Our modeling approach captures the storage option

of the shipping certificate by solving two optimal timing problems: one to determine the optimal liquidation strategy for physical grain and another for the optimal exercise strategy for the shipping certificate.

We have proposed two stochastic diffusion models for the spot grain and storage rate dynamics, one in which the storage rate process is OU and the spot price less storage costs is a martingale, and the other where the spot price admits exponential OU dynamics along with a locally stochastic market storage rate. Under both models, explicit prices are provided for the shipping certificate and associated futures curve. Furthermore, we fit our models to empirical data during the periods of observed non-convergence. Our models not only capture the non-convergence phenomenon, but they also demonstrate adequate fit against the futures curve data when the market in backwardation or contango.

In order to develop tractable models with analytical solutions that are amenable to interpretation and calibration, we did not consider the seasonality of grain prices, among other features. To compare the basis over different months of the year, we illustrate in Figure 27 the average basis for all three commodities. As shown, the basis is typically higher during the fall harvest months (August to October) when available storage capacity is low and market storage rates are high. This suggests that the value of storage optionality, captured in our models here, is particularly high in these months. In contrast, the basis is typically smaller from the winter through the summer while the grain silos are being emptied before the next harvest, and thus, storage rates are reduced during the low season.

Overall, both of our proposed models are capable of generating model prices corresponding to a variety of market situations, such as high/low storage costs, and backwardated/contango futures curves, and fit well for different commodities. Therefore, the proposed models seem to have sufficient components and strong economic rationale to reflect and quantify non-convergence in the grains markets. There is certainly room for incorporating additional characteristics, such as seasonality and other contractual features, such as quality and delivery options. However, the relatively small number of traded futures contracts for

each commodity may limit the number of model parameters, and thus, model sophistication.

A better understanding of the price behaviors of commodity futures is also relevant to broader financial market, especially in the current era of so-called financialization of the commodity market (see Tang and Xiong (2012)), whereby commodity prices have become more correlated with the equity market. Moreover, commodity futures also play a role in the exchange-traded fund (ETF) market since most commodity ETFs are essentially dynamic portfolios of commodity futures; see Guo and Leung (2015); Leung and Ward (2015), among others. Therefore, for investors seeking spot exposure through commodity ETFs, any model which sheds light on the non-convergence phenomenon will affect investment decisions.

While our models have both empirical explanatory power and theoretical foundation, our results do not rule out the possible scenario called the 'failure of arbitrage' in the grain markets, as suggested by the speculator hypothesis. Nevertheless, alternative theories of non-convergence can potentially be incorporated into our models. The unique feature of our models is the embedded double timing option. This should motivate future research to investigate the valuation of such a timing option under different stochastic storage rate dynamics. Other directions include adding to futures multiple options, such as the delivery option, quality option, and location option. Furthermore, we choose our models in this chapter for analytical tractability which give closed-form certificate prices. One can also examine certificate prices under more complex stochastic models, for example, with stochastic interest rate, as well as stochastic volatility and jumps in the spot price or storage rate.

4.6 Appendix

4.6.1 Proofs: Proposition 5

We derive the certificate price by first determining the liquidation value function $J(S_\tau, \delta_\tau)$ and then substituting the value to solve the certificate problem $V(S_T, \delta_T)$. After applying

the martingale property of $(M_t)_{t\geq 0} = \left(e^{-rt}S_t - \int_0^t \delta_u e^{-ru}du\right)_{t\geq 0}$, and applying the optional sampling theorem, the liquidation value function simplifies to

$$\begin{aligned}
J(S_\tau, \delta_\tau) &= e^{r\tau}\left(\sup_{\eta\in\mathcal{T}_{\tau,\infty}} \mathbb{E}\left[e^{-r\eta}(S_\eta - c_2) - \int_\tau^\eta \delta_u e^{-ru}du|\mathcal{F}_\tau\right]\right) \\
&= e^{r\tau}\left(\sup_{\eta\in\mathcal{T}_{\tau,\infty}} \mathbb{E}\left[M_\eta + \int_0^\eta \delta_u e^{-ru}du - \int_\tau^\eta \delta_u e^{-ru}du - c_2 e^{-r\eta}|\mathcal{F}_\tau\right]\right) \\
&= e^{r\tau}\left(M_\tau + \int_0^\tau \delta_u e^{-ru}du + \sup_{\eta\in\mathcal{T}_{\tau,\infty}} \mathbb{E}\left[-c_2 e^{-r\eta}|\mathcal{F}_\tau\right]\right) \\
&= S_\tau.
\end{aligned}$$

From the last step, we see that $\eta = \infty$ is optimal. Furthermore, after substituting $J(S_t, \delta_t) = S_t$ into the certificate pricing problem, and again using the fact that M_t is a martingale, we obtain a solution for $V(S_T, \delta_T)$ which is separable in S_T and δ_T :

$$\begin{aligned}
V(S_T, \delta_T) &= e^{rT}\left(\sup_{\tau\in\mathcal{T}_{T,\infty}} \mathbb{E}\left[e^{-r\tau}(S_\tau - c_1) - \int_T^\tau \widehat{\delta} e^{-ru}du|\mathcal{F}_T\right]\right) \\
&= e^{rT}\left(M_T + \int_0^T \delta_u e^{-ru}du + \sup_{\tau\in\mathcal{T}_{T,\infty}} \mathbb{E}\left[\int_T^\tau (\delta_u - \widehat{\delta}) e^{-ru}du - c_1 e^{-ru}|\mathcal{F}_T\right]\right) \\
&= S_T + \sup_{\tau\in\mathcal{T}_{T,\infty}} \mathbb{E}\left[\int_T^\tau (\delta_u - \widehat{\delta}) e^{-r(u-T)}du - c_1 e^{-r(\tau-T)}|\mathcal{F}_T\right]. \qquad (4.6.1)
\end{aligned}$$

We denote the second term in (4.6.1) by $P(\delta_T)$, where the function $P(\delta)$ satisfies the variational inequality

$$\max\left\{\mathcal{L}P(\delta) - rP(\delta) + \delta - \widehat{\delta}, -P - c_1\right\} = 0,$$

where $\mathcal{L} \equiv \mathcal{L}^{\kappa,\nu,\zeta}$ is the infinitesimal generator defined in (4.3.7). In order to determine $P(\delta)$

and the optimal stopping strategy τ^*, we first conjecture that τ^* takes the form

$$\tau^* = \inf\{t \geq T : \delta_t \leq \delta^*\}$$

for critical stopping level δ^* to be determined. In other words, when the market storage rate δ_t is sufficiently small, the agent exercises to take advantage of the cheaper market storage rate, instead of paying the higher certificate rate $\widehat{\delta}$. Thus, for $\delta_t > \delta^*$, we look for the solution of the ODE $\mathcal{L}P(\delta) - rP(\delta) + \delta - \widehat{\delta} = 0$, and for $\delta \leq \delta^*$ we require that $P(\delta) = -c_1$. This leads to the solution to the variational inequality

$$P(\delta) = \left[AH(\delta) + \frac{1}{\kappa + r}\left(\delta - \widehat{\delta} + \frac{\kappa(\nu - \widehat{\delta})}{r}\right)\right]\mathbf{1}\{\delta \geq \delta^*\} - c_1\mathbf{1}\{\delta < \delta^*\},$$

along with the boundary conditions: $P(\delta^*) = -c_1$ and $P'(\delta^*) = 0$. The latter is the smooth pasting condition, which implies that

$$A = -\frac{1}{H'(\delta^*)(\kappa + r)}.$$

Enforcing these boundary conditions together also yields the optimal exercise level δ^* in (4.3.11).

Consider the function defined from (4.3.11)

$$f(\delta^*) := \delta^* - \frac{H(\delta^*)}{H'(\delta^*)}.$$

First, the properties of H imply that $H/H' \geq 0$, so that $f(\delta^*) \leq \delta^*$. Taking the limit as $\delta^* \to -\infty$, we have $f(-\infty) = -\infty$. Furthermore, under the restriction $\zeta^2 \leq 2\kappa$, and

examining the terms inside the integrals of H and H', namely,

$$H(\delta^*) = \int_0^\infty v^{\frac{r}{\kappa}-1} e^{\sqrt{\frac{2\kappa}{\zeta^2}}(x-\nu)v - \frac{v^2}{2}} dv,$$
$$H'(\delta^*) = \int_0^\infty v^{\frac{r}{\kappa}} \sqrt{\frac{2\kappa}{\zeta^2}} e^{\sqrt{\frac{2\kappa}{\zeta^2}}(x-\nu)v - \frac{v^2}{2}} dv,$$

we conclude that $H/H' \leq 1$. Therefore, $f(\delta^*) \geq \delta^* - 1$, and $f(\infty) = \infty$. Finally, for $\delta^* \in (-\infty, \infty)$, $f' = HH'/H'' > 0$. Therefore, we have

$$\lim_{\delta^* \to -\infty} f(\delta^*) = -\infty, \qquad \lim_{\delta^* \to \infty} f(\delta^*) = \infty, \qquad f'(\delta^*) > 0.$$

The solution δ^* to (4.3.11) is unique.

4.6.2 Proofs: Proposition 6

We consider a candidate interval type strategy for both τ and η. First, since the certificate price is monotonically increasing in the spot price, we consider the optimal liquidation time η^* to be of the form: $\eta^* = \inf\{t \geq \tau^* : U_t \geq u^*\}$. In the liquidation problem represented by J, we hold the commodity until the storage cost δ_t, which is increasing in the commodity price U_t, is sufficiently large relative to the commodity price. We solve a variational inequality for the value function $J(u)$ and match the boundary condition at u^* to get the solution. Assuming the conjectured form for η^*, $J(u)$ satisfies

$$\begin{cases} \mathcal{L}J(u) - rJ(u) = \beta u + \delta & \text{if } u < u^*, \\ J(u) = e^u - c_2 & \text{if } u \geq u^*, \end{cases}$$

where $\mathcal{L} \equiv \mathcal{L}^{\alpha,\mu,\sigma}$ is the infinitesimal generator defined in (4.3.7). We apply the continuity and smooth pasting conditions to $J(u)$, and get

$$J(u^*) = e^{u^*} - c_2, \qquad J'(u^*) = e^{u^*},$$

This gives the solution (4.4.3) with u^* satisfying

$$f(u^*) = \frac{e^{u^*} + \beta/(\alpha + r)}{H'(u^*)} H(u^*) - \frac{1}{\alpha + r}\left[\beta u^* + \gamma + \frac{\alpha(\beta\mu + \gamma)}{r}\right] - e^{u^*} + c_2 = 0.$$

When $\sigma < \sqrt{2\alpha}$, the level u^* admits a unique solution. First we can write

$$f(u^*) = e^{u^*}\left(\frac{H(u^*)}{H'(u^*)} - 1\right) + \frac{\beta}{\alpha + r}\left(\frac{H(u^*)}{H'(u^*)} - u^*\right) + C,$$

for some constant C not depending on u^*. Since $\frac{H}{H'} \leq 1$ then $f(u^*) \leq \frac{\beta}{\alpha+r}(1 - u^*) + C$ so $\lim_{u^*\to\infty} f(u^*) = -\infty$. Also, since $\frac{H}{H'} \geq 0$, then $f(u^*) \geq -e^{u^*} - \frac{\beta}{\alpha+r}u^* + C$ so $\lim_{u^*\to-\infty} f(u^*) = \infty$. Finally, we can look at

$$f'(u^*) = -\frac{H(u^*)}{H'(u^*)}\left[e^{u^*}\left(\frac{H''(u^*)}{H'(u^*)} - 1\right) + \frac{\beta}{\alpha + r}\frac{H''(u^*)}{H'(u^*)}\right].$$

Using similar arguments as from the previous appendix, we canshow $\frac{H''}{H'} \geq 1$, so $f'(u^*) \leq -\frac{H(u^*)}{H'(u^*)}\frac{\alpha}{\alpha+r} < 0 \ \forall u^* \in \mathbb{R}$. To recap, we have shown that

$$\lim_{u^*\to-\infty} f(u^*) = \infty, \qquad \lim_{u^*\to\infty} f(u^*) = -\infty, \qquad f'(u^*) < 0,$$

so our solution u^* is unique.

On the other hand, in the exercise problem V, the optimal strategy τ^* takes the form

$$\tau^* = \inf\{t \geq T : U_t \leq \underline{u}^{**} \text{ or } U_t \geq \overline{u}^{**}\},$$

In other words, hold the commodity until either (i) the storage cost is at or lower than $\underline{u}^{**}$ where the agent exercises, or (ii) the commodity price is reaches the upper level $\overline{u}^{**}$ at which the agent exercises *and* liquidates. As such, the value function satisfies

$$\begin{cases} V(u) = e^u - c_1 - c_2 & \text{if } u > \overline{u}^{**}, \\ \mathcal{L}V(u) - rV(u) = \widehat{\delta} & \text{if } \underline{u}^{**} \leq u \leq \overline{u}^{**}, \\ V(u) = AH(u) - \frac{1}{\alpha+r}\left[\beta u + \delta + \frac{\alpha(\beta\mu+\delta)}{r}\right] - c_1 & \text{if } u < \underline{u}^{**}. \end{cases}$$

The boundary conditions for $\underline{u}^{**}$ and $\overline{u}^{**}$ are

$$V(\overline{u}^{**}) = e^{\overline{u}^{**}} - c_1 - c_2, \qquad V(\underline{u}^{**}) = J(\underline{u}^{**}) = AH(\underline{u}^{**}) - \frac{1}{\alpha+r}\left[\beta\underline{u}^{**} + \delta + \frac{\alpha(\beta\mu+\delta)}{r}\right] - c_1,$$
$$V'(\overline{u}^{**}) = e^{\overline{u}^{**}}, \qquad V'(\underline{u}^{**}) = J'(\underline{u}^{**}) = AH'(\underline{u}^{**}) - \frac{\beta}{\alpha+r}.$$

We match the boundary conditions at $\underline{u}^{**}$ and $\overline{u}^{**}$ to get the solution (4.4.4).

Bibliography

Adjemian, M. K., Garcia, P., Irwin, S., and Smith, A. (2013). Non-convergence in domestic commodity futures markets: causes, consequences, and remedies. *USDA Economic Research Service*, 115(155381).

Ahn, A., Haugh, M., and Jain, A. (2012). Consistent pricing of options on leveraged ETFs. working paper, Columbia University.

Aulerich, N. M., Fishe, R. P. H., and Harris, J. H. (2011). Why do expiring futures and cash prices diverge for grain markets? *The Journal of Futures Markets*, 31(6):503–533.

Aulerich, N. M. and Hoffman, L. A. (2013). Recent convergence performance of futures and cash prices for corn, soybeans and wheat. *USDA Report from Economic Research Service*, 13L(1).

Avellaneda, M. and Zhang, S. (2010). Path-dependence of leveraged ETF returns. *SIAM Journal of Financial Mathematics*, 1:586–603.

Baur, D. G. and McDermott, T. K. (2010). Is gold a safe haven? International evidence. *Journal of Banking and Finance*, 34(8):1886âĂŞ1898.

Benninga, S., Eldor, R., and Zilcha, I. (1985). Optimal international hedging in commodity and currency forward markets. *Journal of International Money and Finance*, 4(4):537 – 552.

Biagini, F. and Bjork, T. (2007). On the timing option in a futures contract. *Mathematical Finance*, 17(2):267–283.

Bloseand, L. E. and Shieh, J. C. (1995). The impact of gold price on the value of gold mining stock. *Review of Financial Economics*, 4(2):125–139.

Borodin, A. N. and Salminen, P. (2002). *Handbook of Brownian Motion- Facts and Formulae*. Birkhauser Verlag.

Brennan, M. (1958). The supply of storage. *American Economic Review*, 48:50–72.

Brennan, M. and Schwartz, E. S. (1985). Evaluating natural resource investments. *The Journal of Business*, 58(2):135–57.

Brown, R. G. and Hwang, P. Y. (1997). *The Extended Kalman Filter*. John Wiley and Sons, 3 edition.

Carmona, R. and Coulon, M. (2013). *A Survey of Commodity Markets and Structural Models for Electricity Prices*. Springer New York.

Cheng, M. and Madhavan, A. (2009). The dynamics of leveraged and inverse exchange-traded funds. *Journal of Investment Management*, 4.

Cortazar, G. and Schwartz, E. (1997). Implementing a real option model for valuing an undeveloped oil field. *International Transactions in Operational Research*, 4(2):125–137.

Dahlgren, E. and Leung, T. (2015). An optimal multiple stopping approach to infrastructure investment decisions. *Journal of Economic Dynamics & Control*, 53:251–267.

Deaton, A. and Laroque, G. (1996). Competitive storage and commodity price dynamics. *Journal of Political Economy*, 104(5):896–293.

Dixit, A. K. (1994). *Investment Under Uncertainty*. Princeton University Press.

Dobi, D. and Avellaneda, M. (2012). Structural slippage of leveraged ETFs. Working Paper.

Erdelyi, Magnus, O. and Tricom (1953). *Higher Transcendental Functions*, volume 2. McGraw-Hill.

Fama, E. F. and French, K. R. (1987). Commodity futures prices: Some evidence on forecast power, premiums, and the theory of storage. *The Journal of Business*, 60(1):55–73.

Fama, E. F. and French, K. R. (1993). Common risk factors in the returns on stocks and bonds. *Journal of Financial Economics*, 33(1):3 – 56.

Florian, M. and Klein, M. (1971). Deterministic production planning with concave costs and capacity constraints. *Management Science*, 18(1):12–20.

Garcia, P., Irwin, S. H., and Smith, A. D. (2014). Futures market failure. *American Journal of Agricultural Economics*, 97(1):40–64.

Ghosh, D., Levin, E. J., MacMillan, P., and Wright, R. E. (2004). Gold as an inflation hedge? *Studies in Economics and Finance*, 22(1):1–25.

Gorton, G. B., Hayashi, F., and Rouwenhorst, K. G. (2012). The fundamentals of commodity futures returns. *Review of Finance*, pages 31–105.

Guedj, I., Li, G., and McCann, C. (2011). Futures-based commodities ETFs. *The Journal of Index Investing*, 2(1):14–24.

Guo, K. and Leung, T. (2015). Understanding the tracking errors of commodity leveraged ETFs. In Aid, R., Ludkovski, M., and Sircar, R., editors, *Commodities, Energy and Environmental Finance, Fields Institute Communications*, pages 39–63. Springer.

Guo, K. and Leung, T. (2017). Understanding the non-converge of agricultural futures via stochastic storage costs and timing options. *Journal of Commodity Markets*, 6:32–49.

Hinz, J. and Fehr, M. (2010). Storage costs in commodity option pricing. *SIAM Journal of Financial Math*, 1(1):729–751.

Hranaiova, J., Jarrow, R. A., and Tomek, W. G. (2005). Estimating the value of delivery options in futures contracts. *Journal of Financial Research*, 28(3):363–383.

Irwin, S. H., Garcia, P., Good, D., and Kunda, E. (2009). Poor convergence performance of cbot corn, soybean and wheat futures contracts: Causes and solutions. *Marketing and Outlook Research Report*.

Irwin, S. H., Garcia, P., Good, D. L., and Kunda, E. L. (2011). Spreads and non-convergence in Chicago Board of Trade corn, soybean, and wheat futures: Are index funds to blame? *Applied Economic Perspectives and Policy*, 33(1):116–142.

Johnson, L. L. (1960). The theory of hedging and speculation in commodity futures. *The Review of Economic Studies*, 27(3):139–151.

Johnson, M. A. J. and Lamdin, D. J. (2015). New evidence on whether gold mining stocks are more like gold or like stocks. *Alternative Investment Analyst Review*. forthcoming.

Jorion, Y. J. P. (2006). Firm value and hedging: Evidence from us oil and gas producers. *The Journal of Finance*, 61(2):893–919.

Jurek, J. W. and Stafford, E. (2013). The cost of capital for alternative investments. *NBER working paper*.

Kaldor, N. (1939). Speculation and economic stability. *Review of Economic Studies*, 7(1):1–27.

Leung, T., Li, J., Li, X., and Wang, Z. (2016). Speculative futures trading under mean reversion. *Asia-Pacific Financial Markets*, 23(4):281–304.

Leung, T. and Li, X. (2015). Optimal mean reversion trading with transaction costs and stop-loss exit. *International Journal of Theoretical & Applied Finance*, 18(3):15500.

Leung, T. and Li, X. (2016). *Optimal Mean Reversion Trading: Mathematical Analysis and Practical Applications*. Modern Trends in Financial Engineering. World Scientific, Singapore.

Leung, T., Li, X., and Wang, Z. (2014). Optimal starting–stopping and switching of a CIR process with fixed costs. *Risk and Decision Analysis*, 5(2):149–161.

Leung, T., Li, X., and Wang, Z. (2015). Optimal multiple trading times under the exponential OU model with transaction costs. *Stochastic Models*, 31(4):554–587.

Leung, T. and Santoli, M. (2013). Leveraged exchange-traded funds: admissible leverage and risk horizon. *Journal of Investment Strategies*, 2:39–61.

Leung, T. and Sircar, R. (2012). Implied volatility of leveraged ETF options. Working paper, Columbia University.

Leung, T. and Ward, B. (2015). The golden target: Analyzing the tracking performance of leveraged gold ETFs. *Studies in Economics and Finance*, 32(3):278–297.

Mackintosh, P. and Lin, V. (2010a). Longer term plays on leveraged ETFs. *Credit Suisse: Portfolio Strategy*, pages 1–6.

Mackintosh, P. and Lin, V. (2010b). Tracking down the truth. *Credit Suisse: Portfolio Strategy*, pages 1–10.

Mason, C., Omprakash, A., and Arouna, B. (2010). Few strategies around leveraged ETFs. *BNP Paribas Equities Derivatives Strategy*, pages 1–6.

McDonald, R. and Siegel, D. (1986). The value of waiting to invest. *The Quarterly Journal of Economics*, 101(4):707.

Merton, R. C. (1974). On the pricing of corporate debt: The risk structure of interest rates. *The Journal of Finance*, 29(2):449–470.

Murphy, R. and Wright, C. (2010). An empirical investigation of the performance of commodity-based leveraged ETFs. *The Journal of Index Investing*, 1(3):14–23.

Naylor, M., Wongchoti, U., and Gianotti, C. (2011). Abnormal returns in gold and silver exchange traded funds. *The Journal of Index Investing*, 2(2):1–34.

Rand, A. (1957). *Atlas Shrugged*. Random House.

Schwartz, E. (1997). The stochastic behavior of commodity prices, implications for valuation and hedging. *Journal of Finance*, 52(3):923–973.

Takahashi, A. and Yamamoto, K. (2008). Hedge fund replication. *CARF Working Paper*.

Tang, K. and Xiong, W. (2012). Index investment and the financialization of commodities. *Financial Analysts Journal*, 68(6):54–72.

Triantafyllopoulos, K. and Montana, G. (2009). Dynamic modeling of mean-reverting spreads for statistical arbitrage. *Computational Management Science*, 8:23–49.

Tufano, P. (1996). Who manages risk? An empirical examination of risk management practices in the gold mining industry. *The Journal of Finance*, 51(4):1097–1137.

Tufano, P. (1998). The determinants of stock price exposure: Financial engineering and the gold mining industry. *The Journal of Finance*, 53(3):1015–1052.

Working, H. (1949). The theory of the price of storage. *American Economic Review*, 39:1254–1262.